The Abdus Salam
International Centre for Theoretical Physics

United Nations
Educational, Scientific and
Cultural Organization

IAEA
International Atomic Energy Agency

1965-11

9th Workshop on Three-Dimensional Modelling of Seismic Waves Generation, Propagation and their Inversion

22 September - 4 October, 2008

Geophysical modelling and GPS, SAR, GRACE and GOCE data for the understanding of lithospheric and mantle processes Part 1 & 2

Roberto Sabadini

Dipartimento di Scienze della Terra "A. Desio"
Università di Milano, Italy

roberto.sabadini@unimi.it

Strada Costiera 11, 34014 Trieste, Italy - Tel. +39 040 2240 111; Fax +39 040 224 163 - sci_info@ictp.it, www.ictp.it

Geophysical modelling and GPS, SAR, GRACE and GOCE data for the understanding of lithospheric and mantle processes - 1

Roberto Sabadini

Dipartimento di Scienze della Terra “A. Desio”
Università di Milano

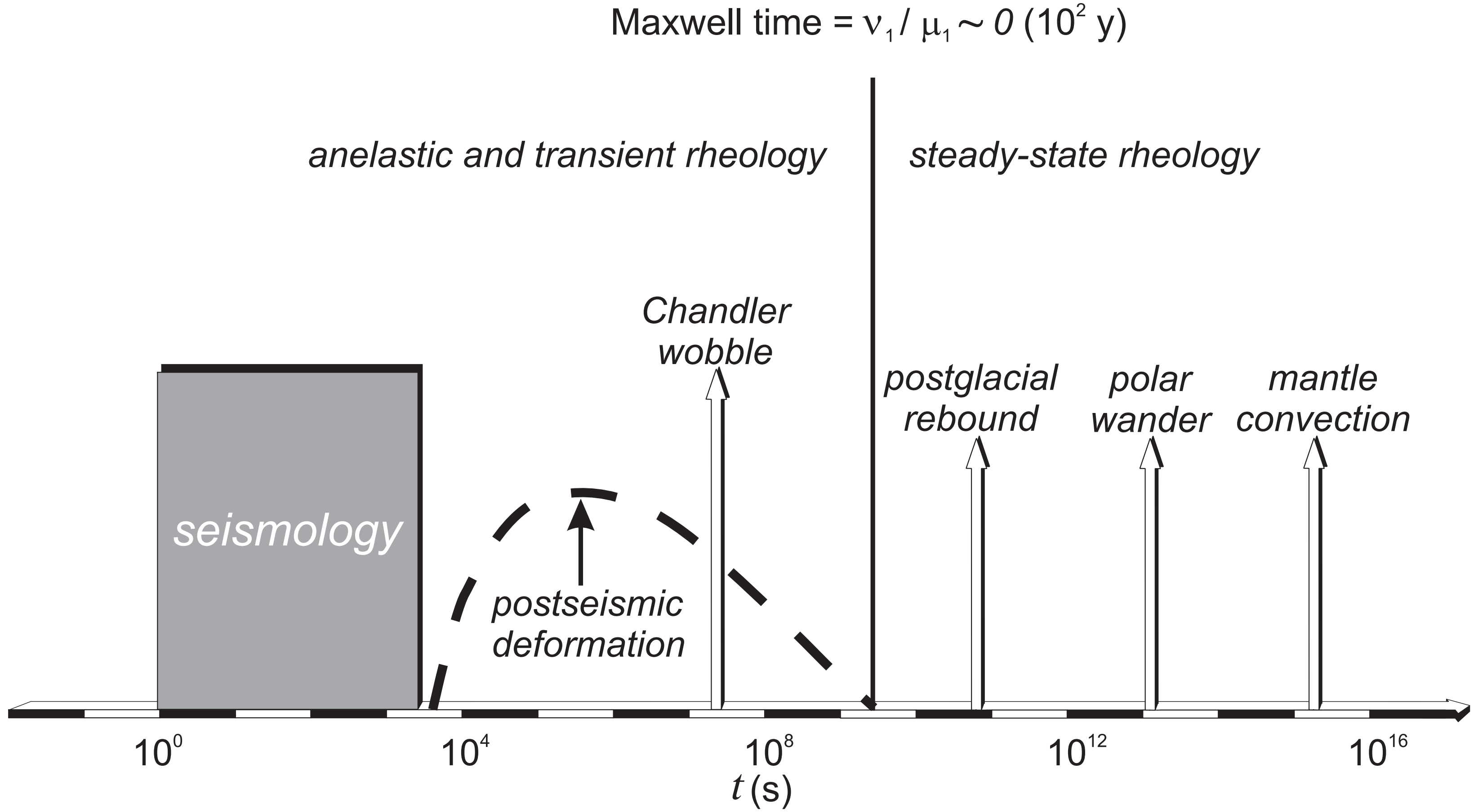

Maxwell time = $\nu_1 / \mu_1 \sim 0\,(10^2$ y)
anelastic and transient rheology
steady-state rheology
Chandler wobble
postglacial rebound
polar wander
mantle convection
seismology
postseismic deformation
10^0
10^4
10^8
10^{12}
10^{16}
t (s)

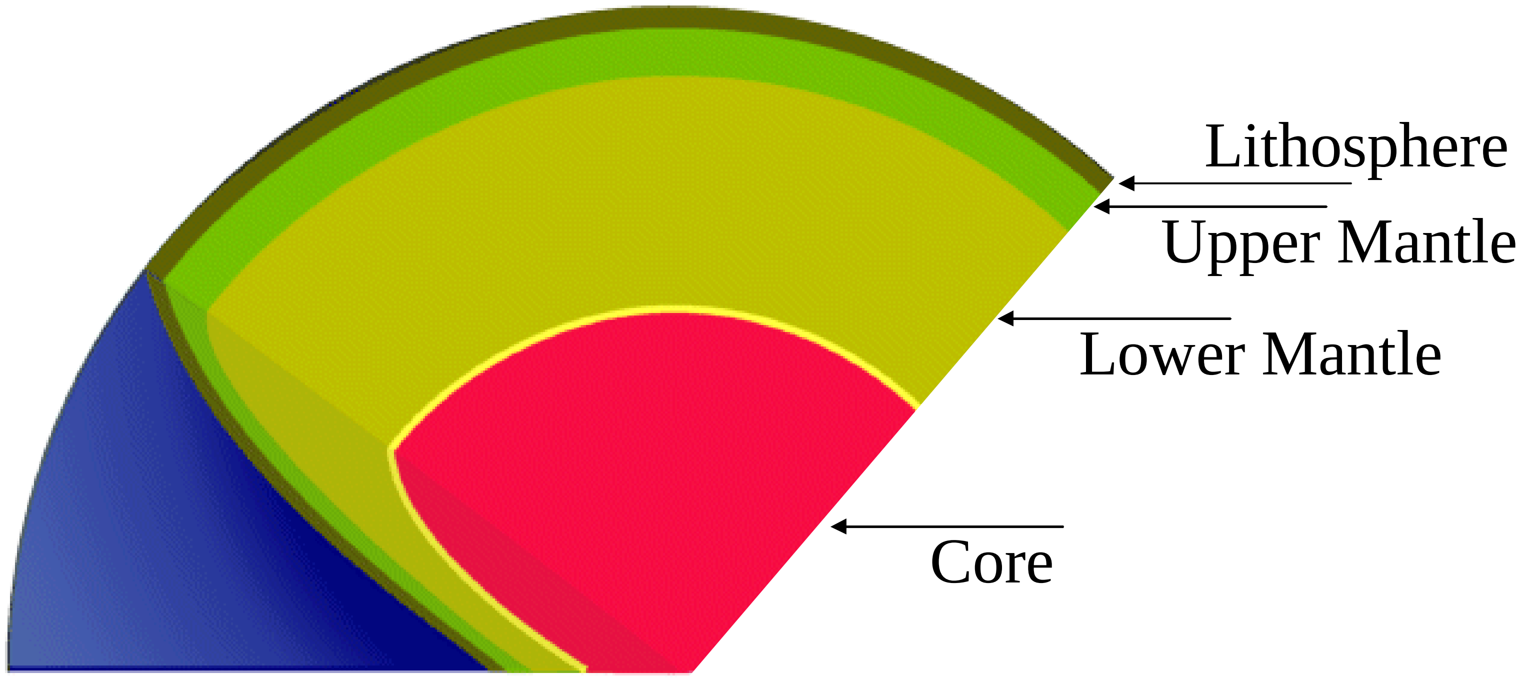
Lithosphere
Upper Mantle
Lower Mantle
Core

$$\nabla \cdot \sigma_1 - \nabla p_0(t_0) - \nabla(\rho_0 g \mathbf{u} \cdot \hat{\mathbf{e}}_r) + \rho \mathbf{F} = 0$$

$$\nabla \cdot \sigma_1 - \nabla(\rho_0 g \mathbf{u} \cdot \hat{\mathbf{e}}_r) - \rho_0 \nabla \phi_1 - \rho_1 g \hat{\mathbf{e}}_r = 0$$

$$\nabla^2 \phi_1 = 4\pi G \rho_1$$

$$\nabla^2 \phi_1 = 0$$

$$
\begin{aligned}
&-\rho_0 \partial_r \phi_1 + \rho_0 g_0 \Delta - \rho_0 \partial_r (u g_0) + \partial_r \sigma_{rr} + r^{-1} \partial_\theta \sigma_{r\theta} \\
&\quad + r^{-1}\left(2\sigma_{rr} - \sigma_{\theta\theta} - \sigma_{\phi\phi} + \sigma_{r\theta} \cot\theta\right) = 0
\end{aligned}
$$

$$
\begin{aligned}
&-\rho_0 r^{-1} \partial_\theta \phi_1 - \rho_0 g_0 r^{-1} \partial_\theta u + \partial_r \sigma_{r\theta} + r^{-1} \partial_\theta \sigma_{\theta\theta} \\
&\quad + r^{-1}\left(\left(\sigma_{\theta\theta} - \sigma_{\phi\phi}\right) \cot\theta + 3\sigma_{r\theta}\right) = 0
\end{aligned}
$$

$$
\begin{aligned}
&r^{-2} \partial_r \left(r^2 \partial_r \phi_1\right) + \left(r^2 \sin\theta\right)^{-1} \partial_\theta (\sin\theta \partial_\theta \phi_1) \\
&\quad = -4\pi G(\rho_0 \Delta + u \partial_r \rho_0)
\end{aligned}
$$

$$u = \sum_{l=0}^{\infty} U_l(r) P_l(\cos\theta)$$

$$v = \sum_{l=0}^{\infty} V_l(r) \partial_\theta P_l(\cos\theta)$$

$$\phi_1 = -\sum_{l=0}^{\infty} \phi_l(r) P_l(\cos\theta)$$

$$P_l(\cos\theta) = \frac{1}{2^l l!} \frac{\mathrm{d}^l}{\mathrm{d}(\cos\theta)^l} \left(\cos^2\theta - 1\right)^l$$

$$\frac{\mathrm{d}\epsilon}{\mathrm{d}t} = \frac{\sigma}{2\nu} + \frac{1}{2\mu}\frac{\mathrm{d}\sigma}{\mathrm{d}t}$$

$$\tilde{\mu}(s) = \frac{\mu s}{s + \mu/\nu}$$

$$\tilde{\sigma}_{ij}(s) = 2\tilde{\mu}(s)\tilde{\epsilon}_{ij}(s)$$

$$U_l(t) = U_{le}\delta(t) + \sum_{j=1}^{M} U_{lj}\mathrm{e}^{s_j t}$$

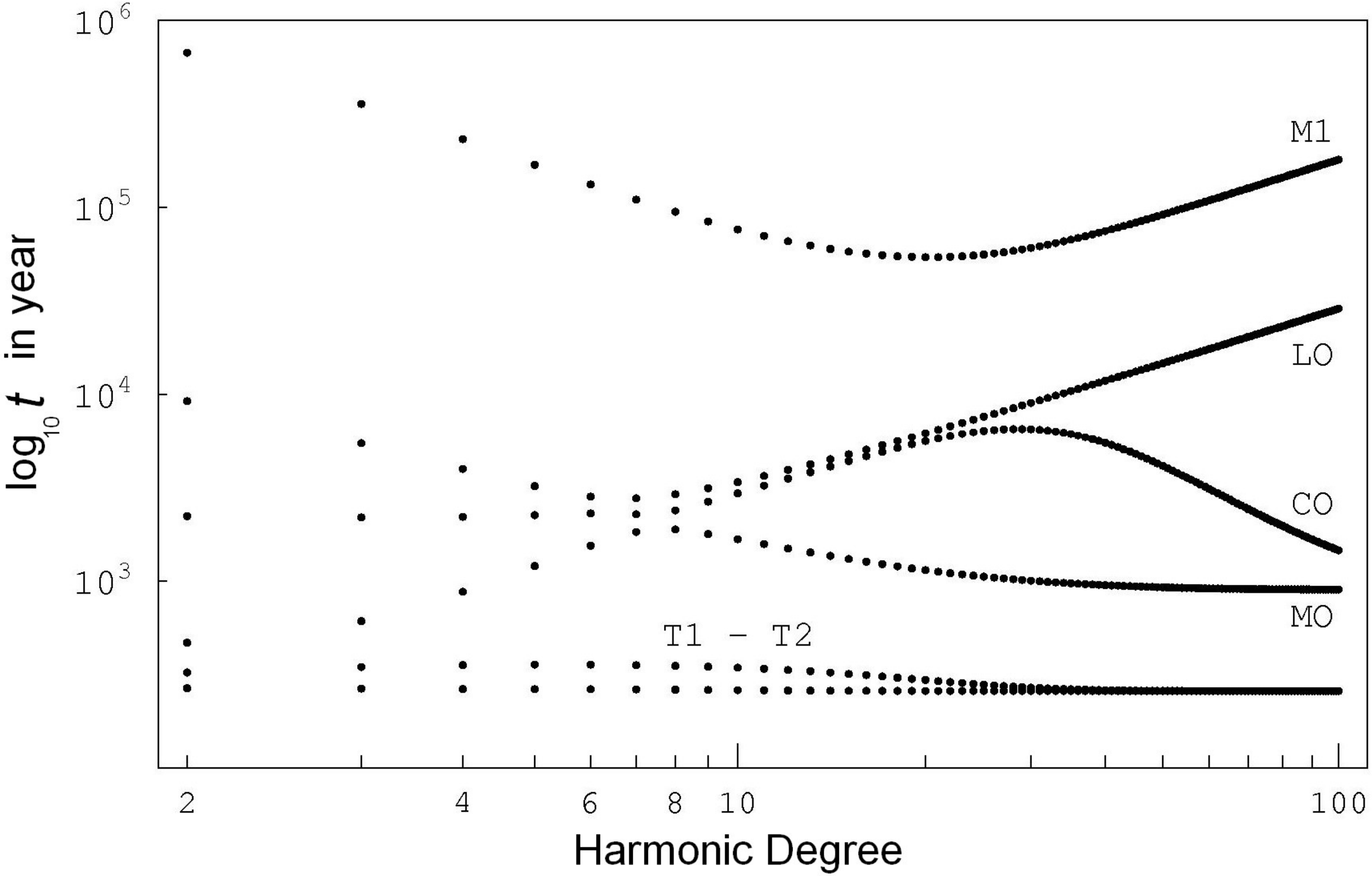

10^6
10^5
10^4
10^3
$\log_{10} t$ in year
M1
LO
CO
MO
T1 - T2
2
4
6
8
10
100
Harmonic Degree

General Scheme

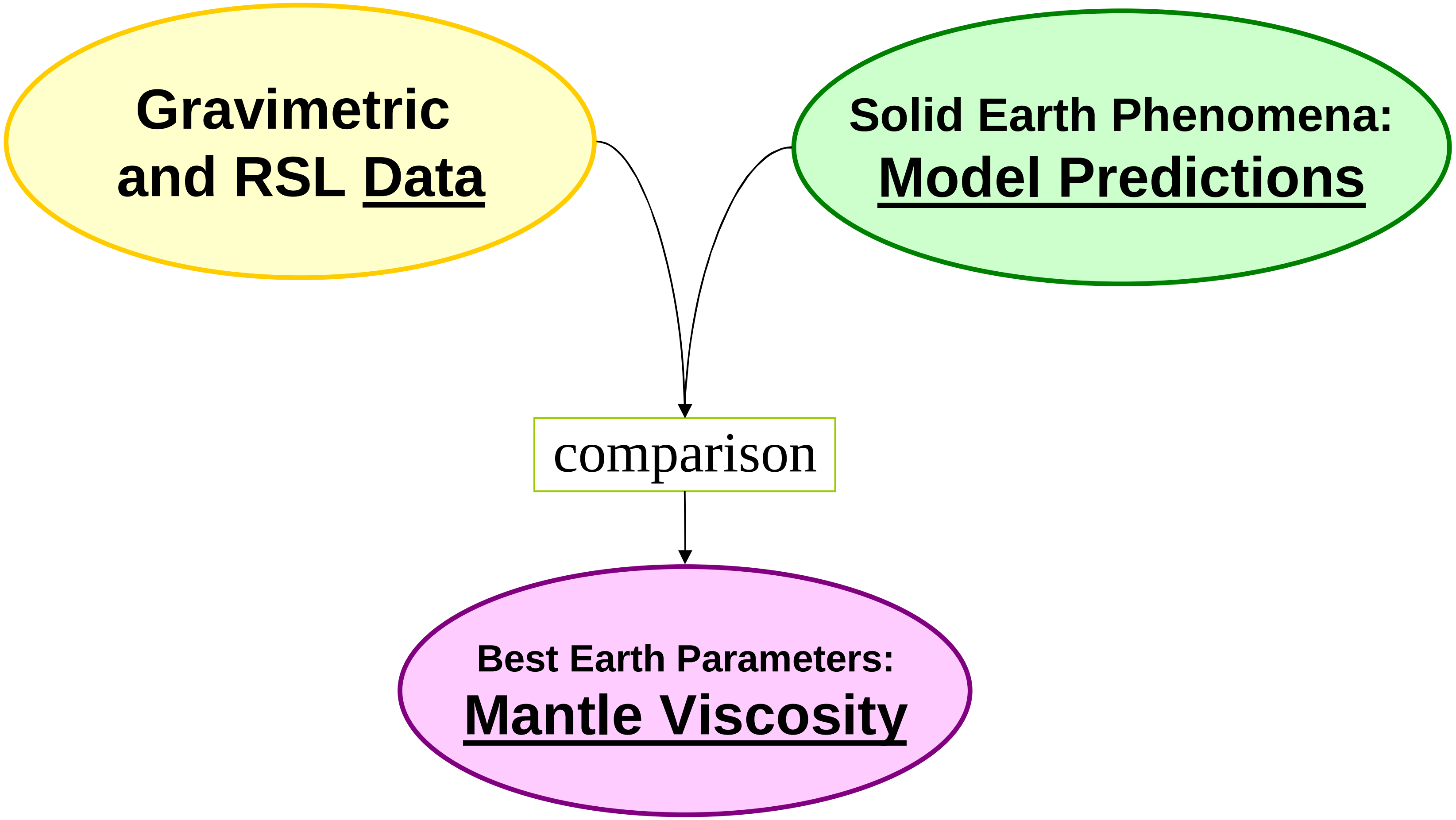

General Scheme

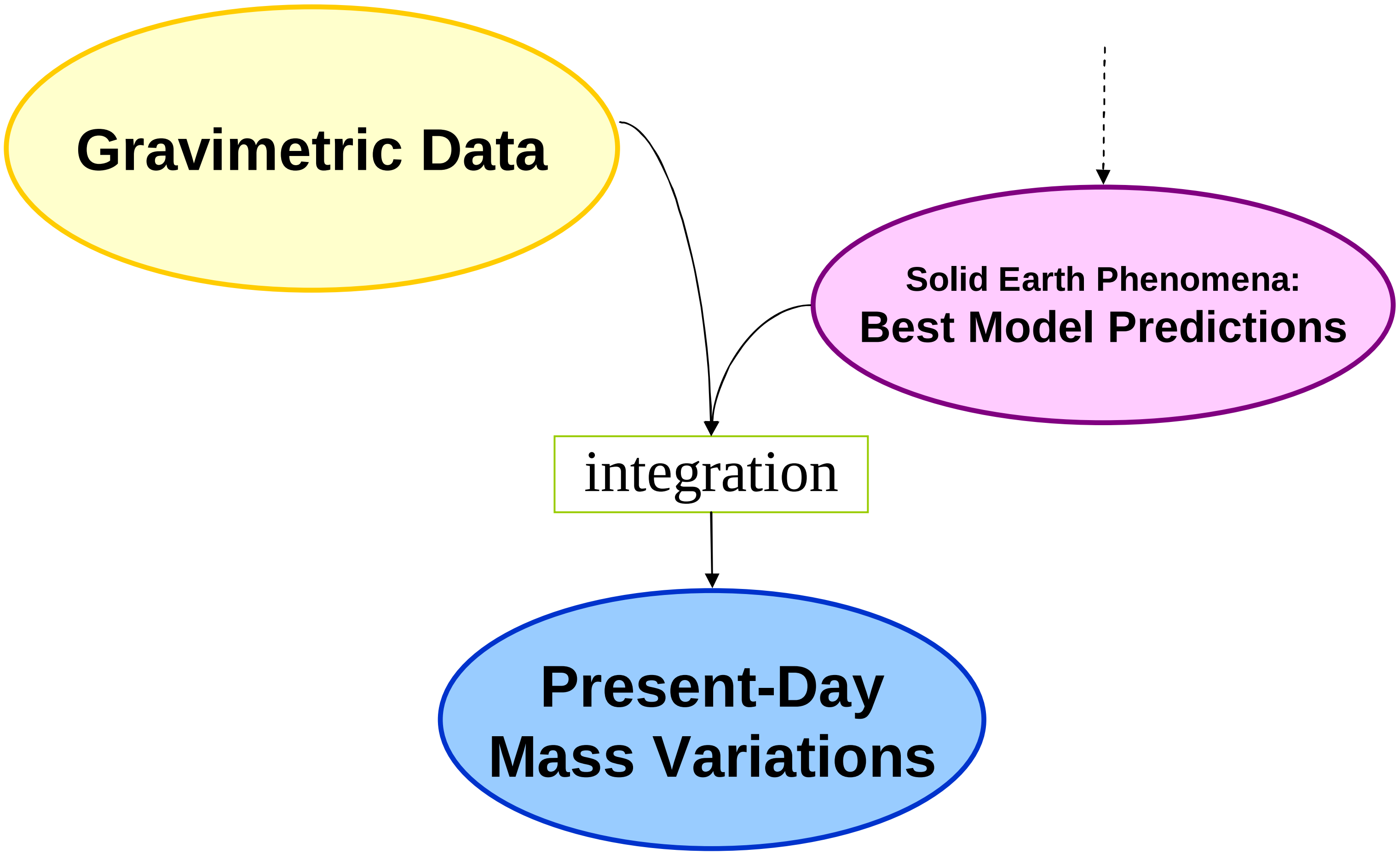

SLR and GRACE

Satellite Laser Ranging

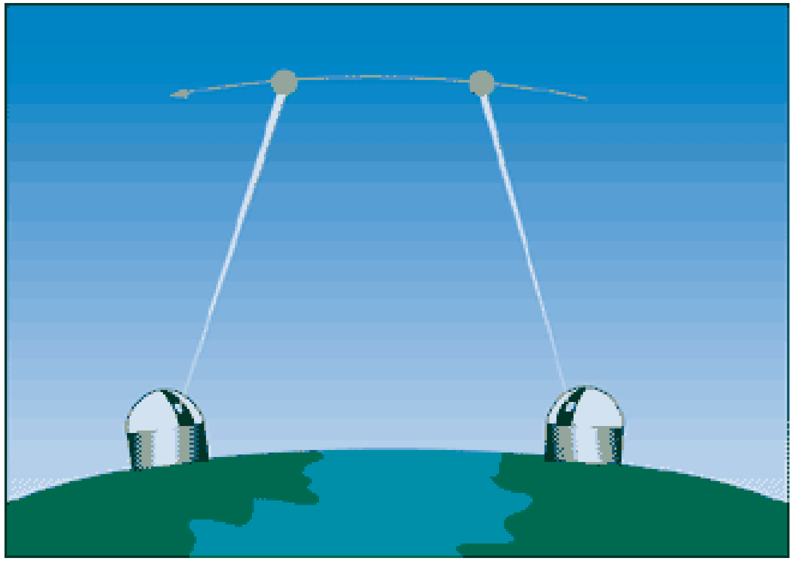

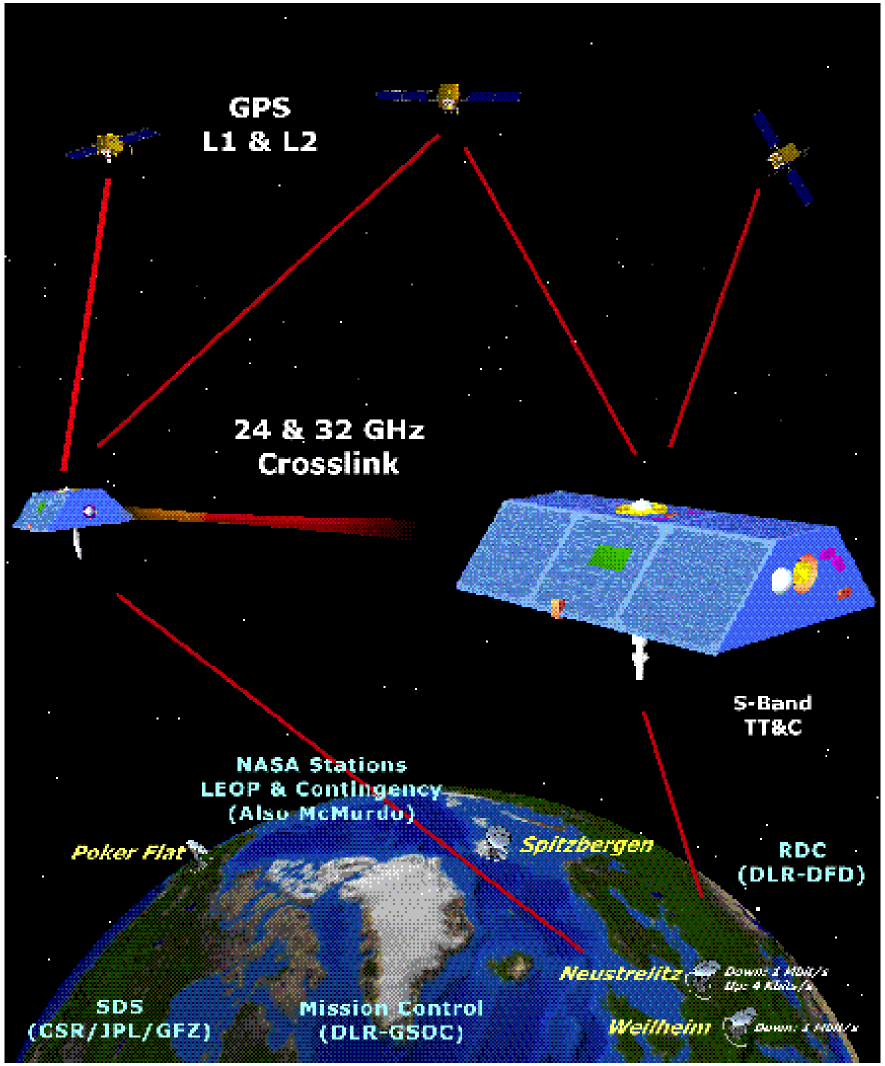

Gravity Anomalies (from GRACE)

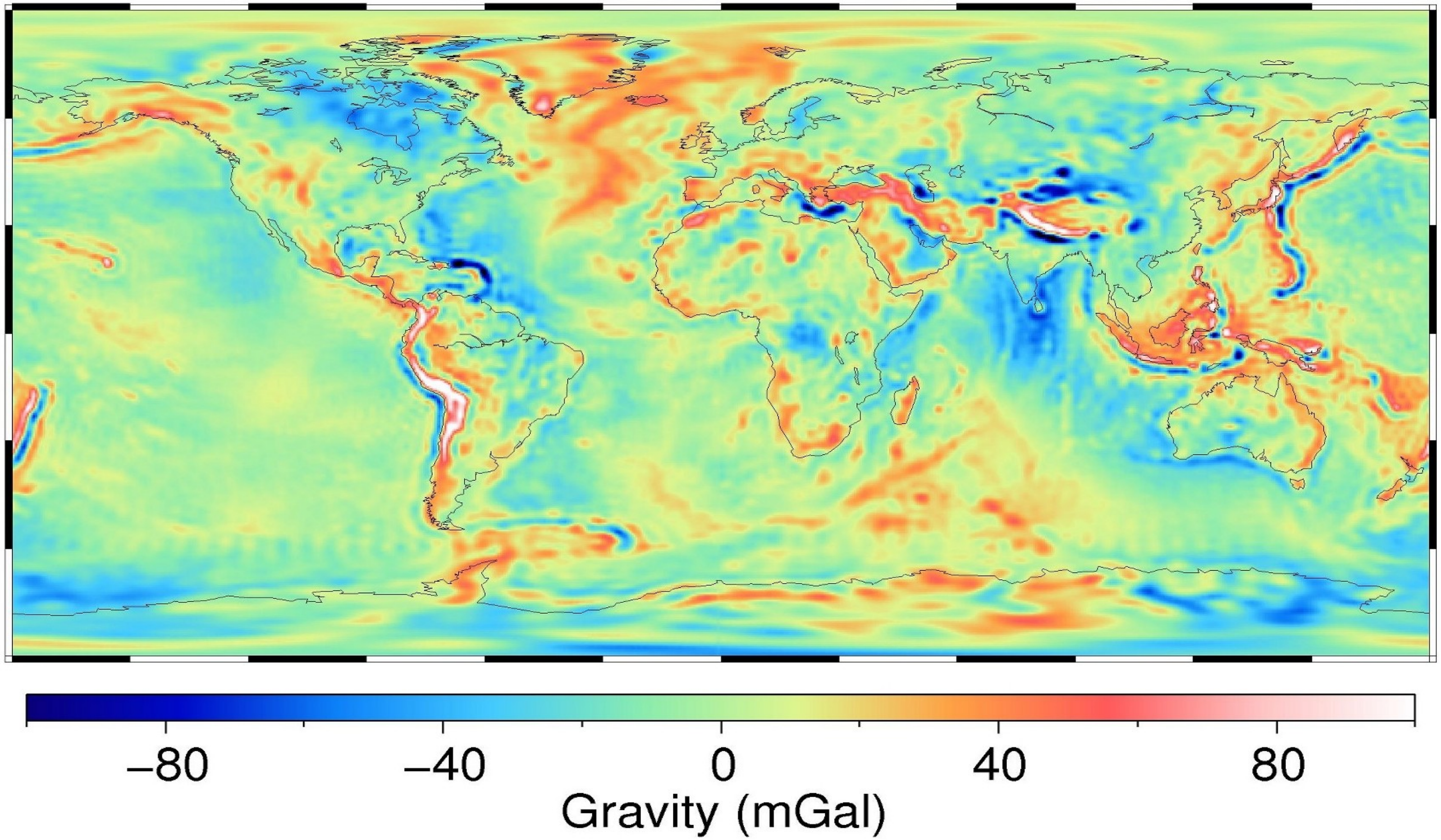

GRACE-LAGEOS 2-year gravity field (EIGEN-GL04S)

Static Geoid (from GRACE)

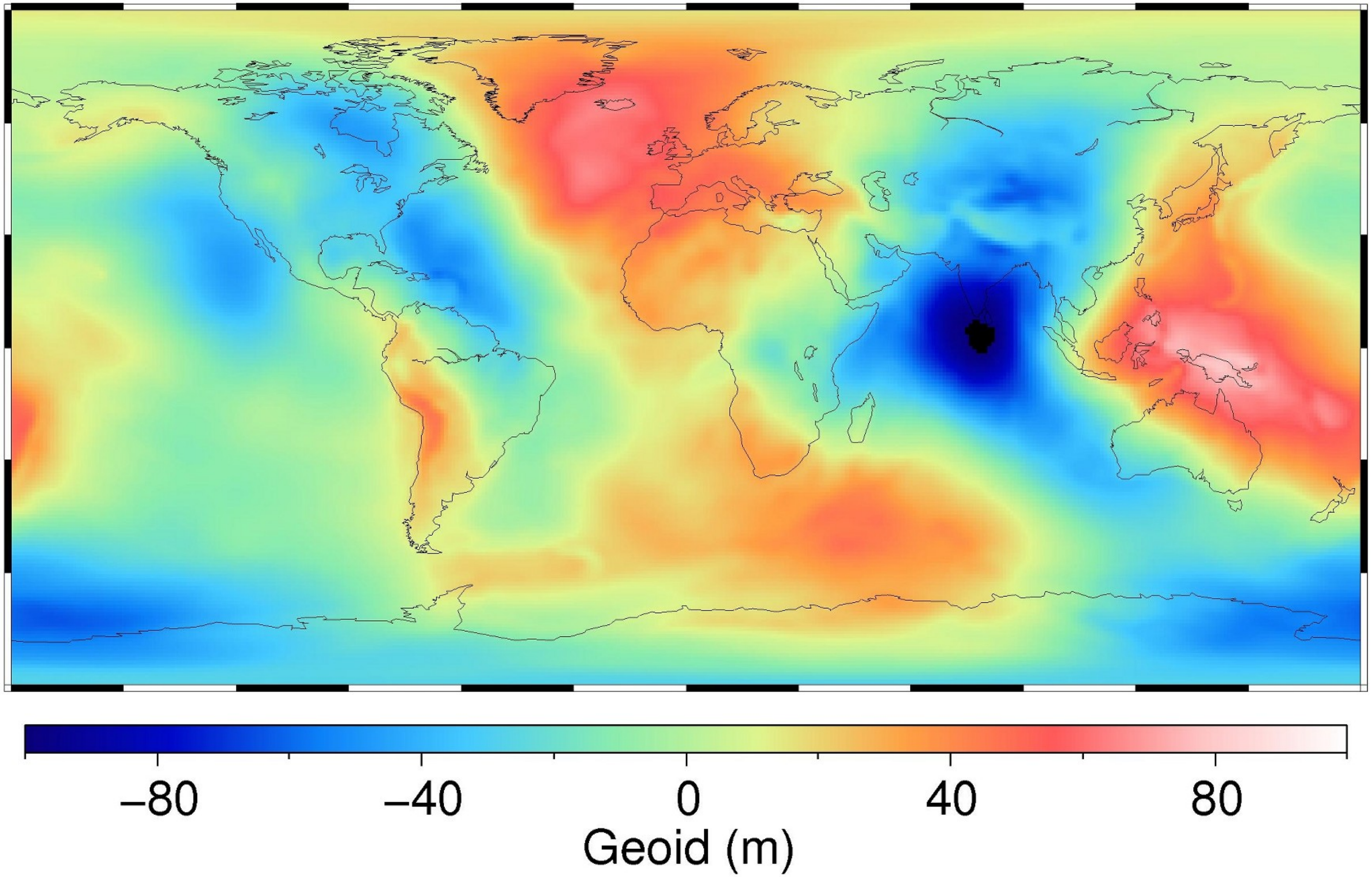

GRACE-LAGEOS 2-year gravity field (EIGEN-GL04S)

Geoid Variation - August 2002

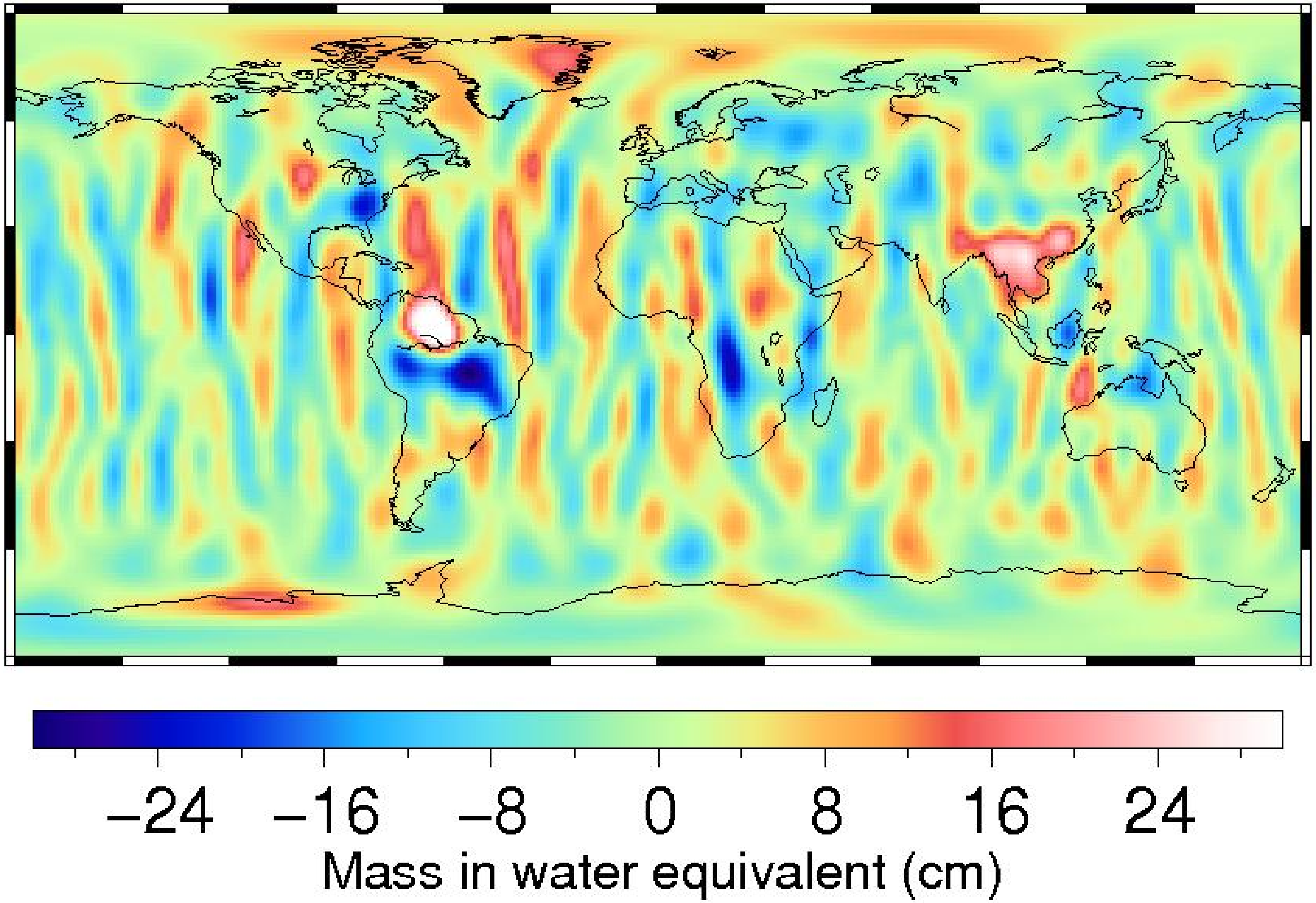

Geoid Variation - October 2002

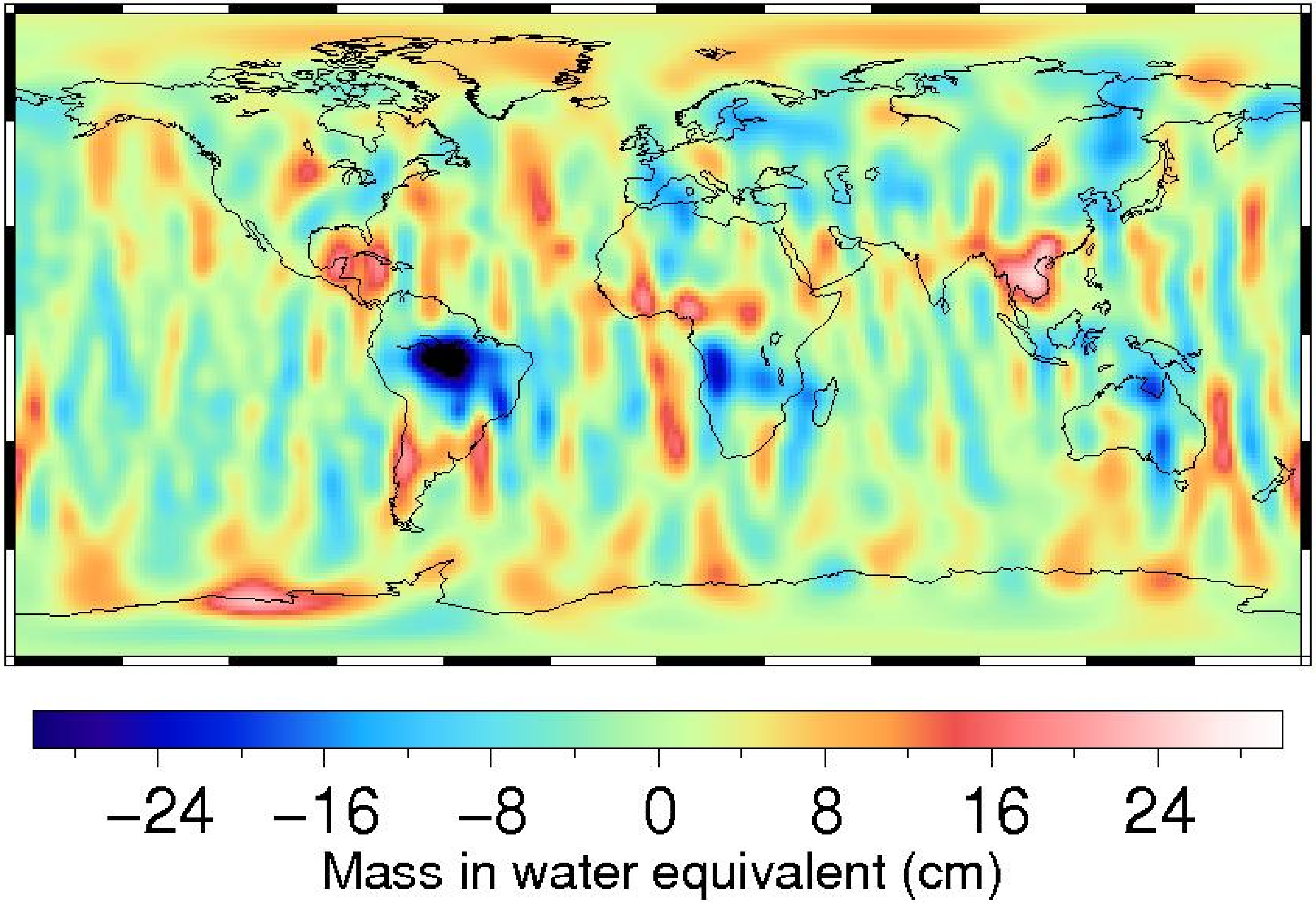

Geoid Variation - November 2002

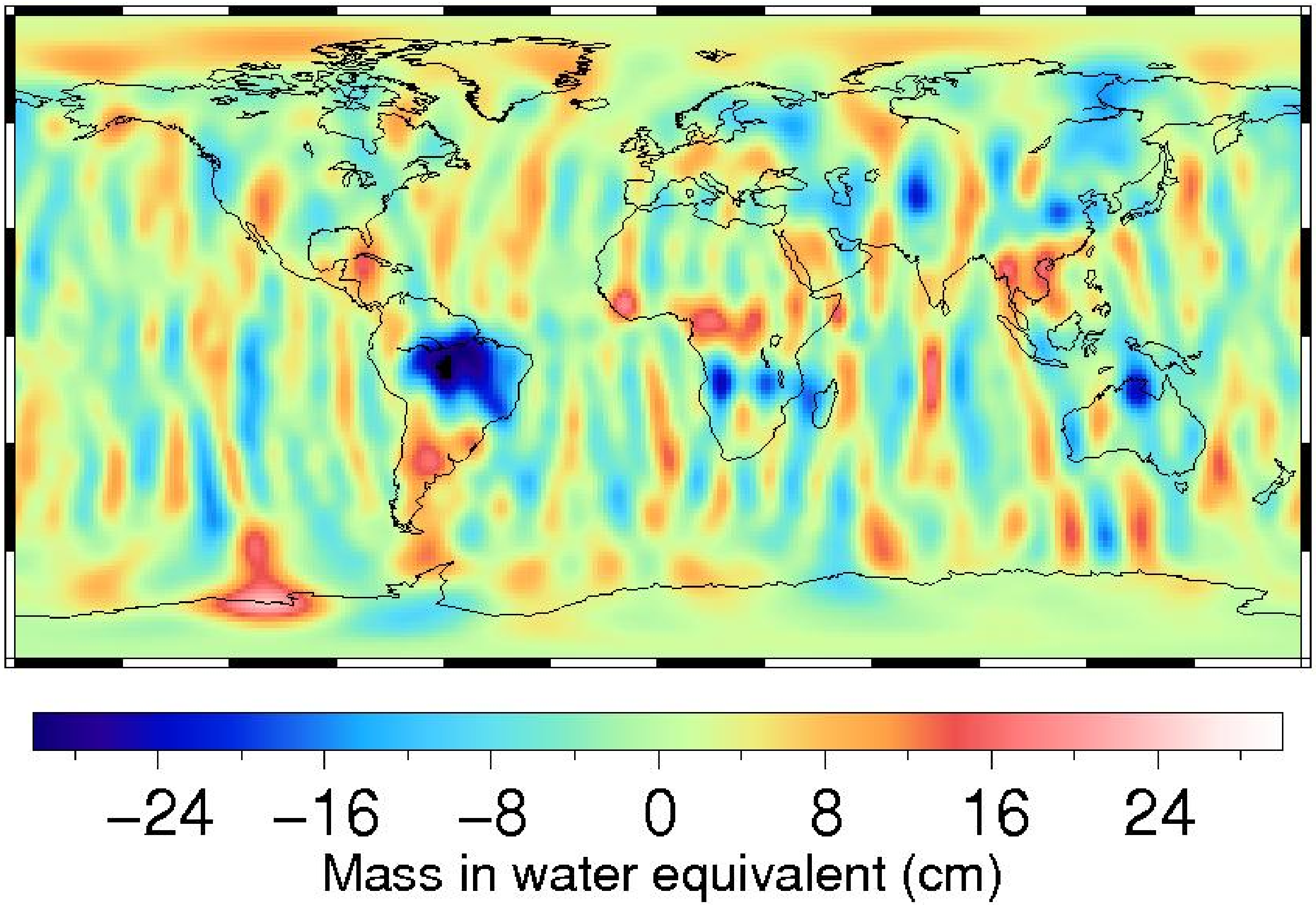

Geoid Variation - February 2003

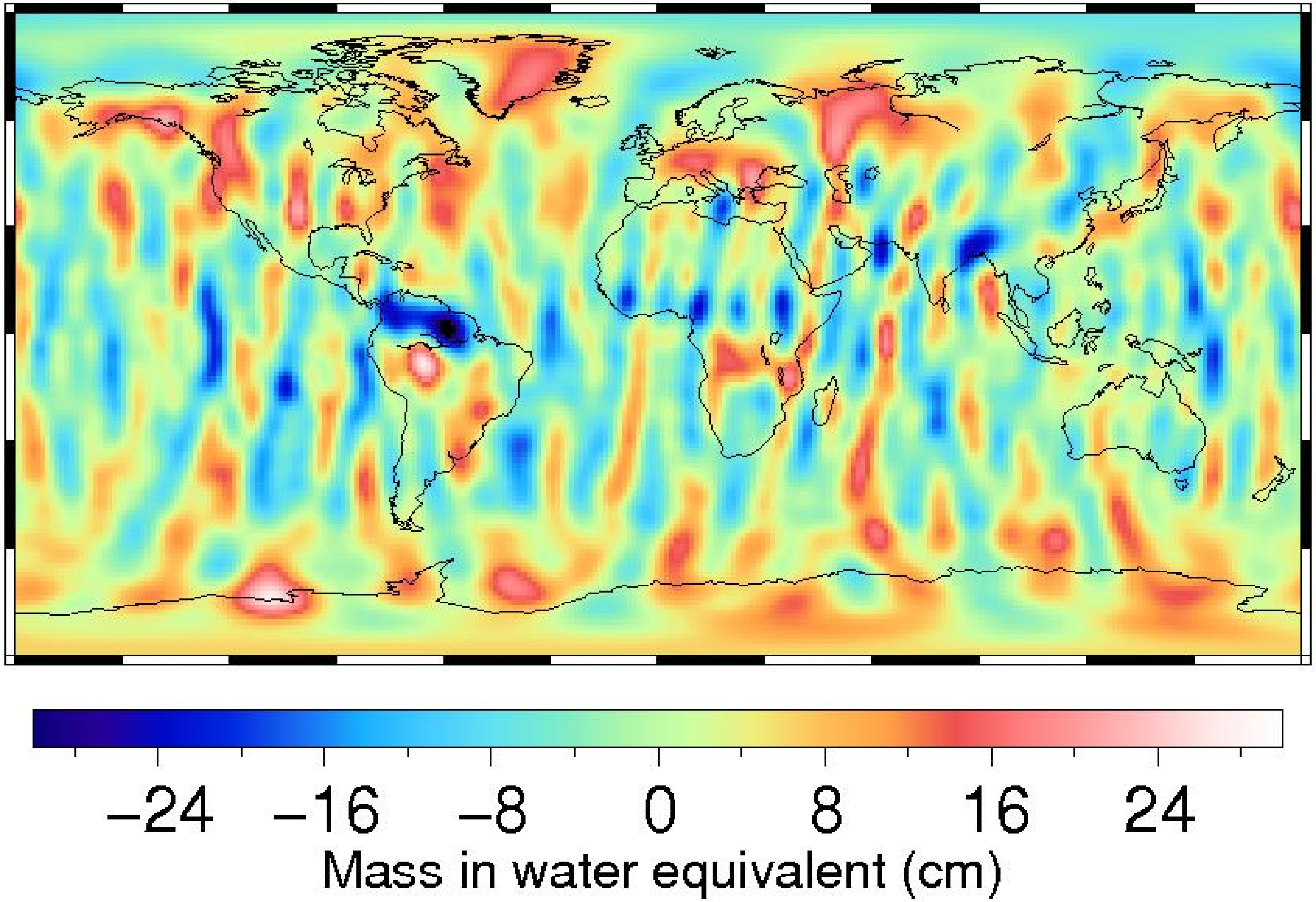

Geoid Variation - March 2003

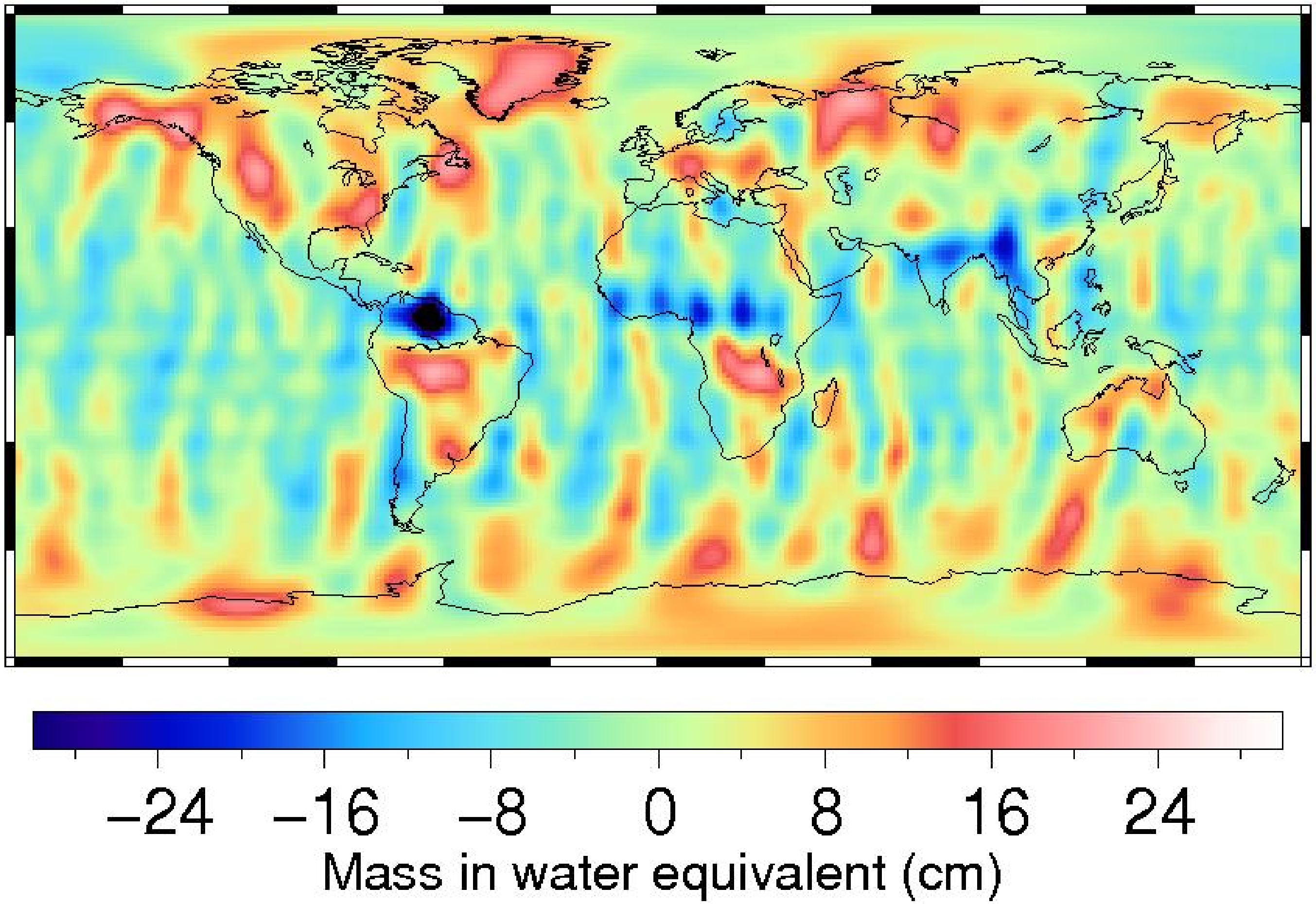

Geoid Variation - April 2003

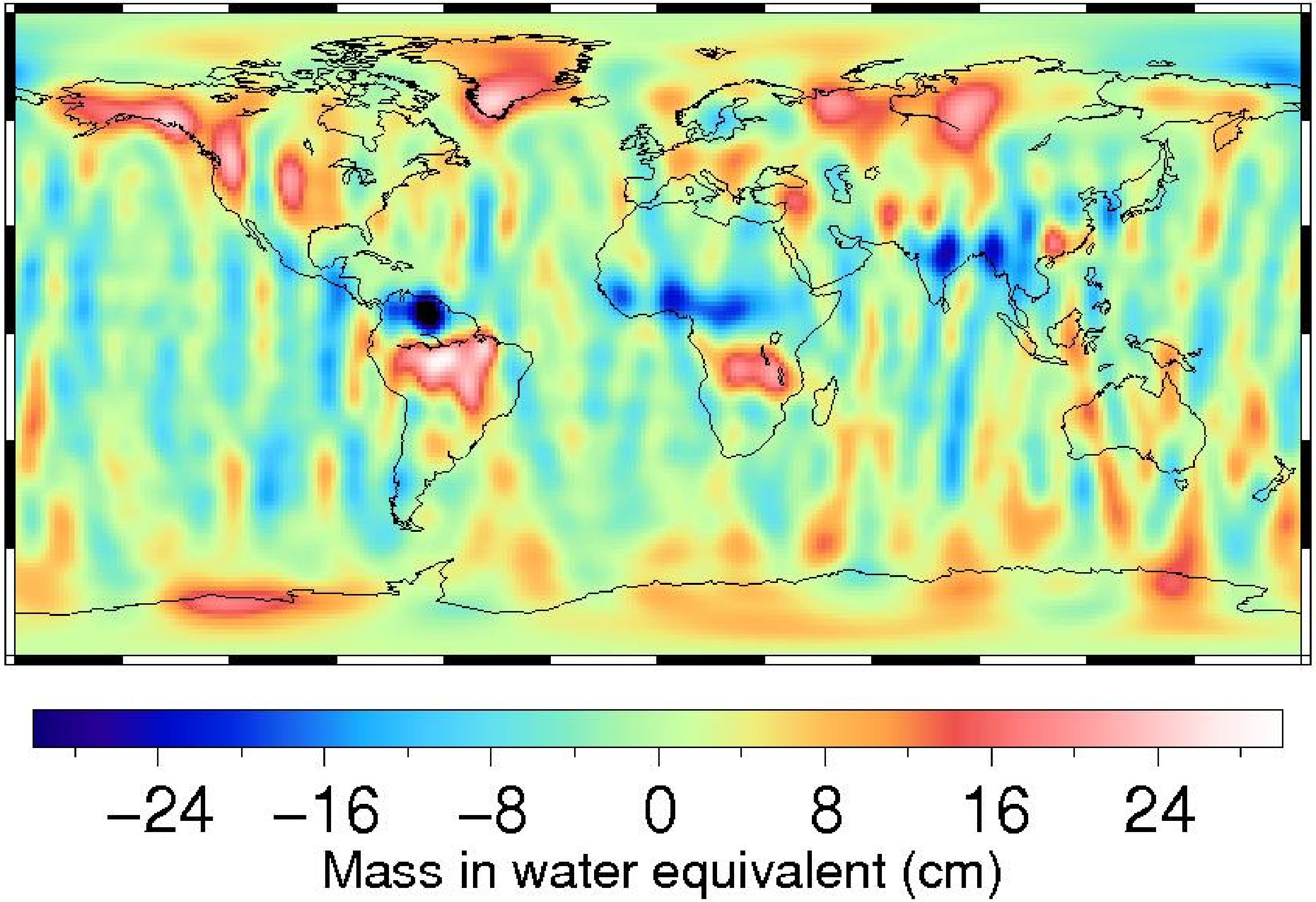

Geoid Variation - May 2003

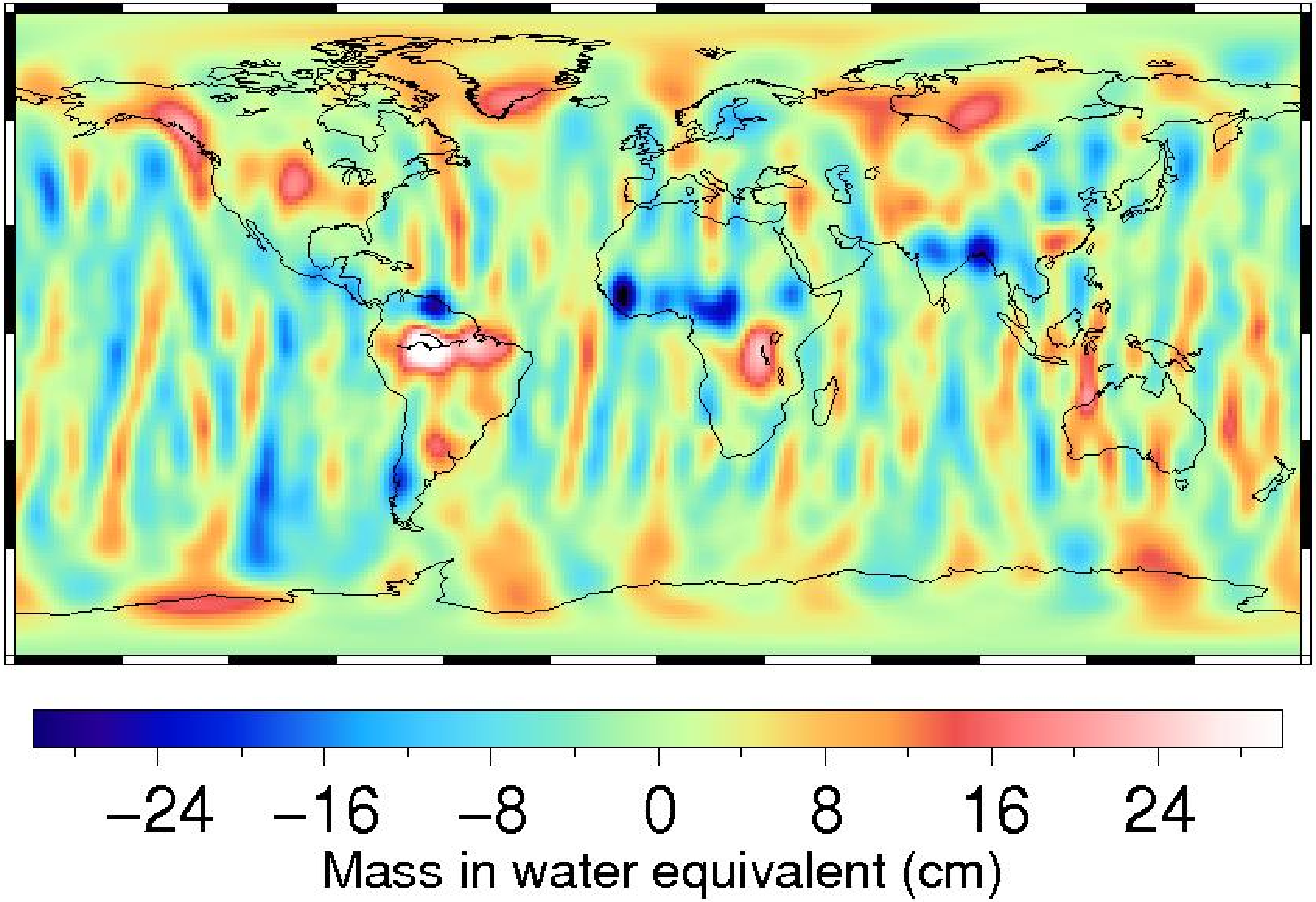

Geoid Variation - July 2003

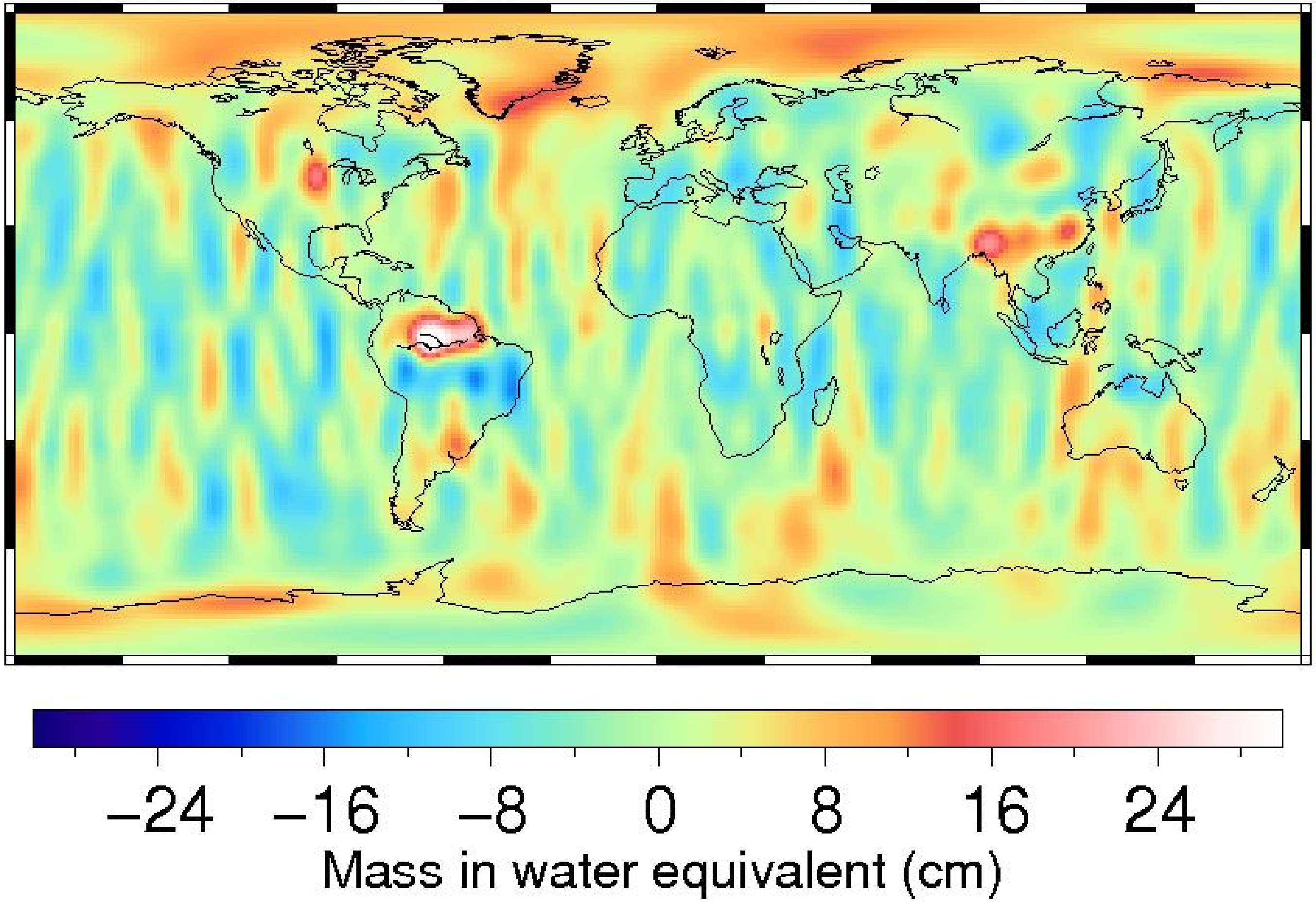

Geoid Variation - Agoust 2003

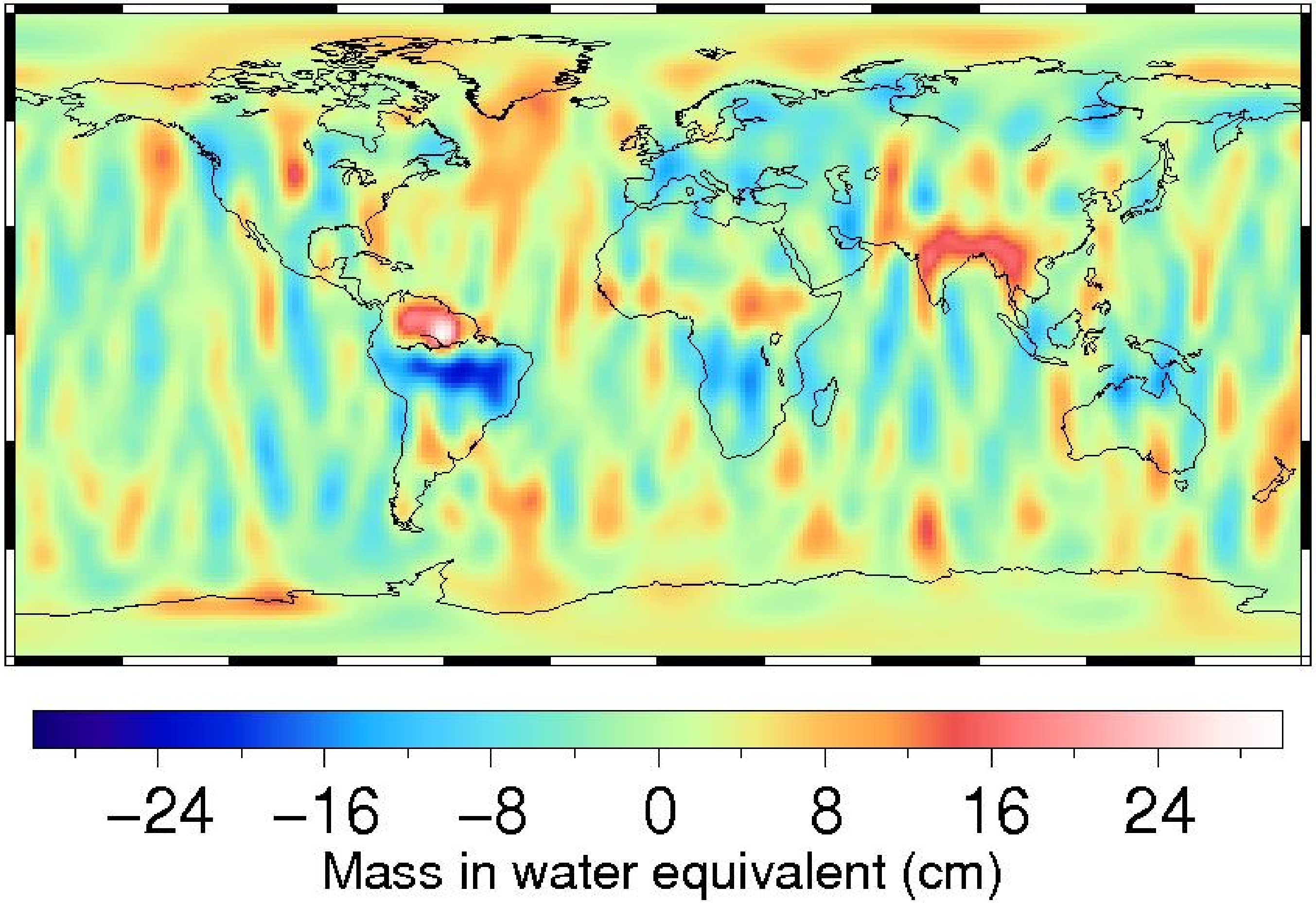

Geoid Variation - September 2003

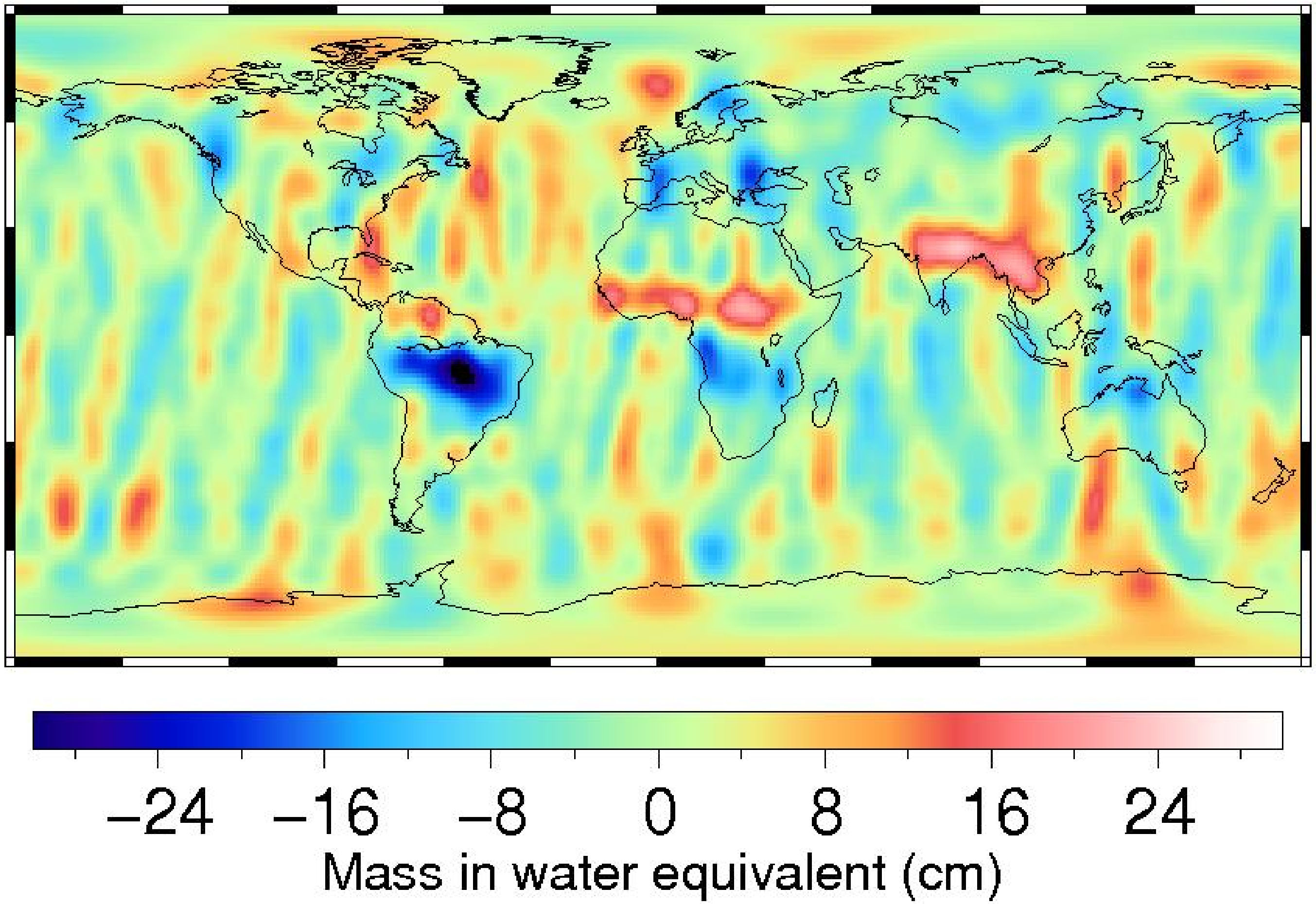

Geoid Variation - October 2003

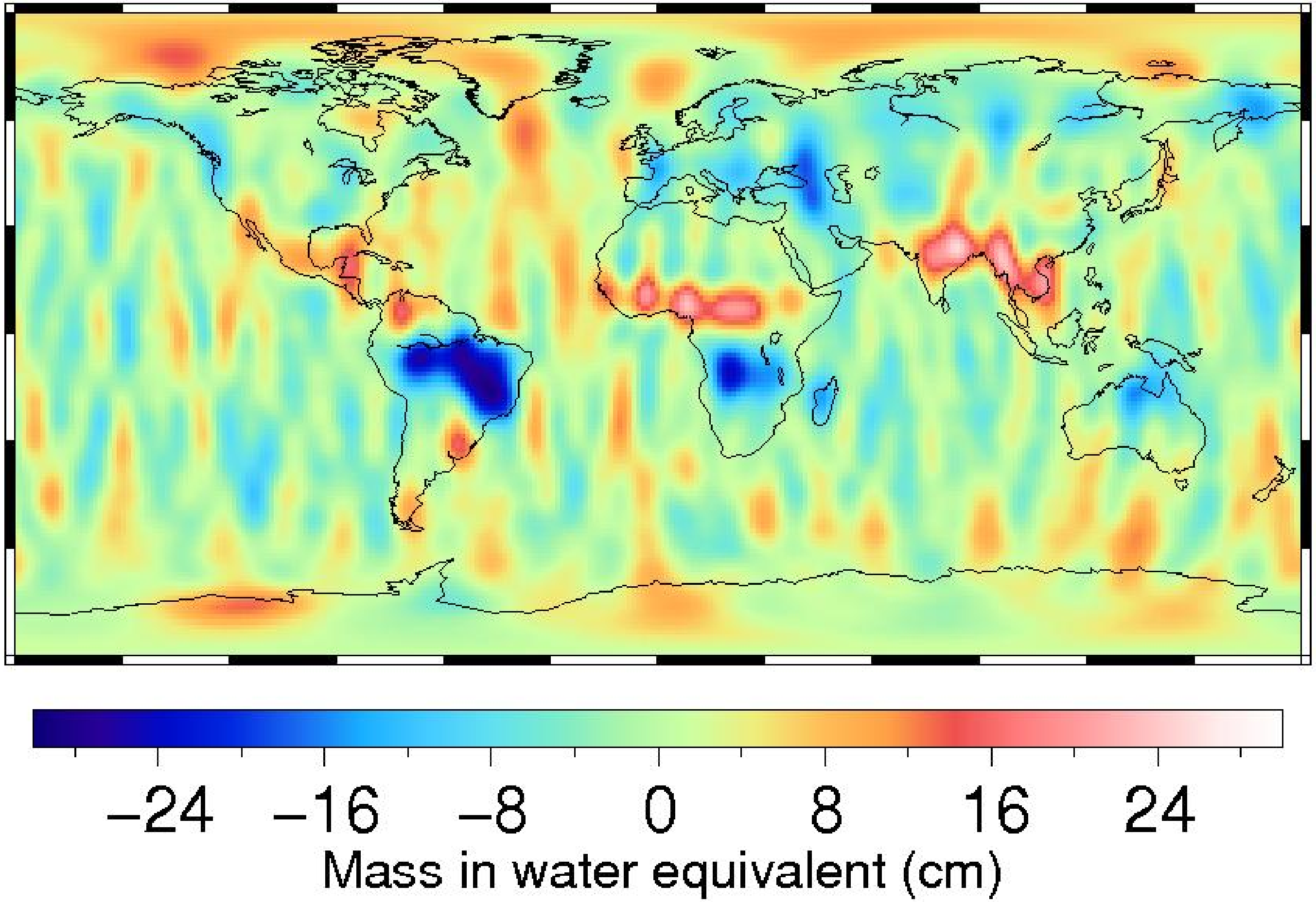

Geoid Variation - November 2003

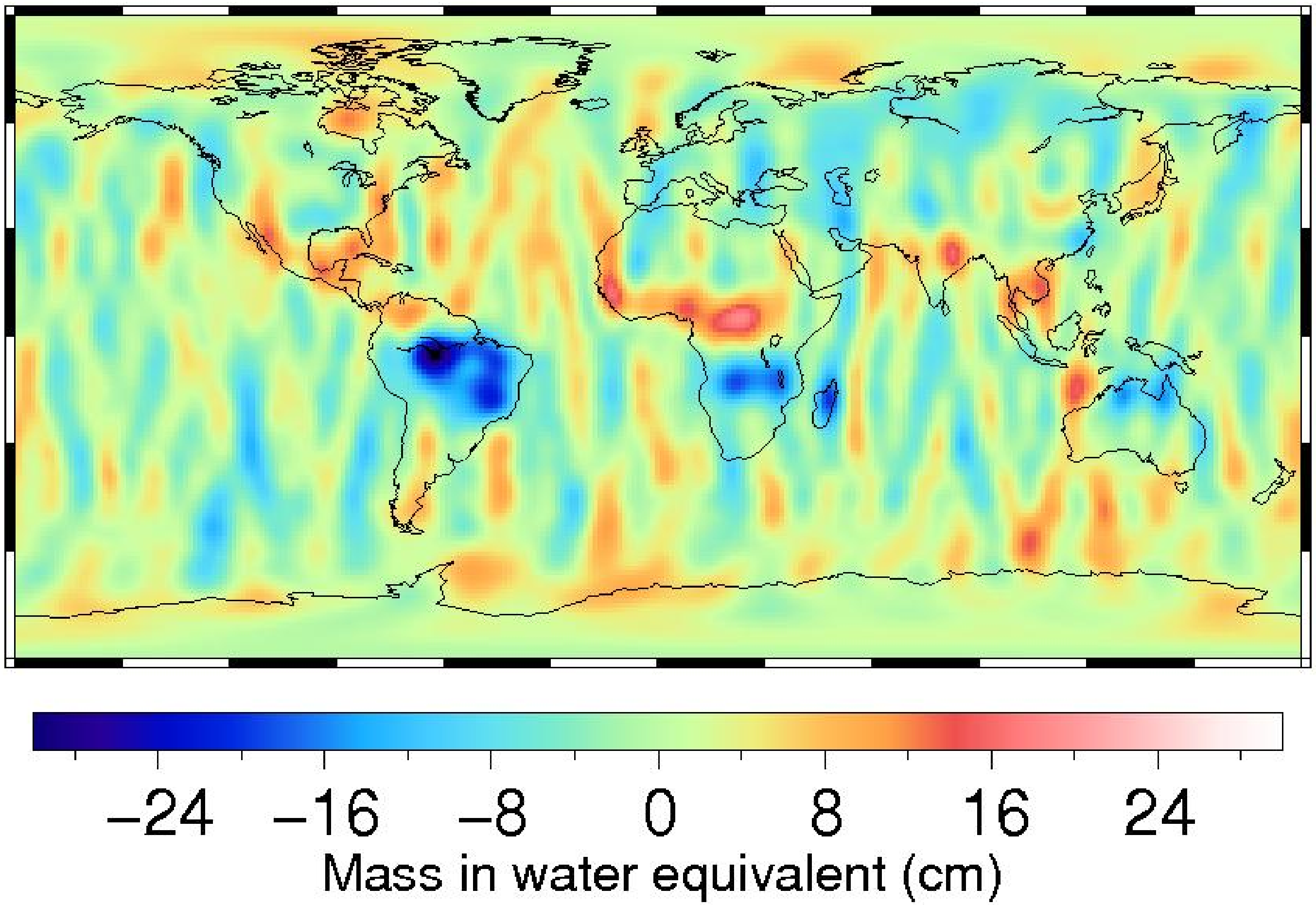

Geoid Variation - December 2003

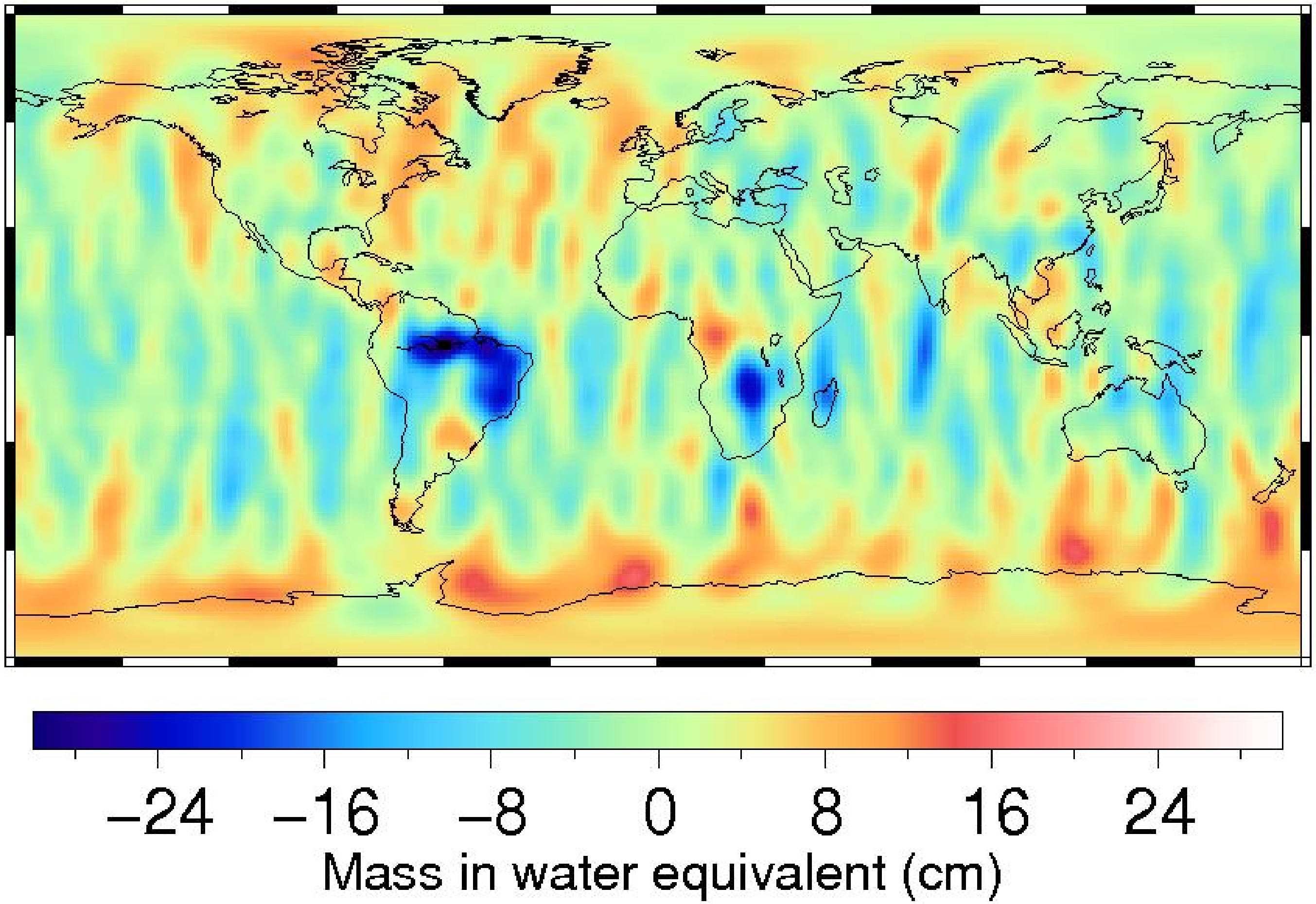

Geoid Variation - February 2004

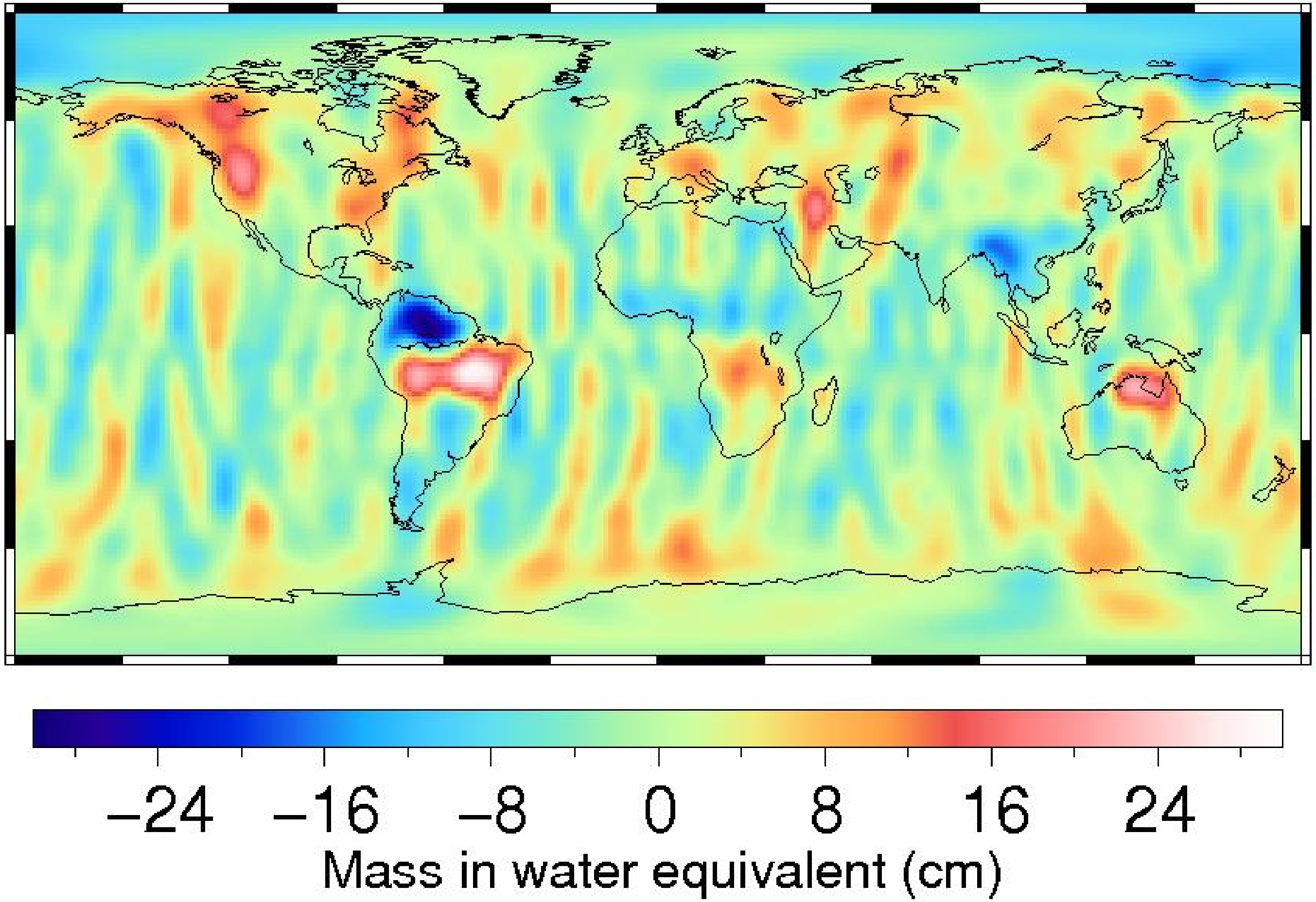

Geoid Variation - March 2004

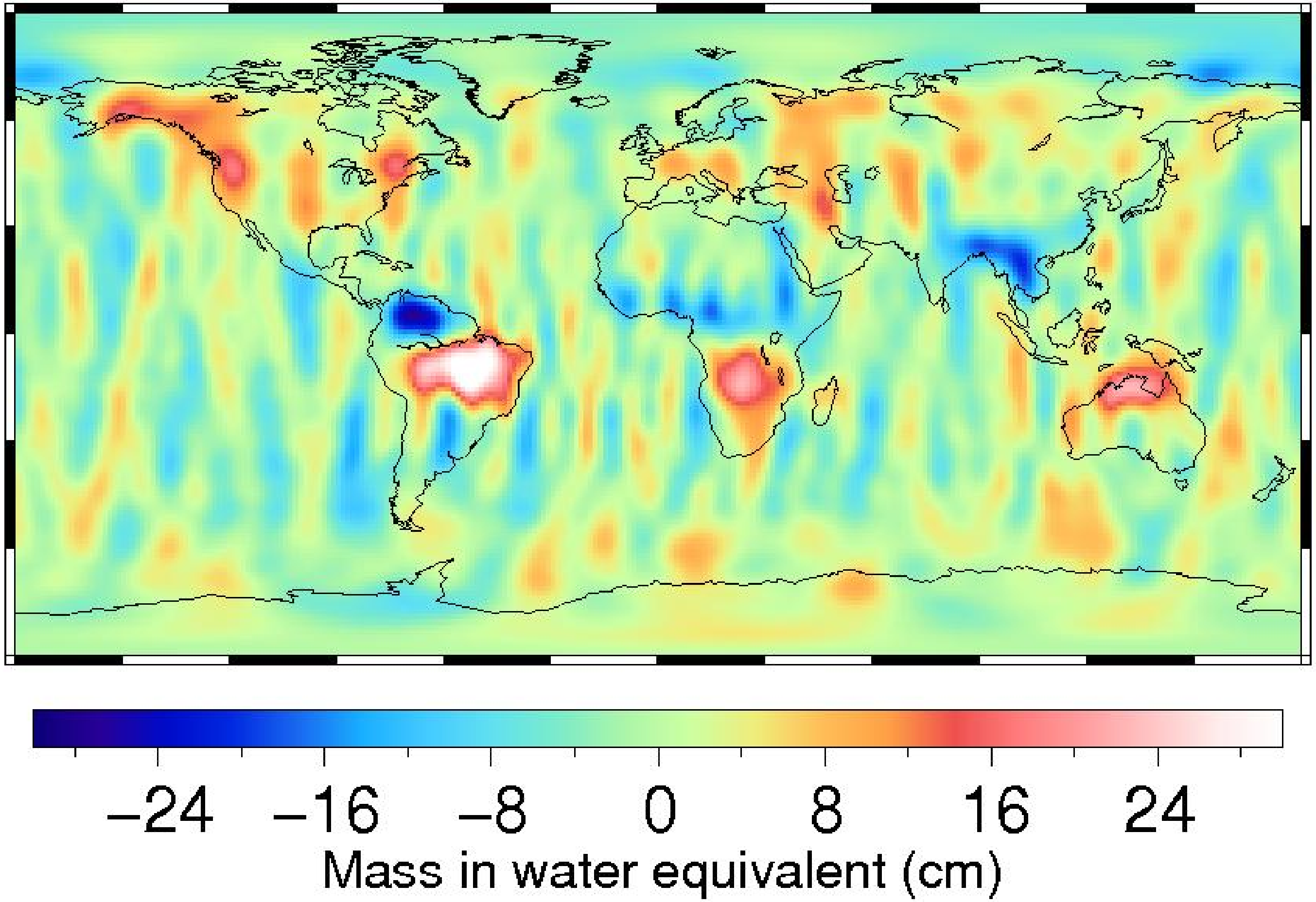

Geoid Variation - April 2004

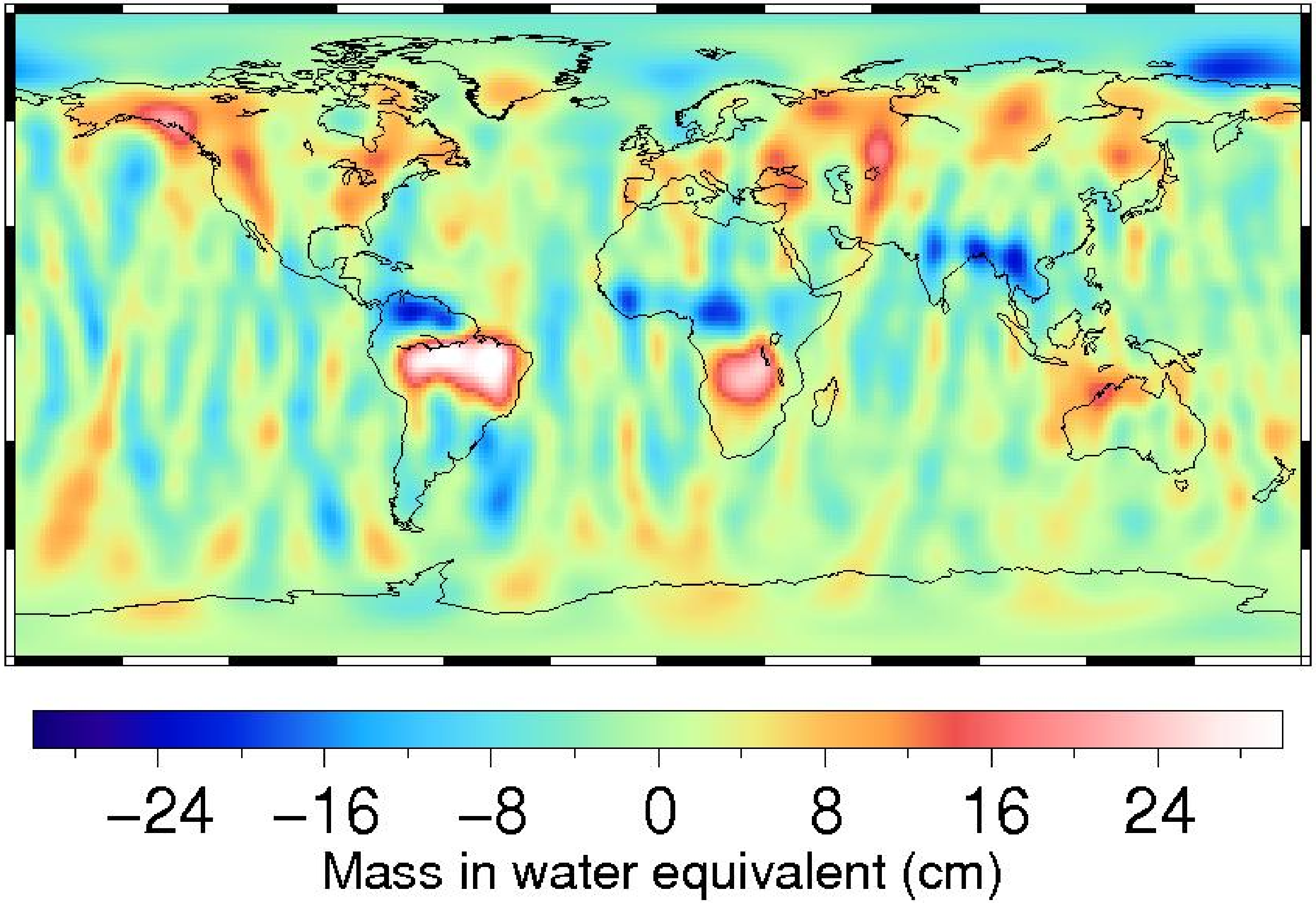

Geoid Variation - May 2004

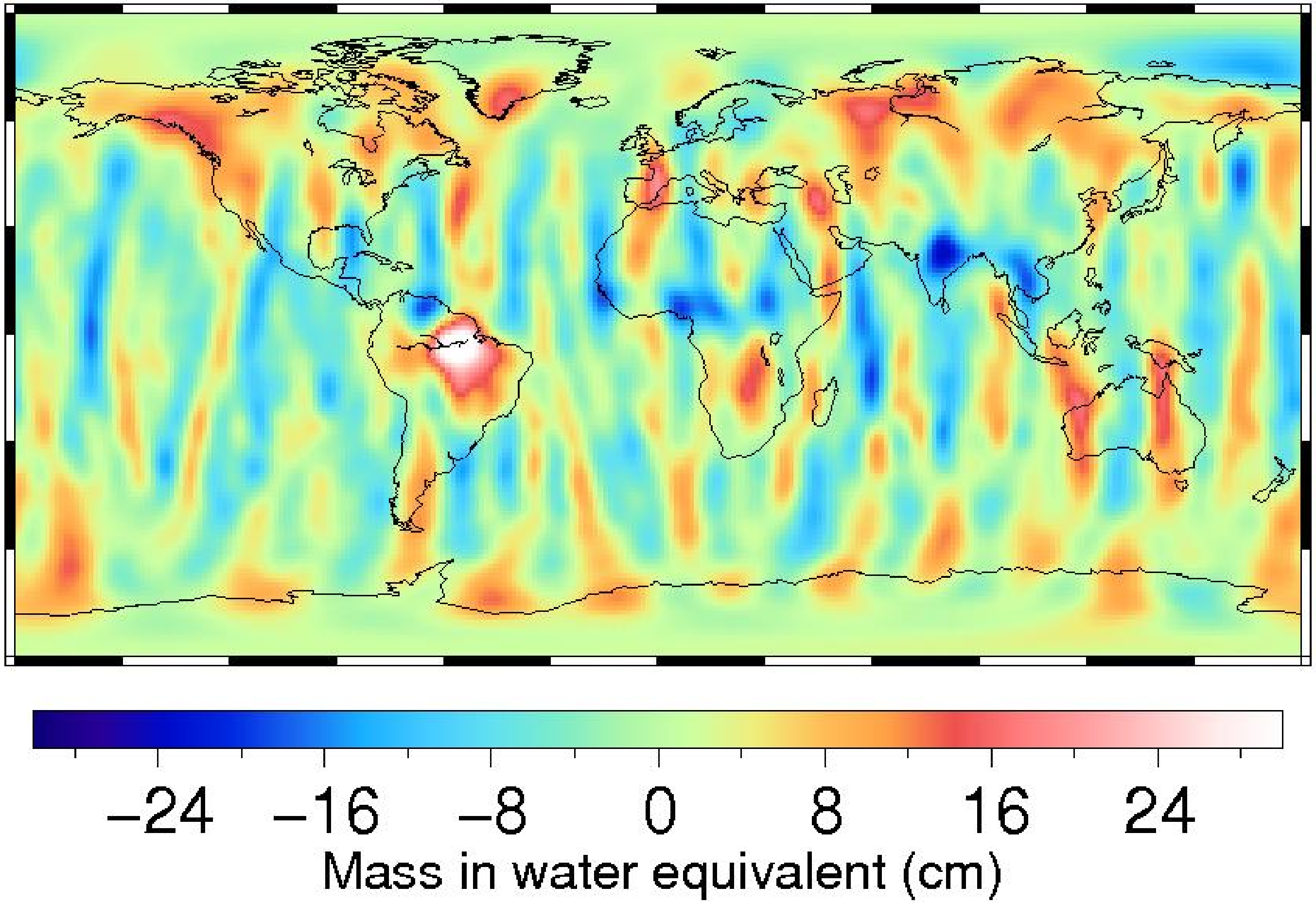

Geoid Variation - June 2004

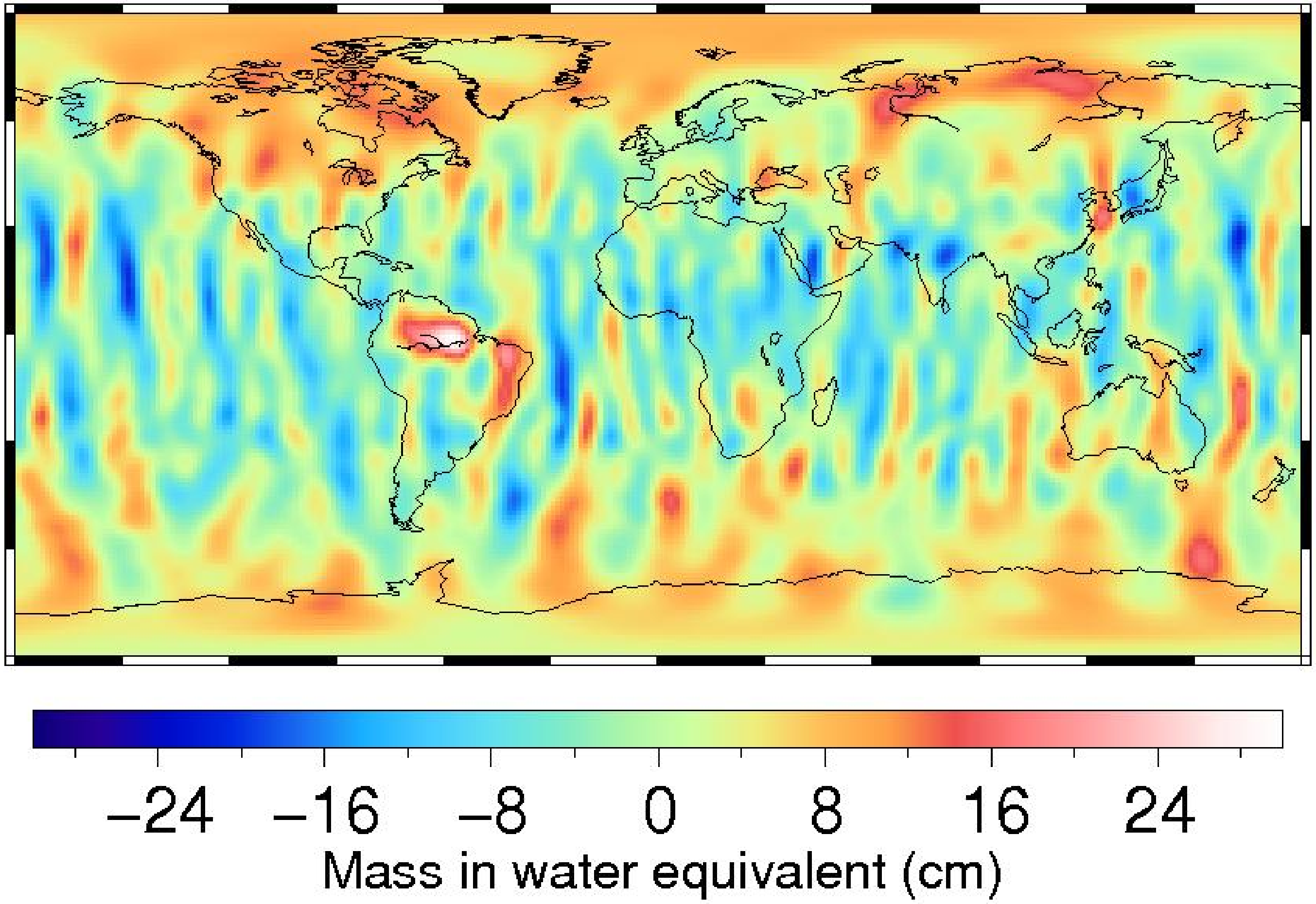

Geoid Variation - July 2004

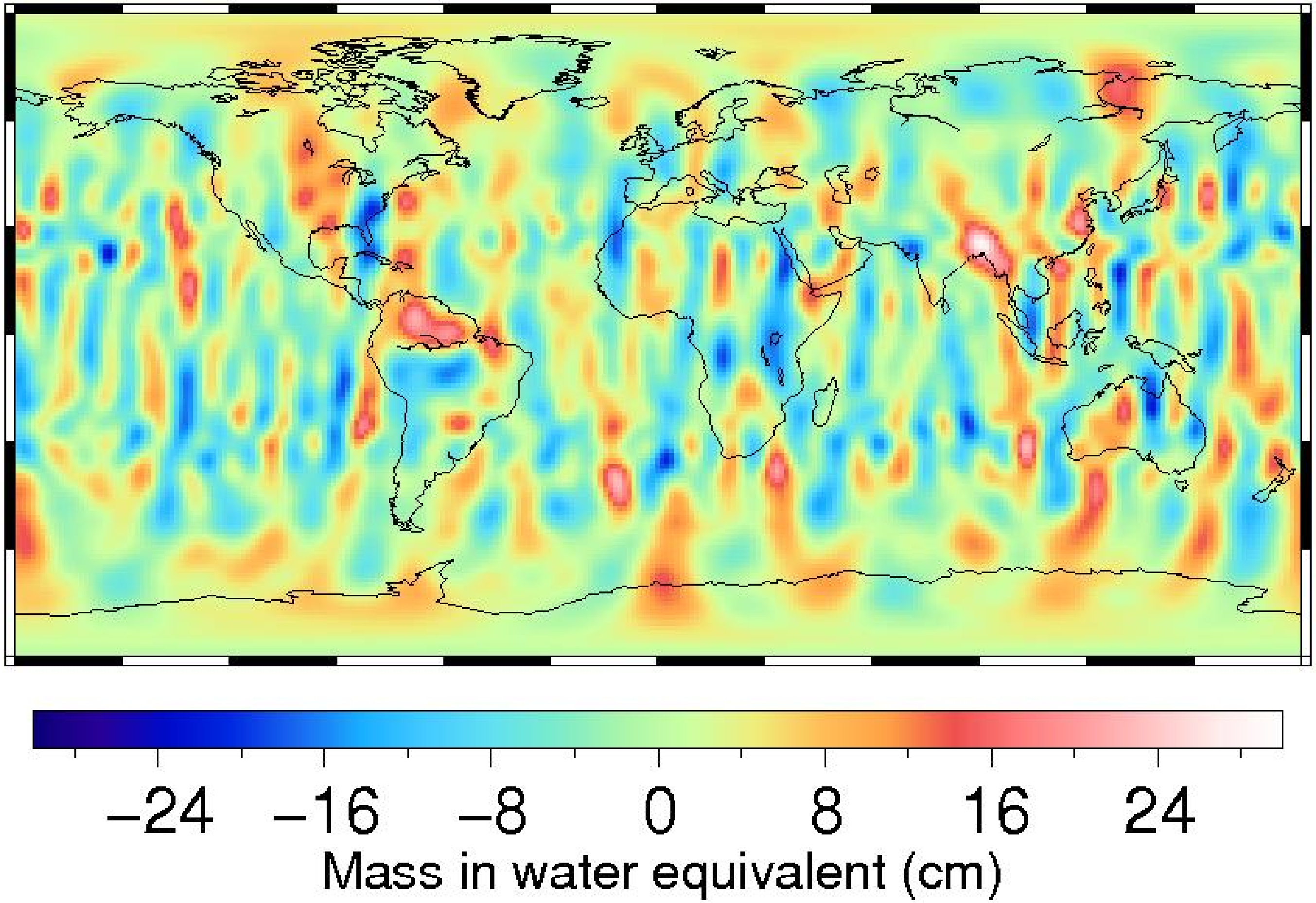

Geoid Variation - August 2004

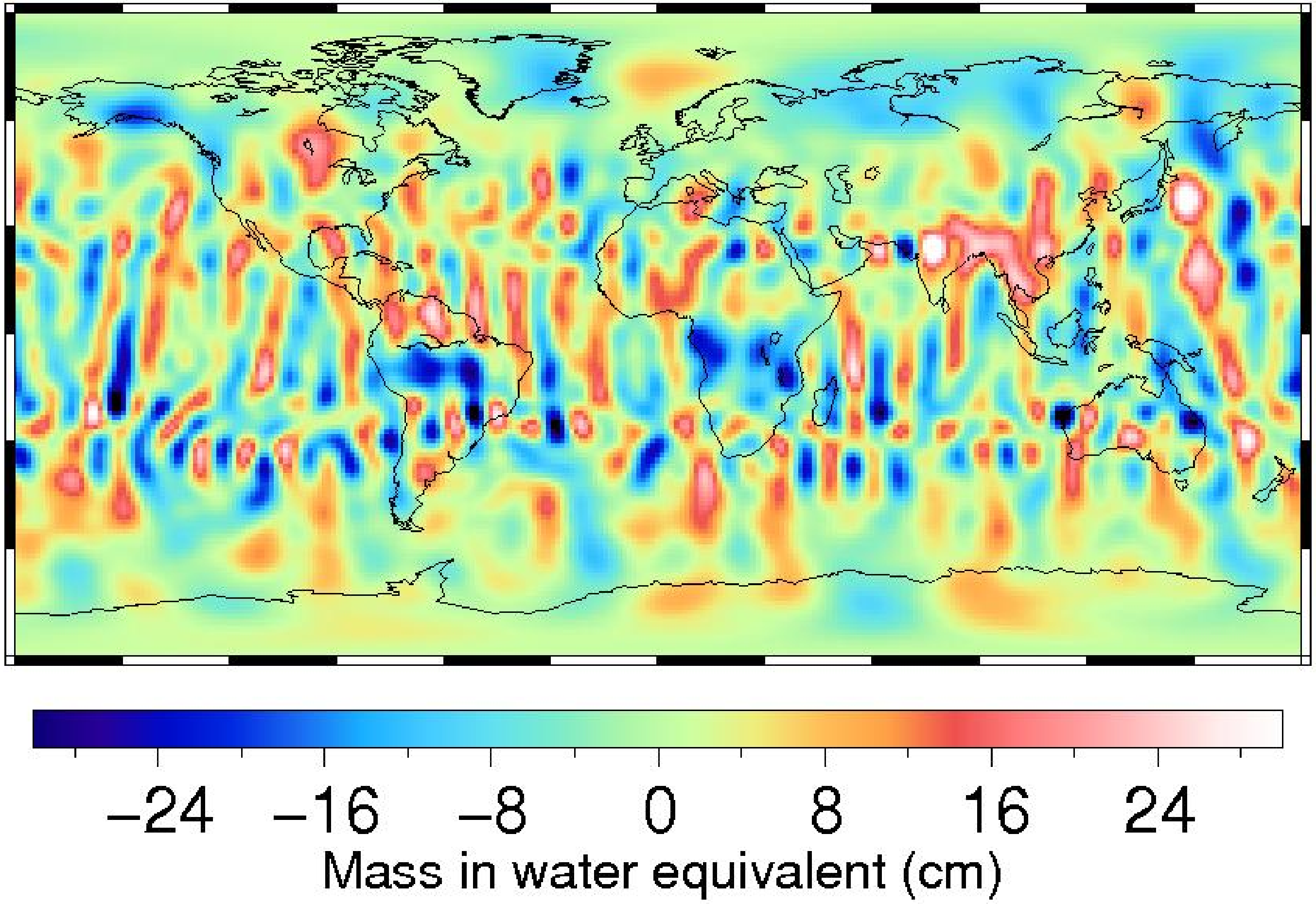

Geoid Variation - September 2004

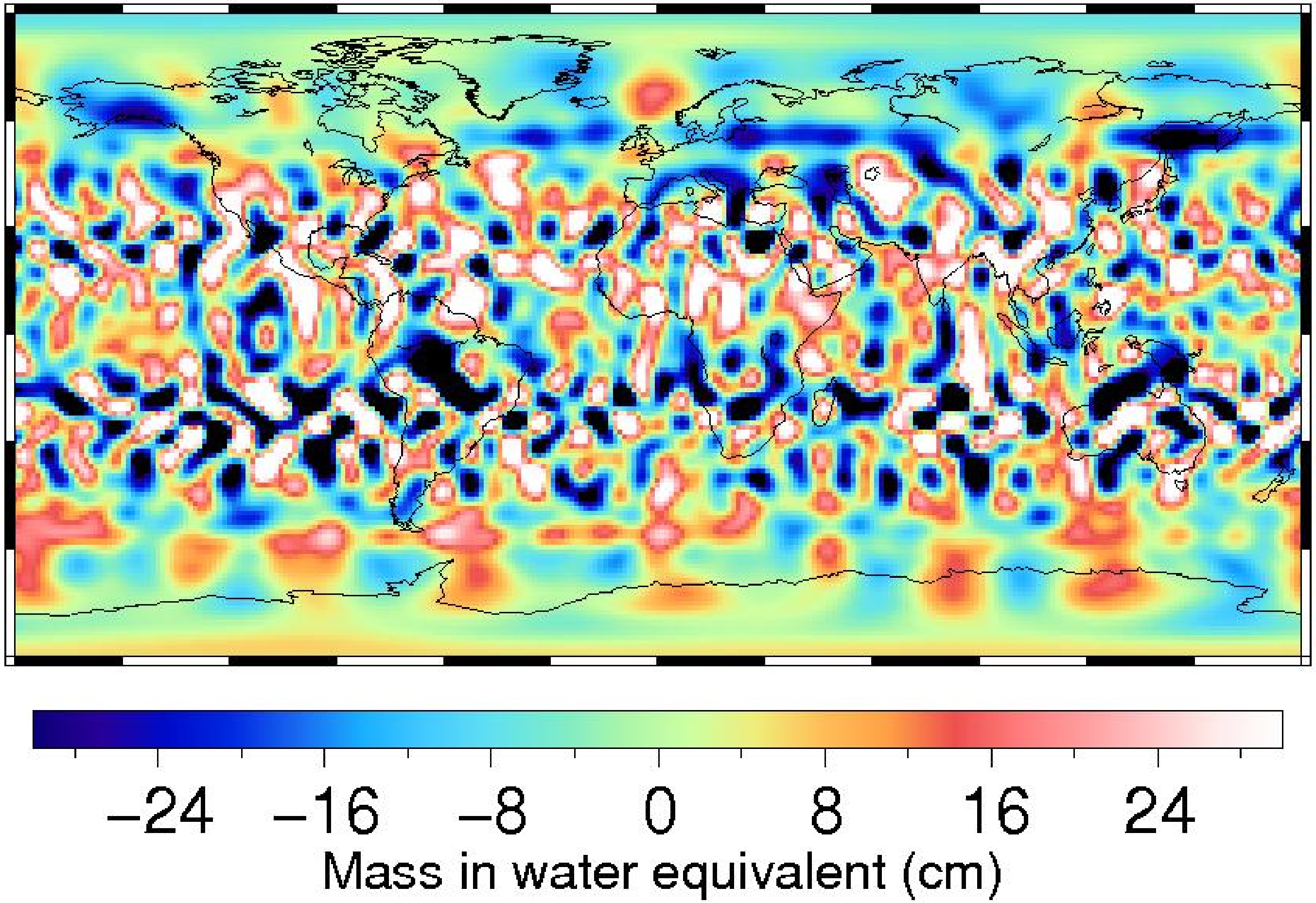

Geoid Variation - October 2004

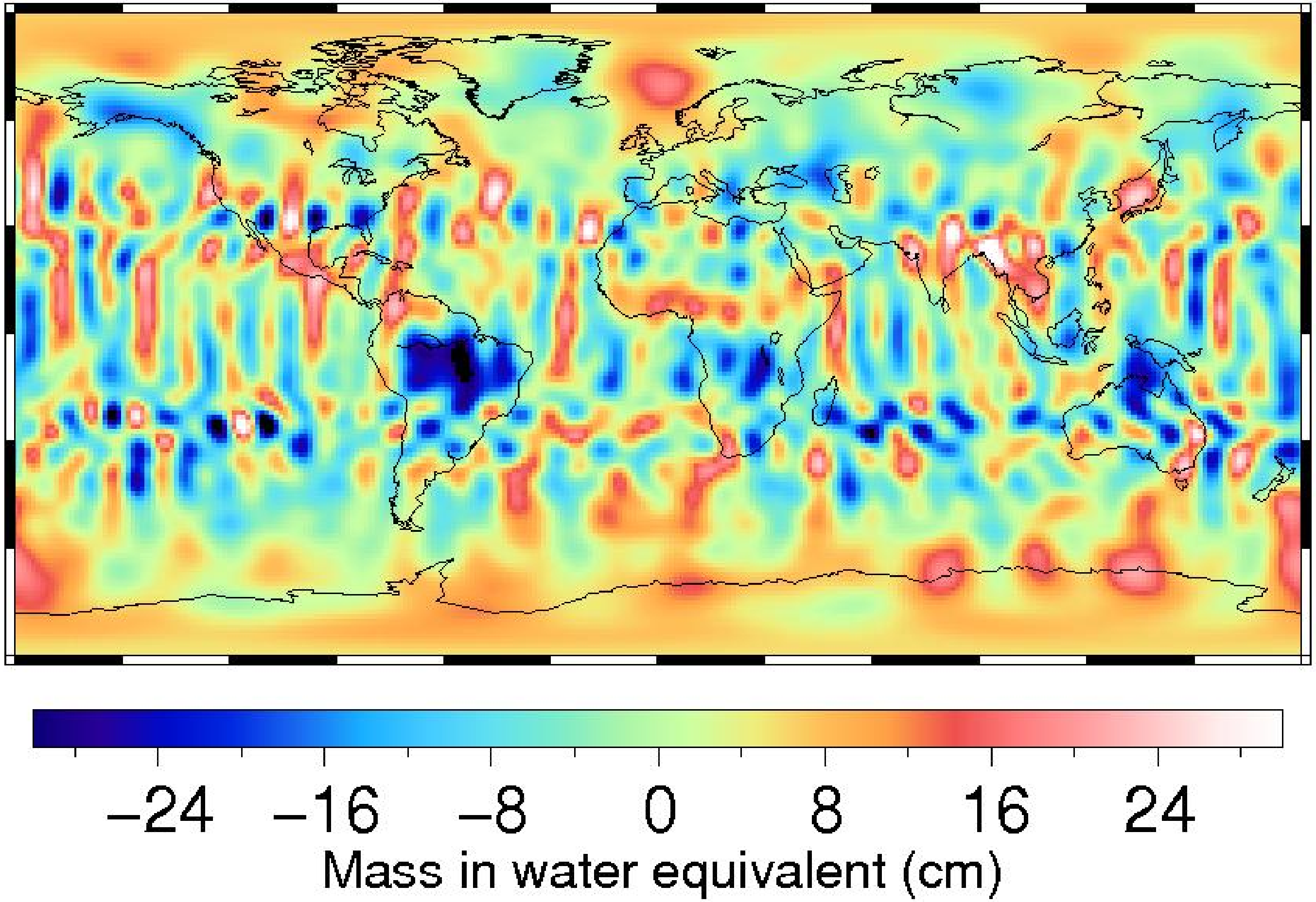

Geoid Variation - November 2004

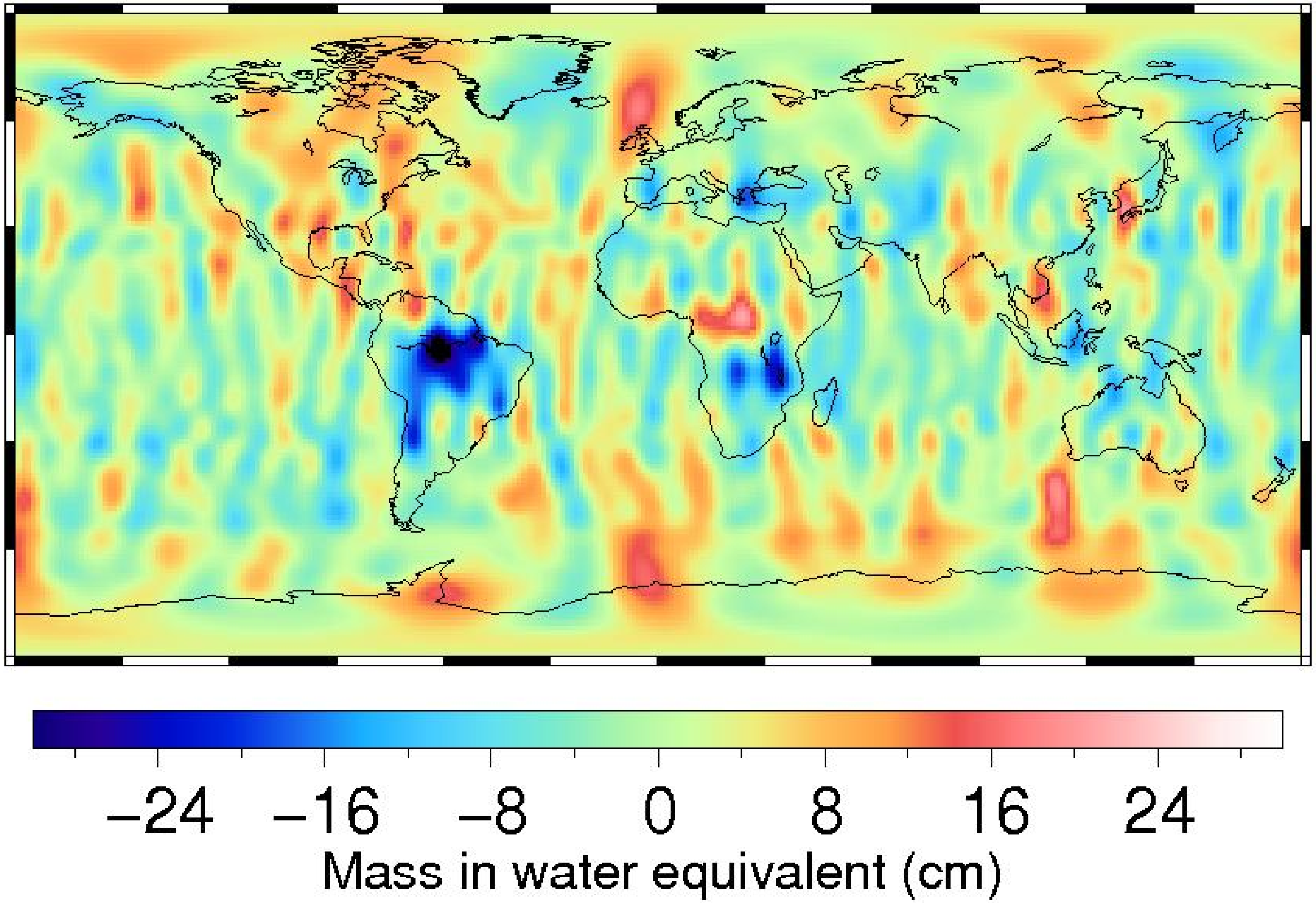

Geoid Variation - December 2004

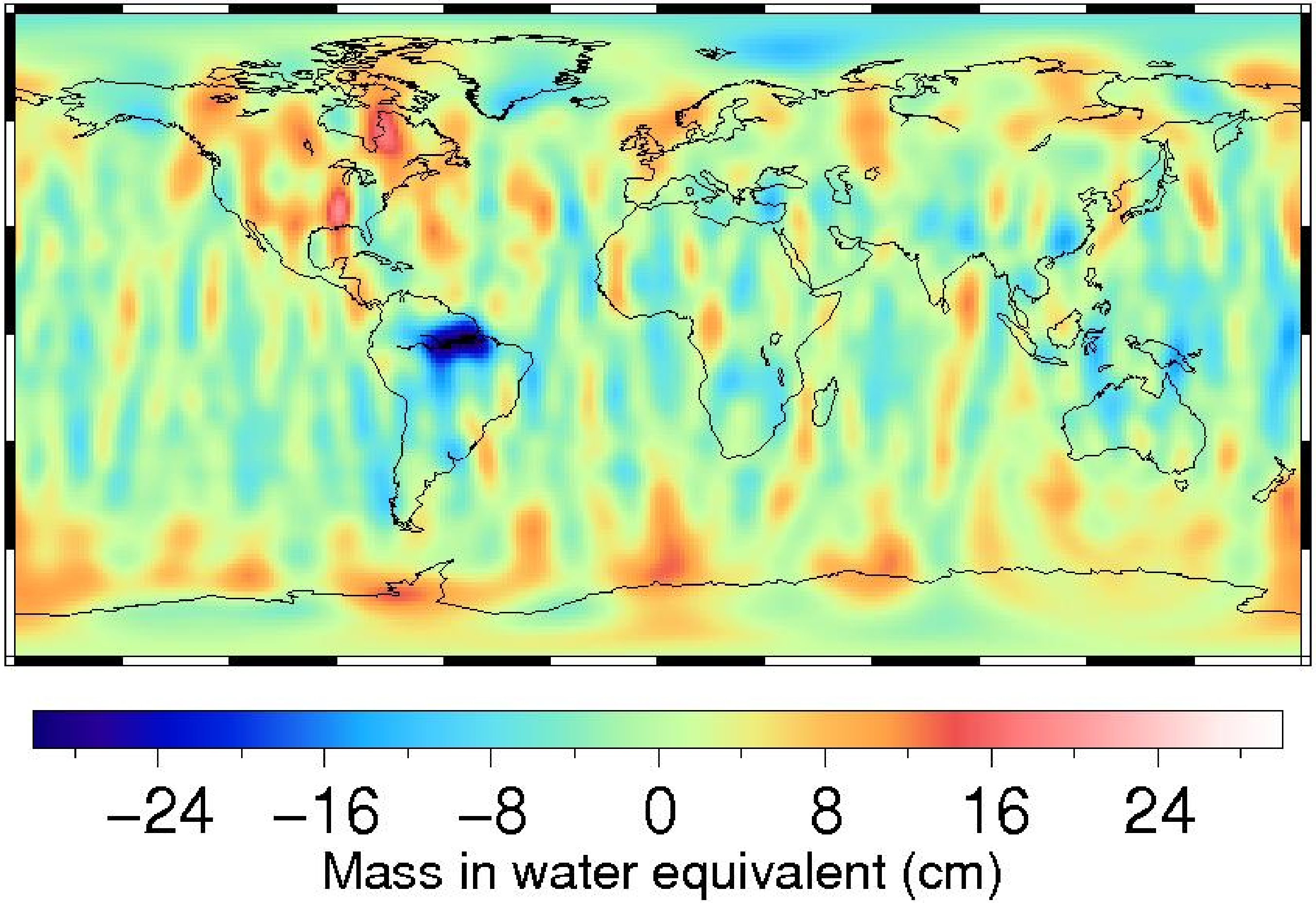

Geoid Variation - January 2005

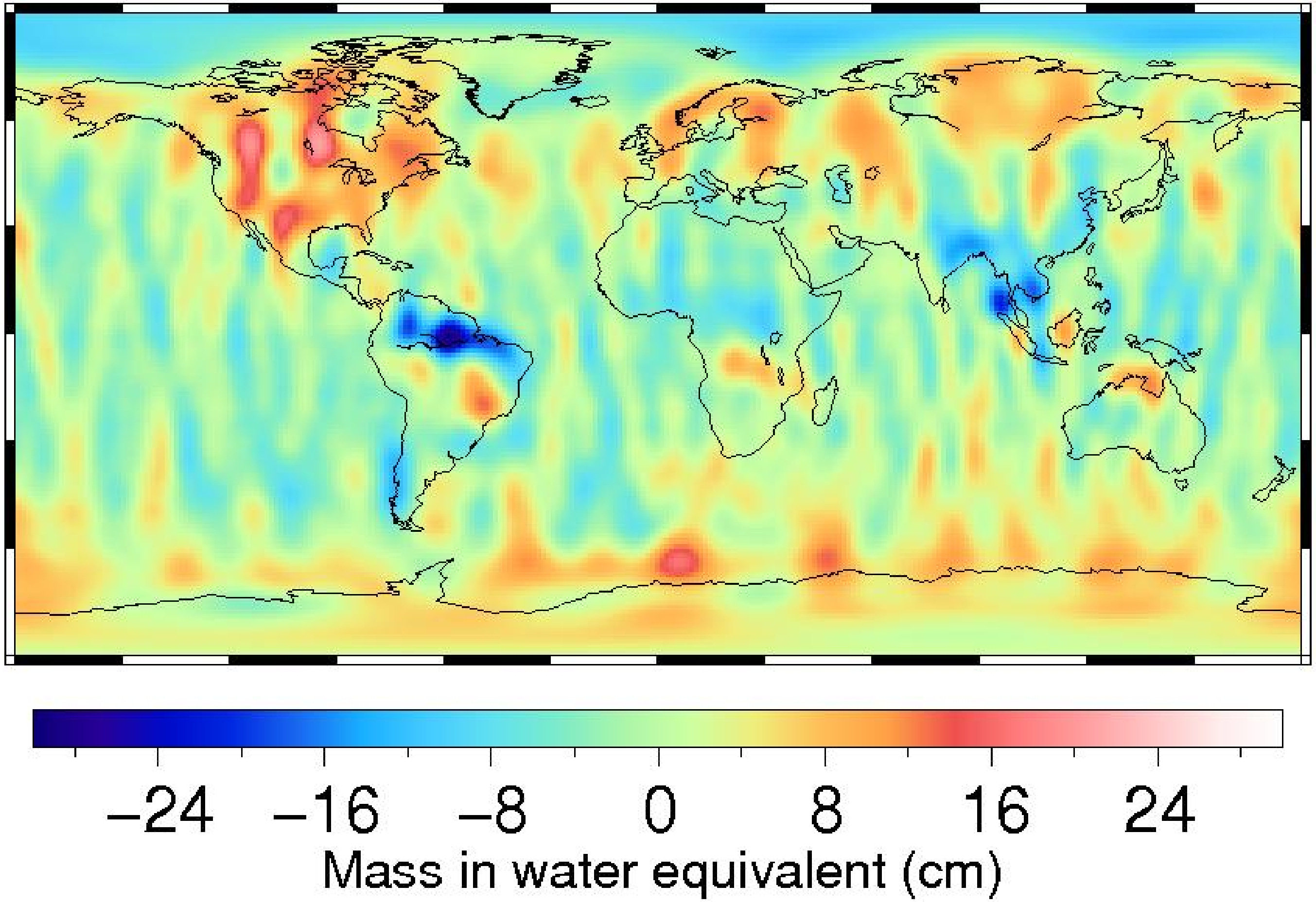

Geoid Variation - February 2005

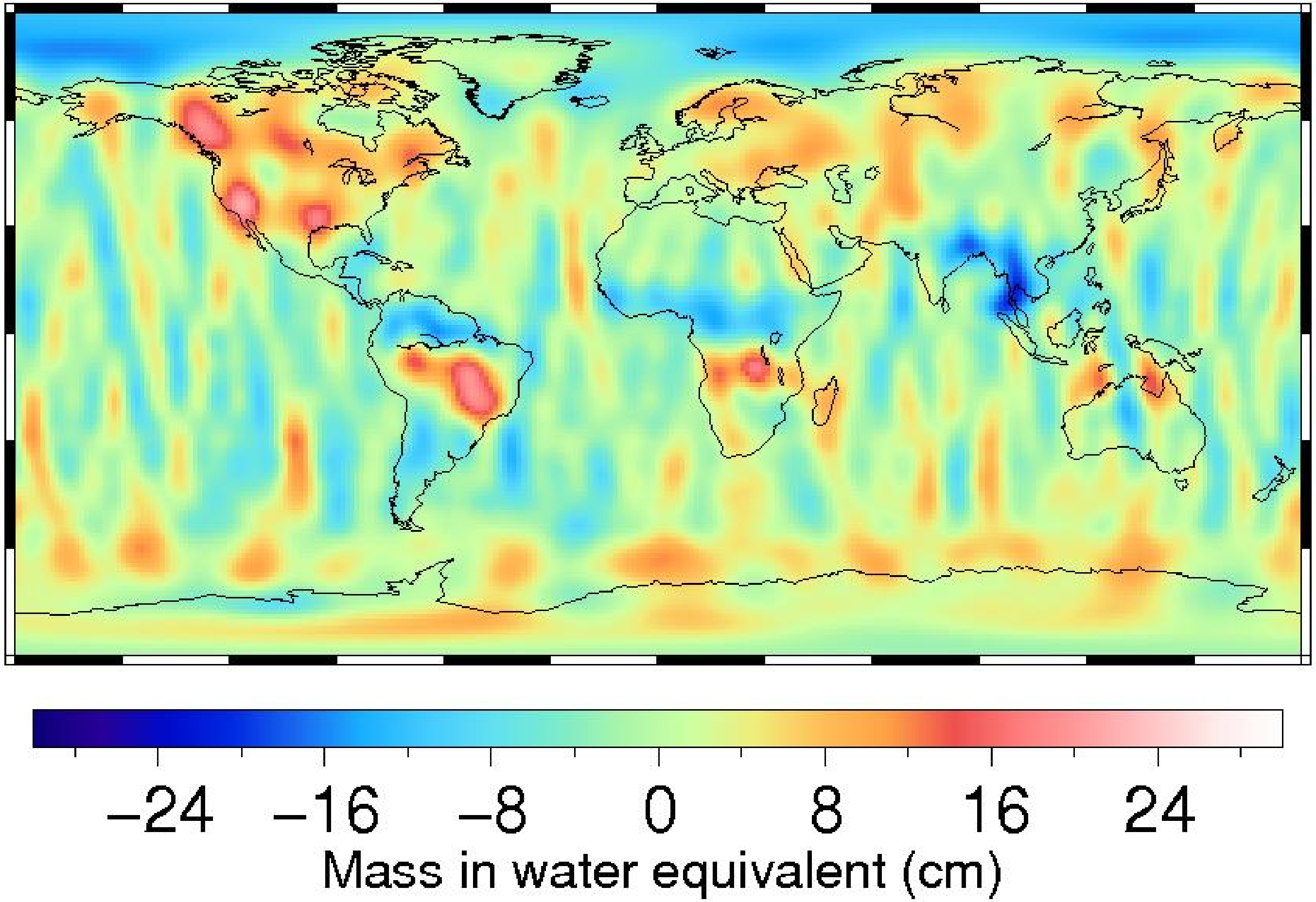

Geoid Variation - March 2005

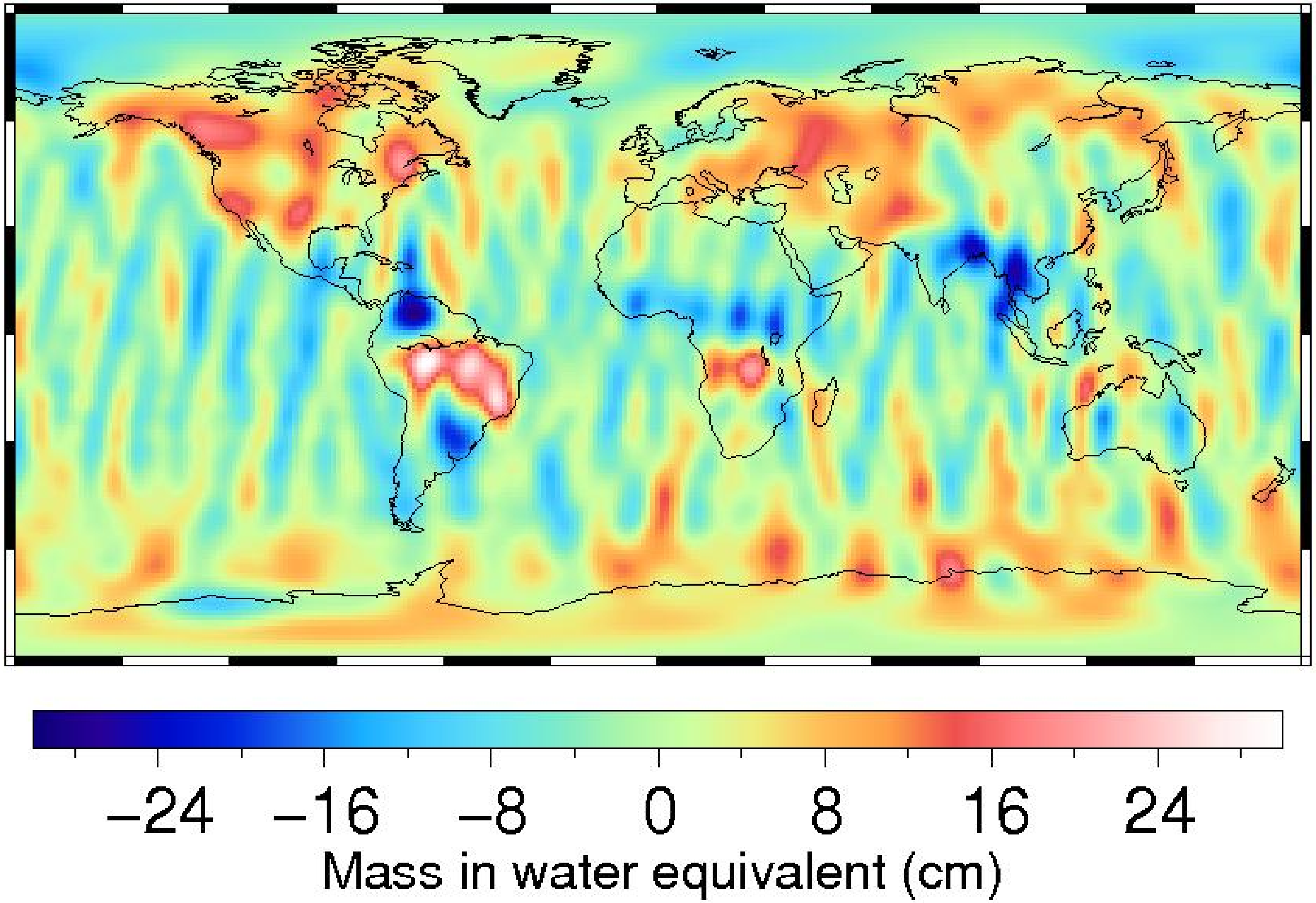

Geoid Variation - April 2005

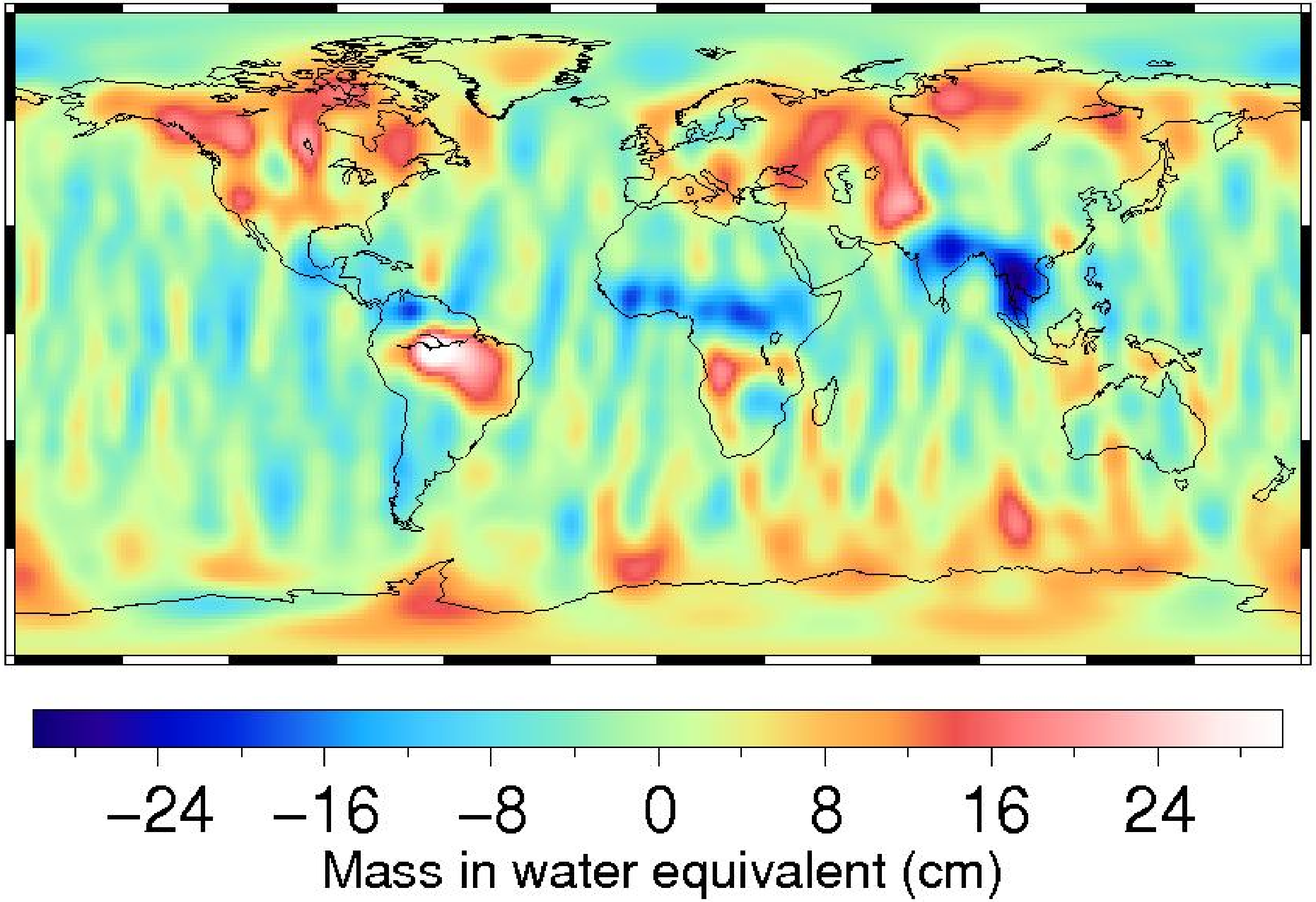

Geoid Variation - May 2005

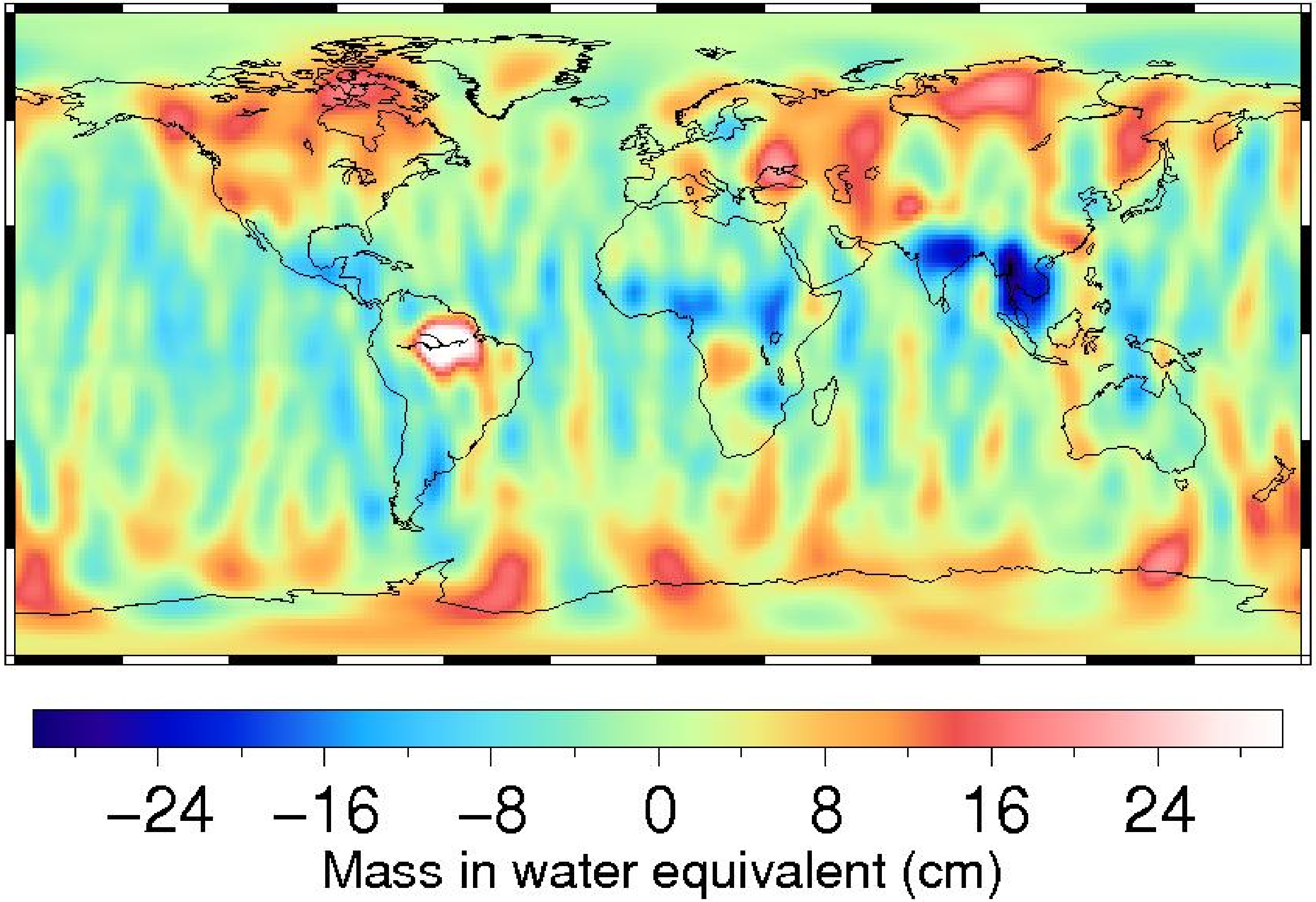

Geoid Variation - June 2005

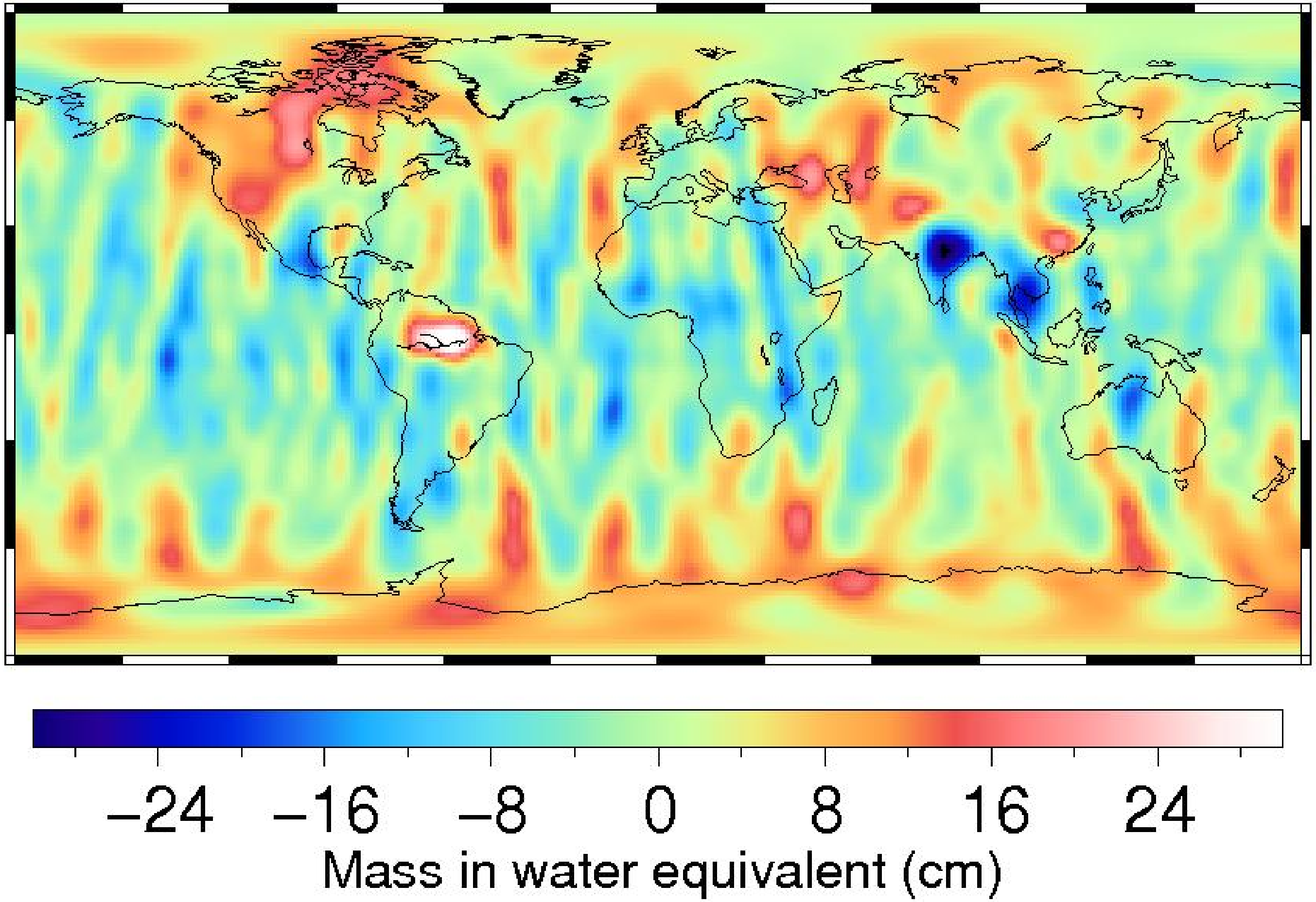

Geoid Variation - July 2005

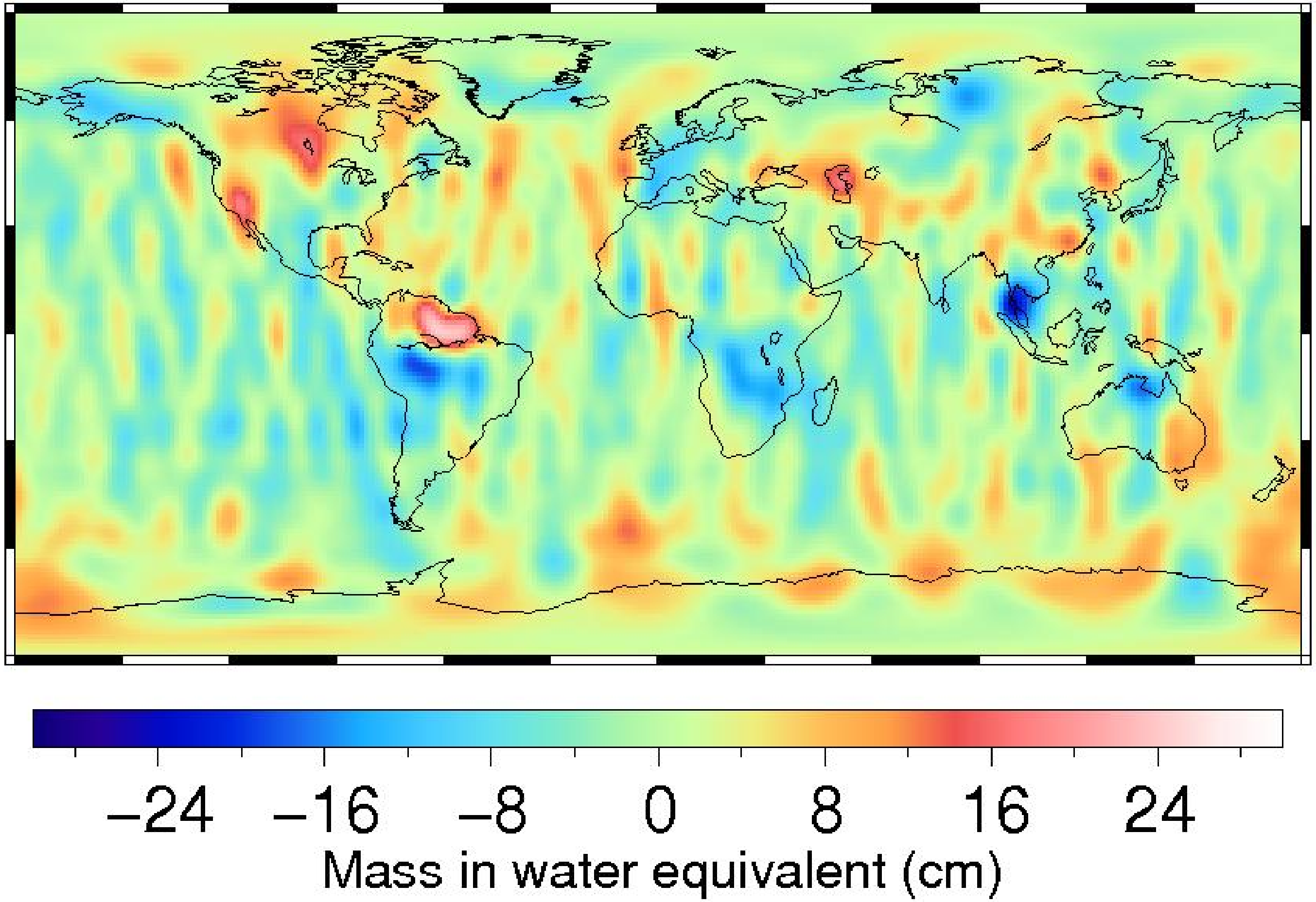

Geoid Variation - August 2005

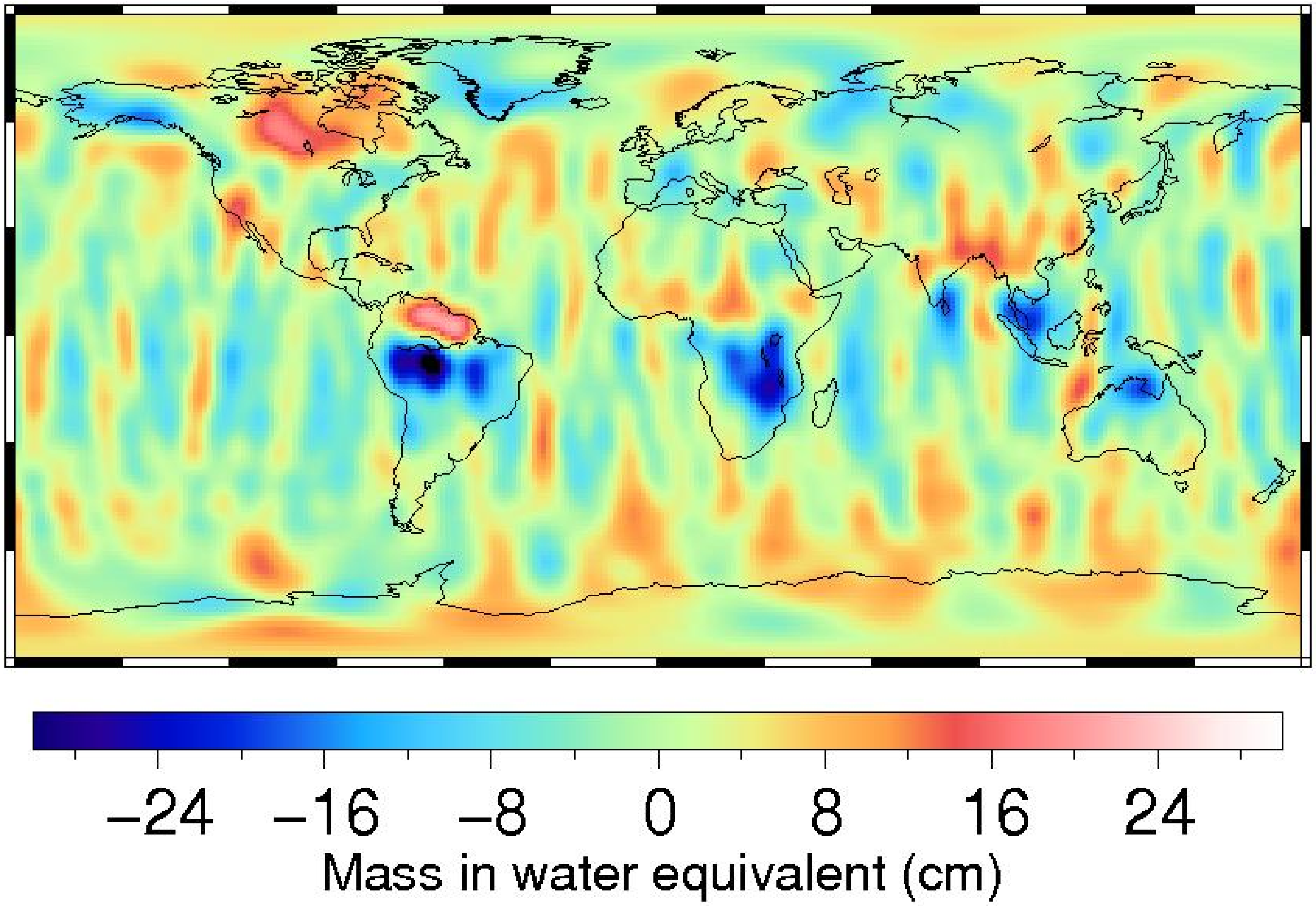

Geoid Variation - September 2005

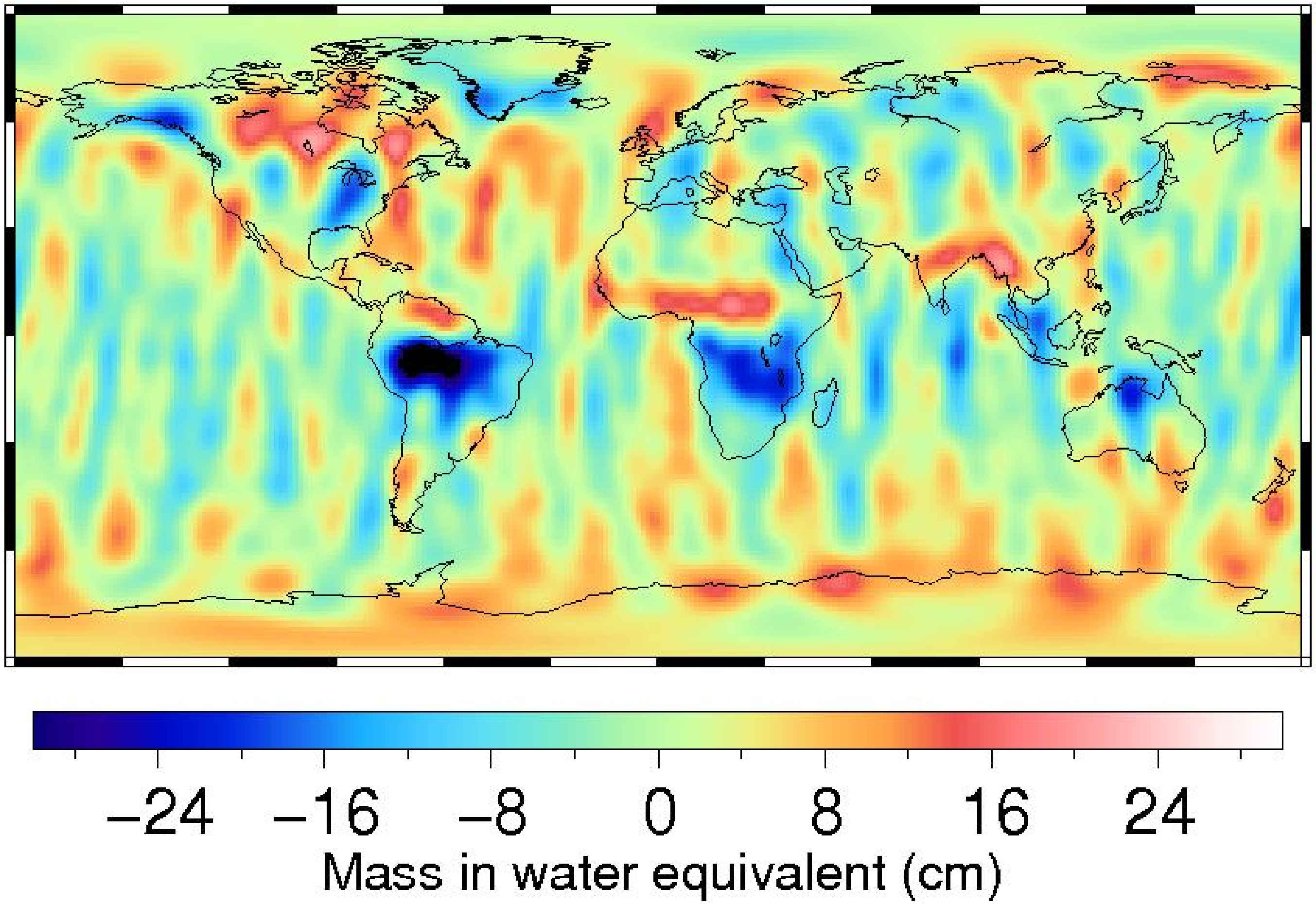

Geoid Variation - October 2005

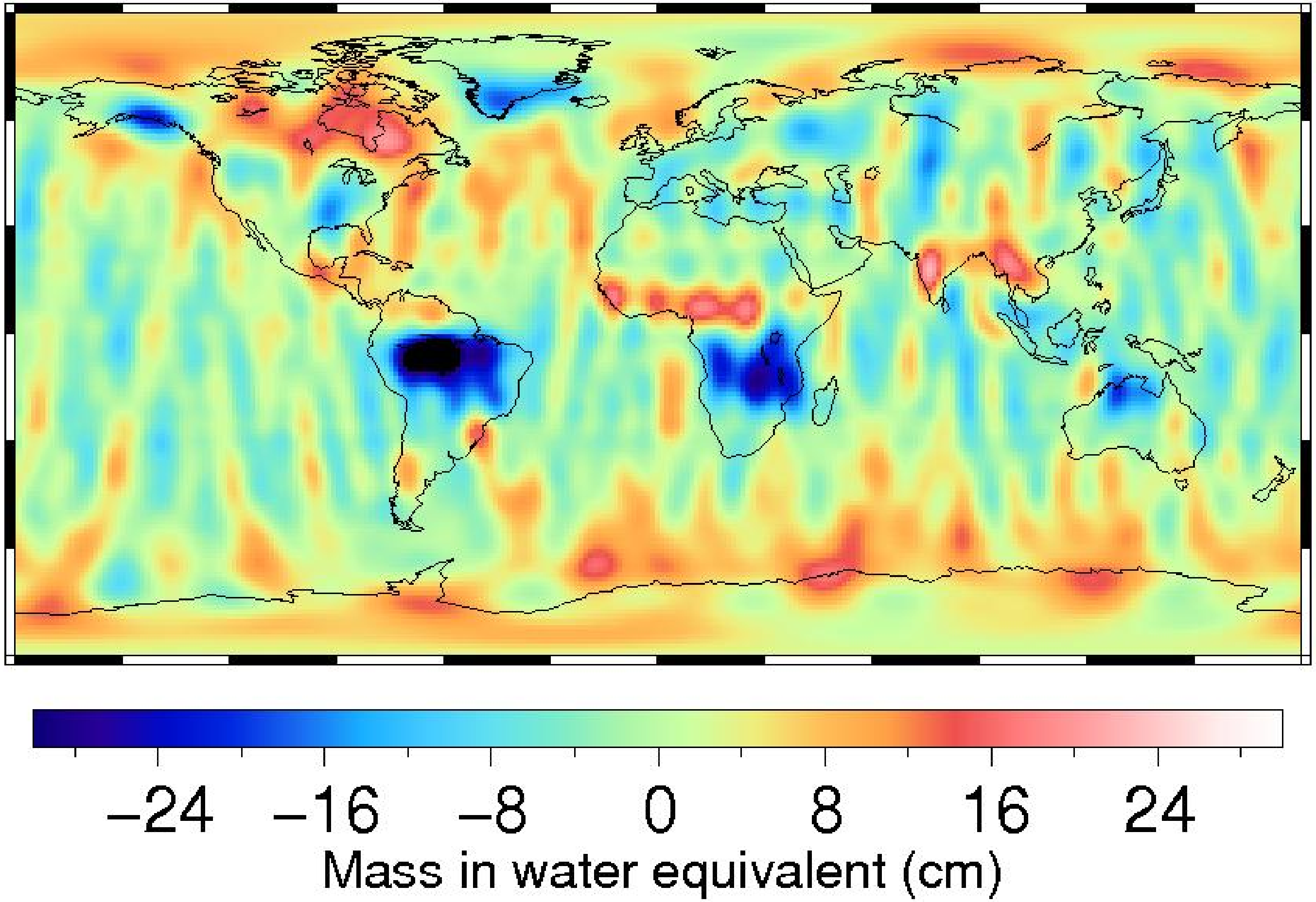

Geoid Variation - November 2005

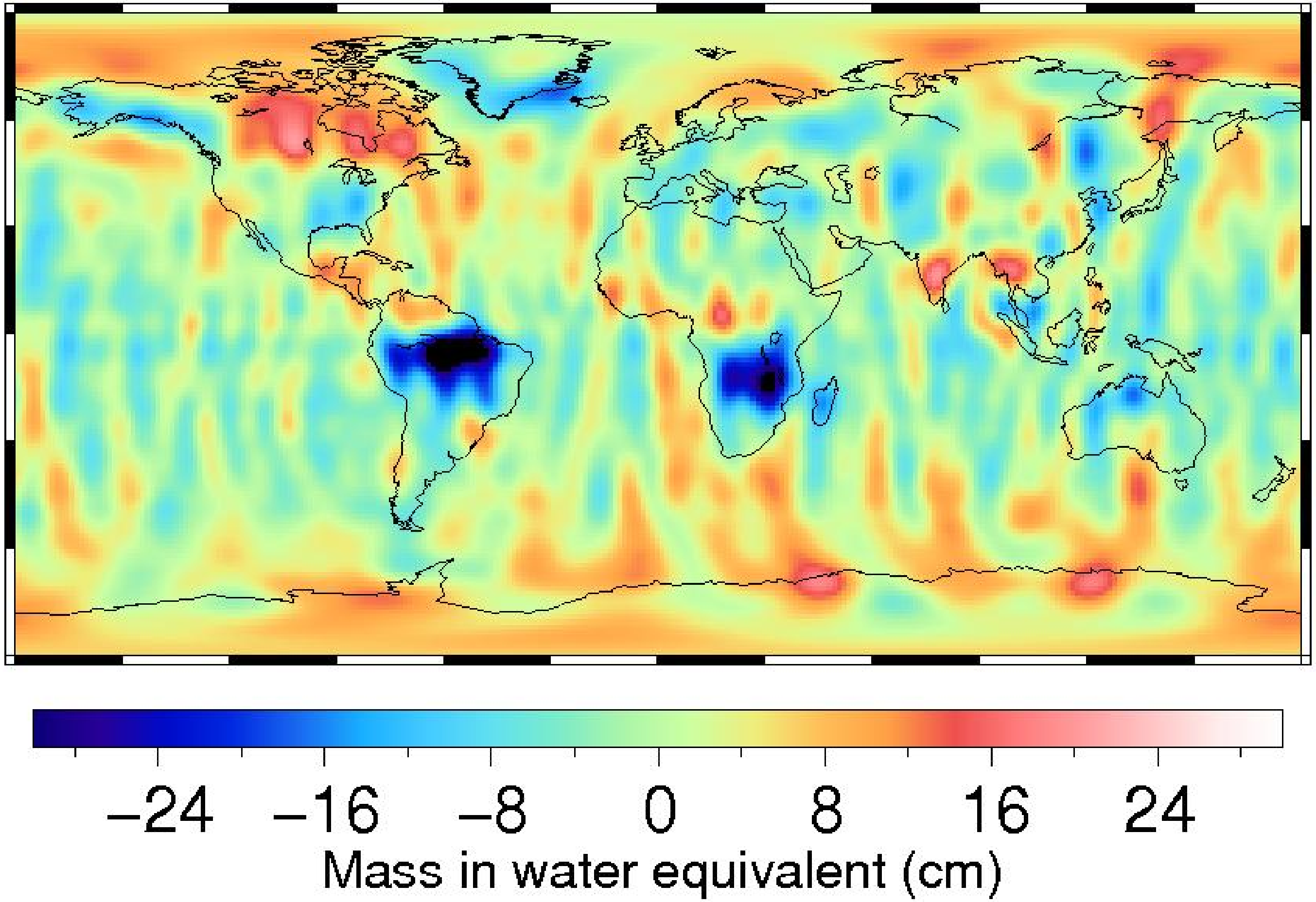

Geoid Variation - December 2005

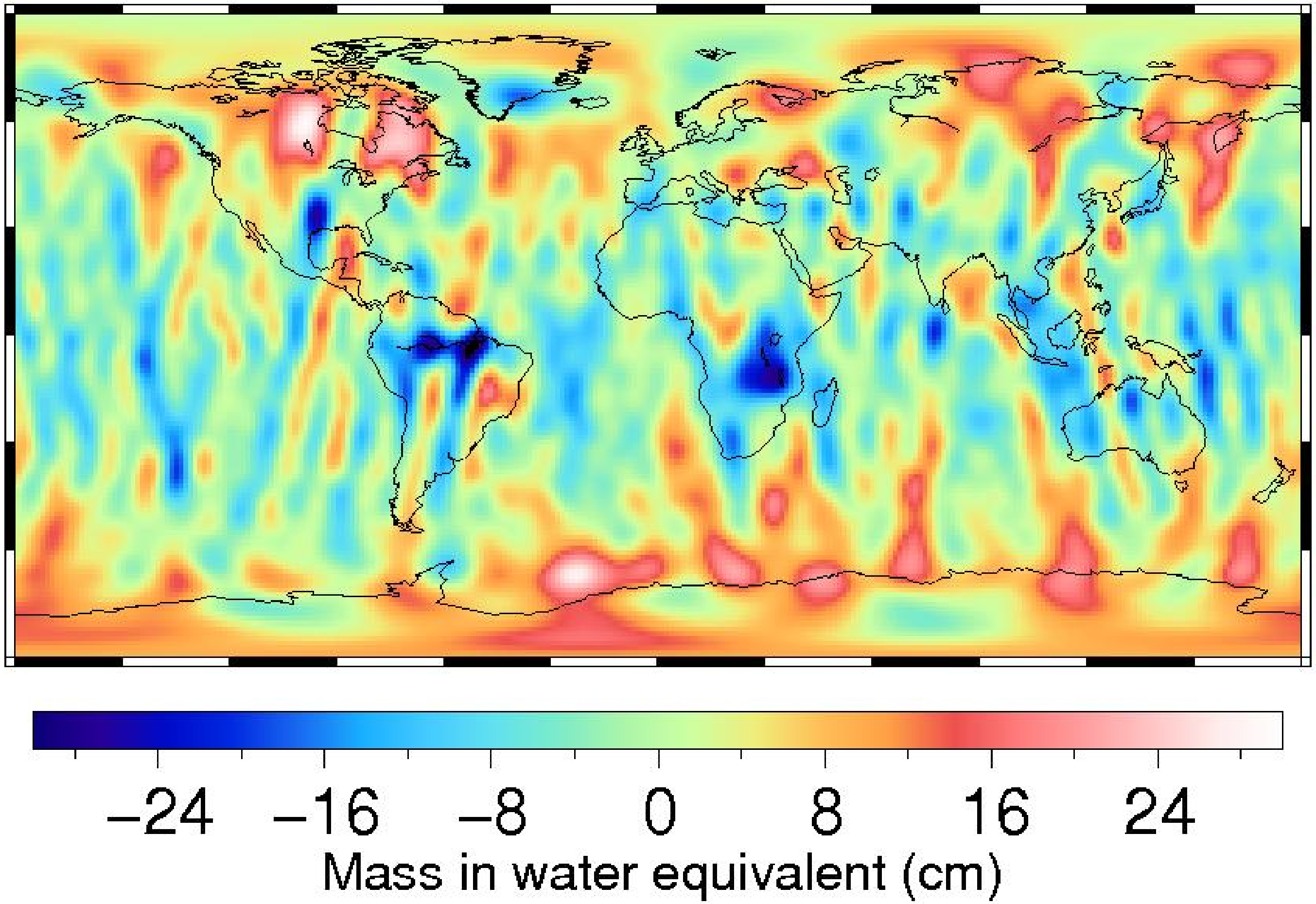

Geoid Variation - January 2006

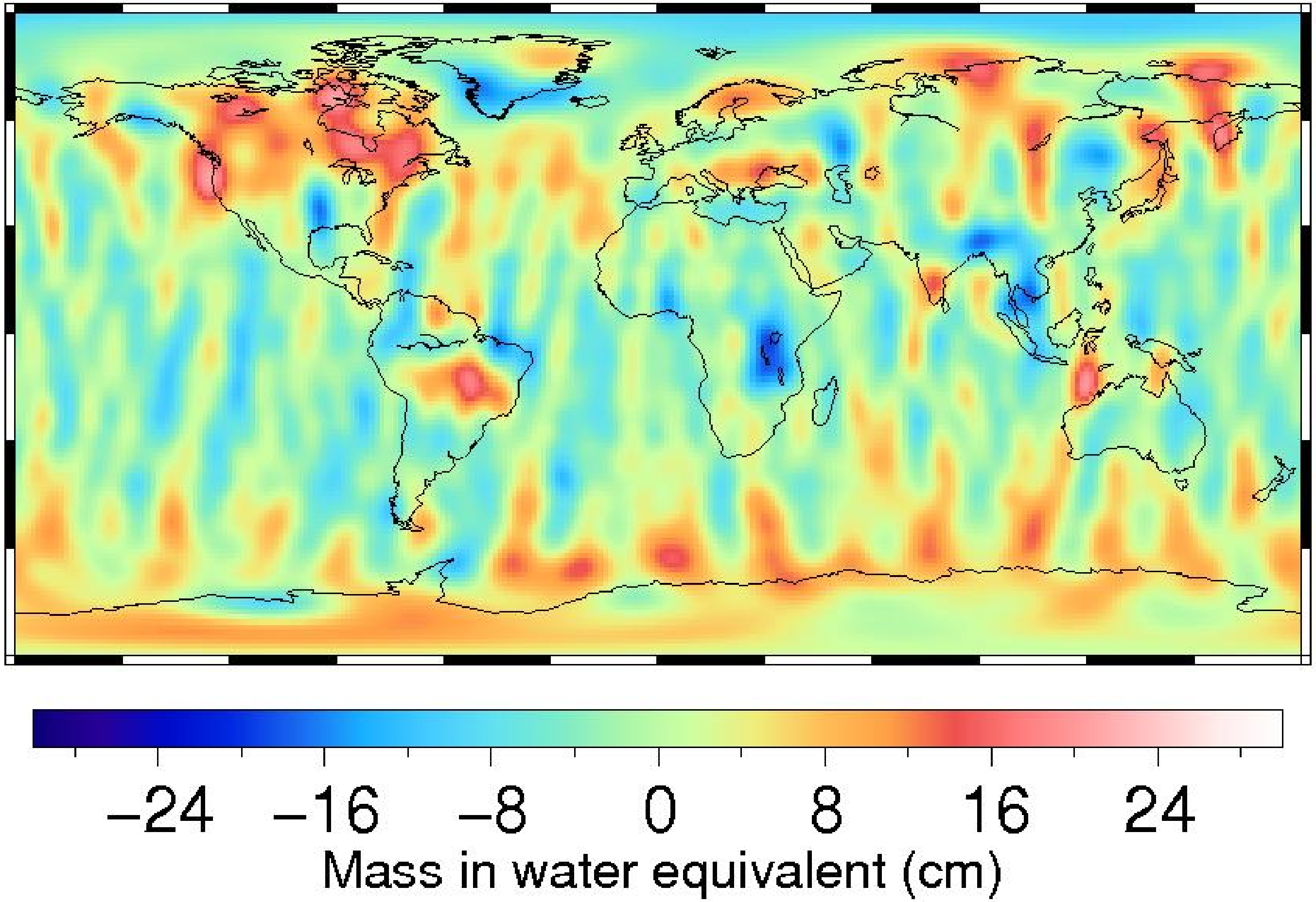

Geoid Variation - February 2006

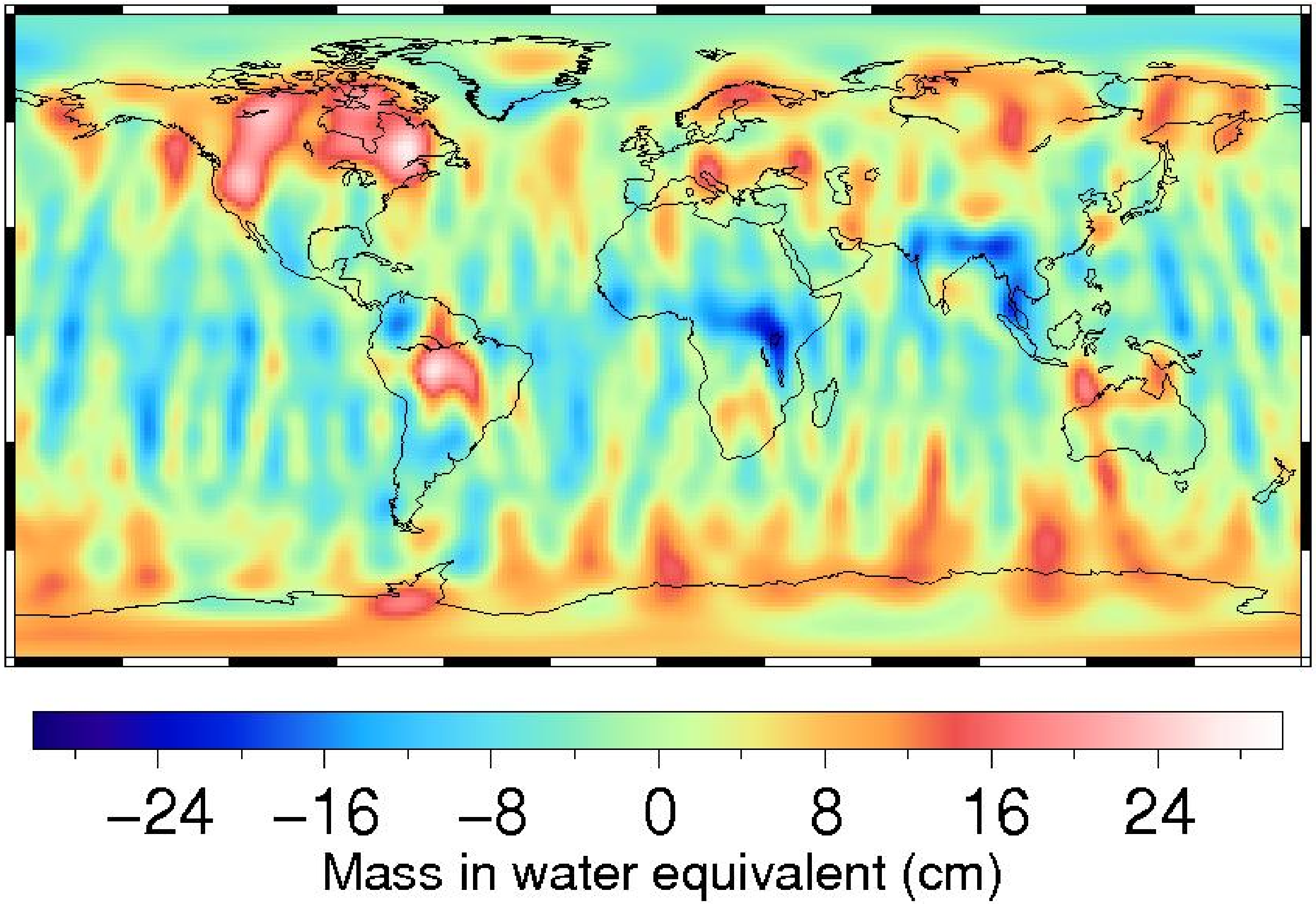

Geoid Variation - March 2006

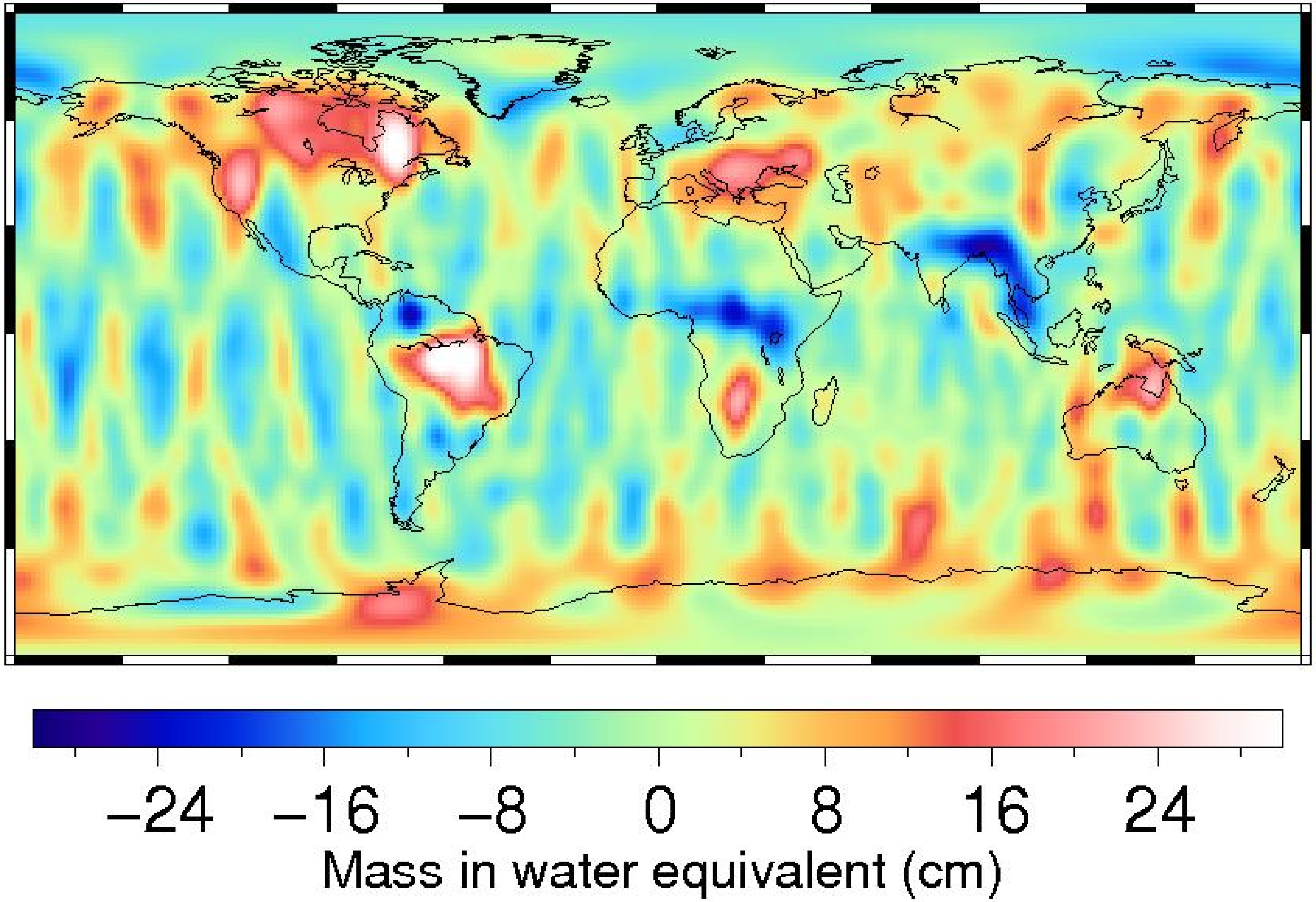

Geoid Variation - April 2006

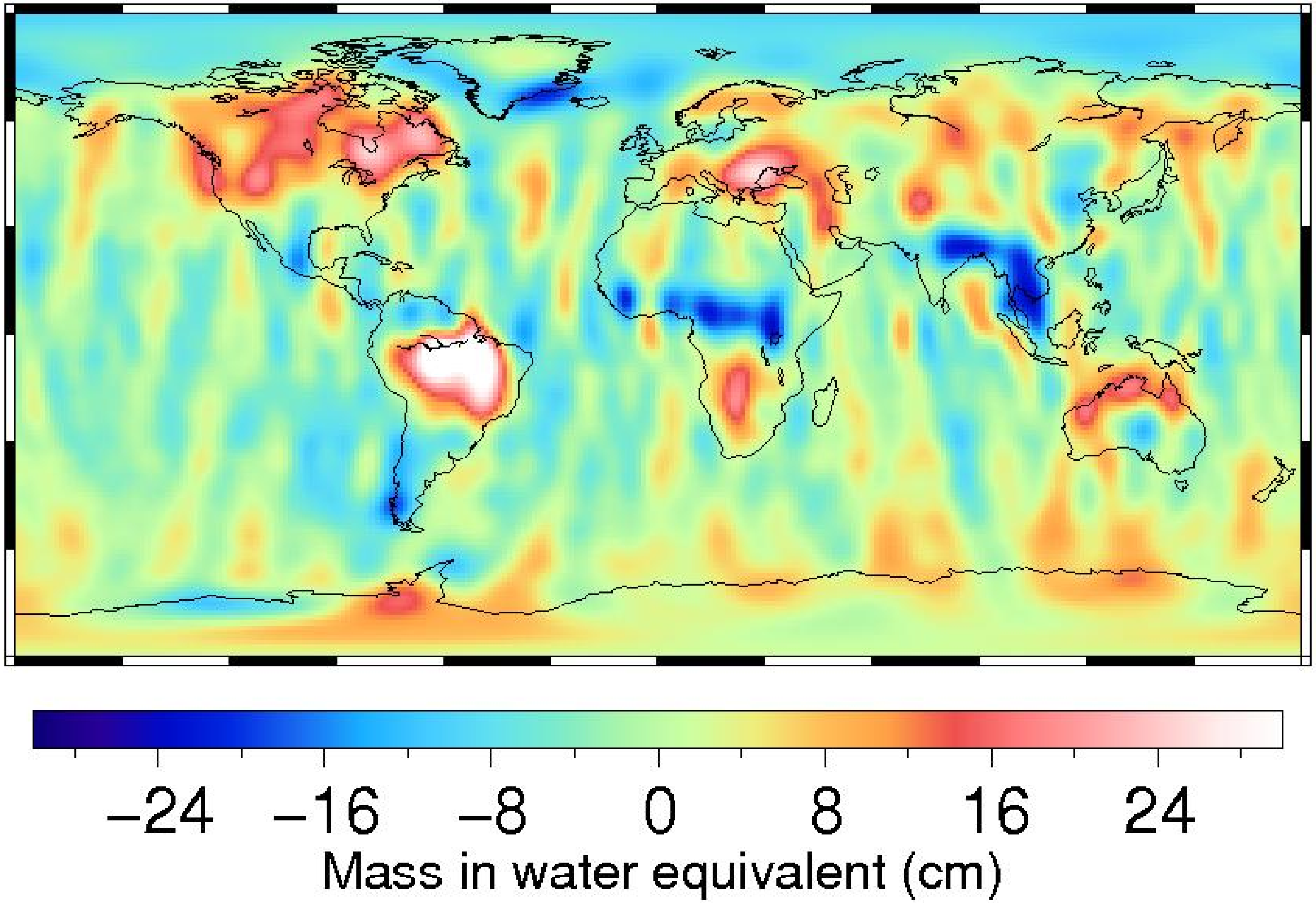

Geoid Variation - May 2006

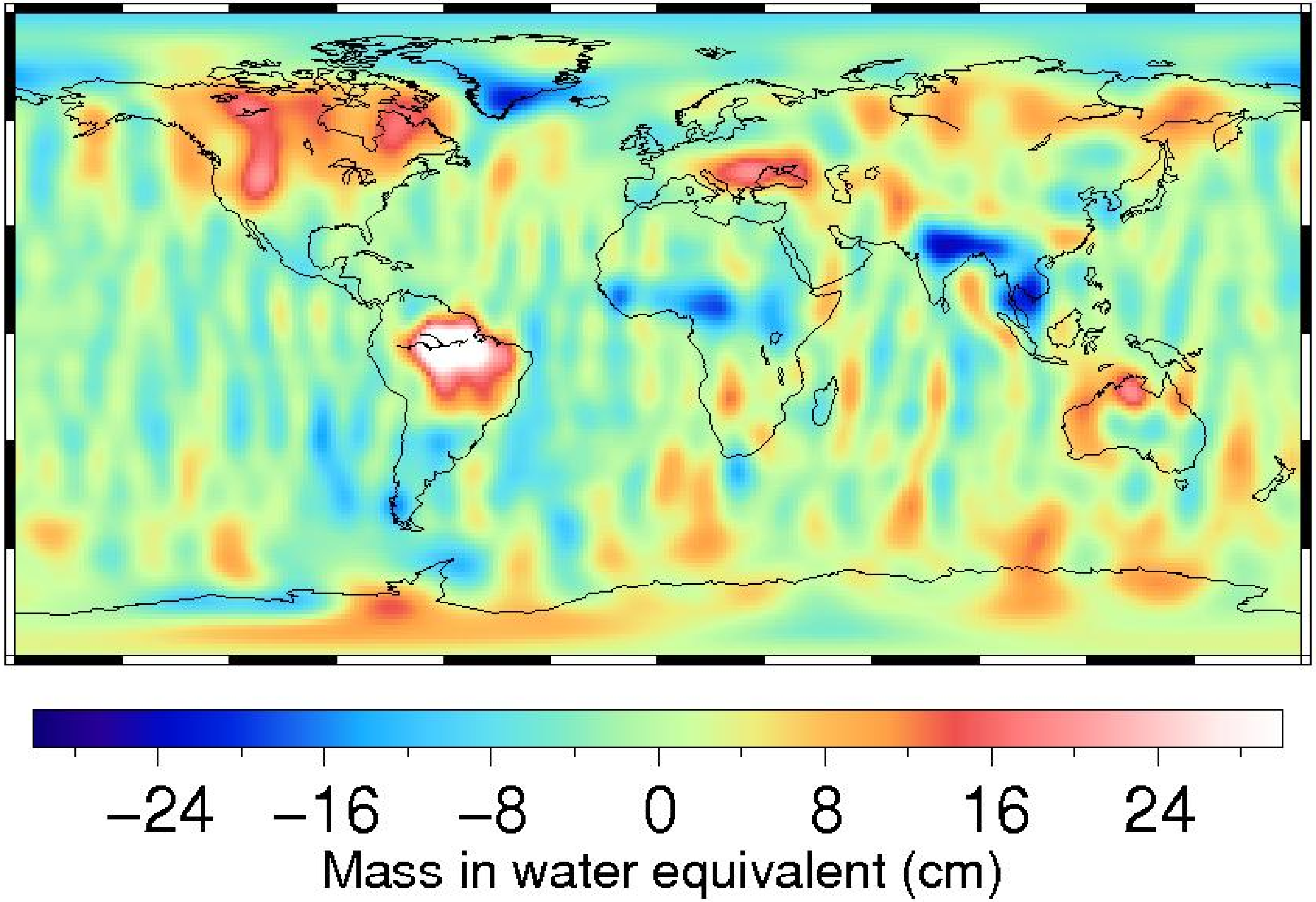

Geoid Variation - June 2006

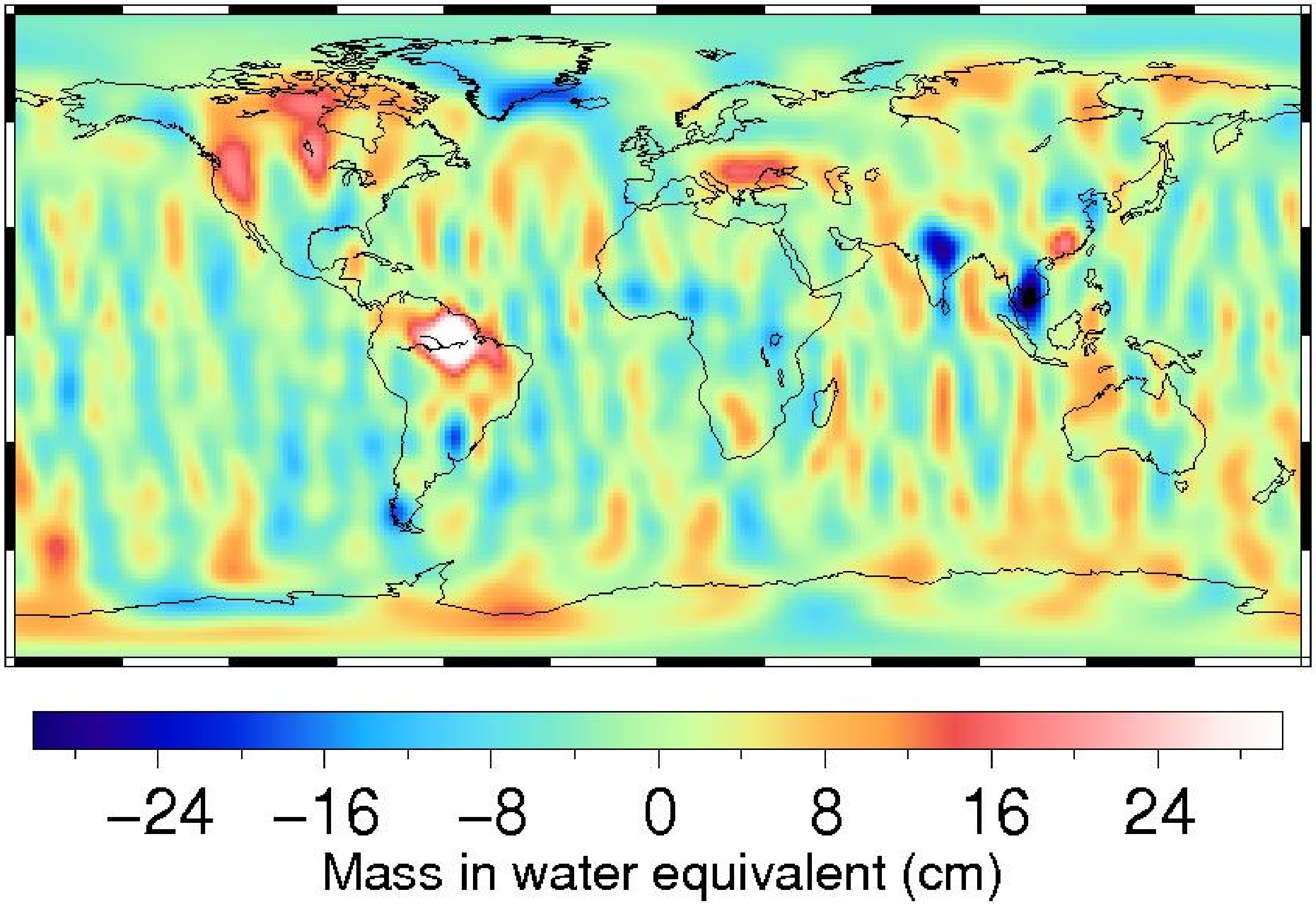

Geoid Variation - July 2006

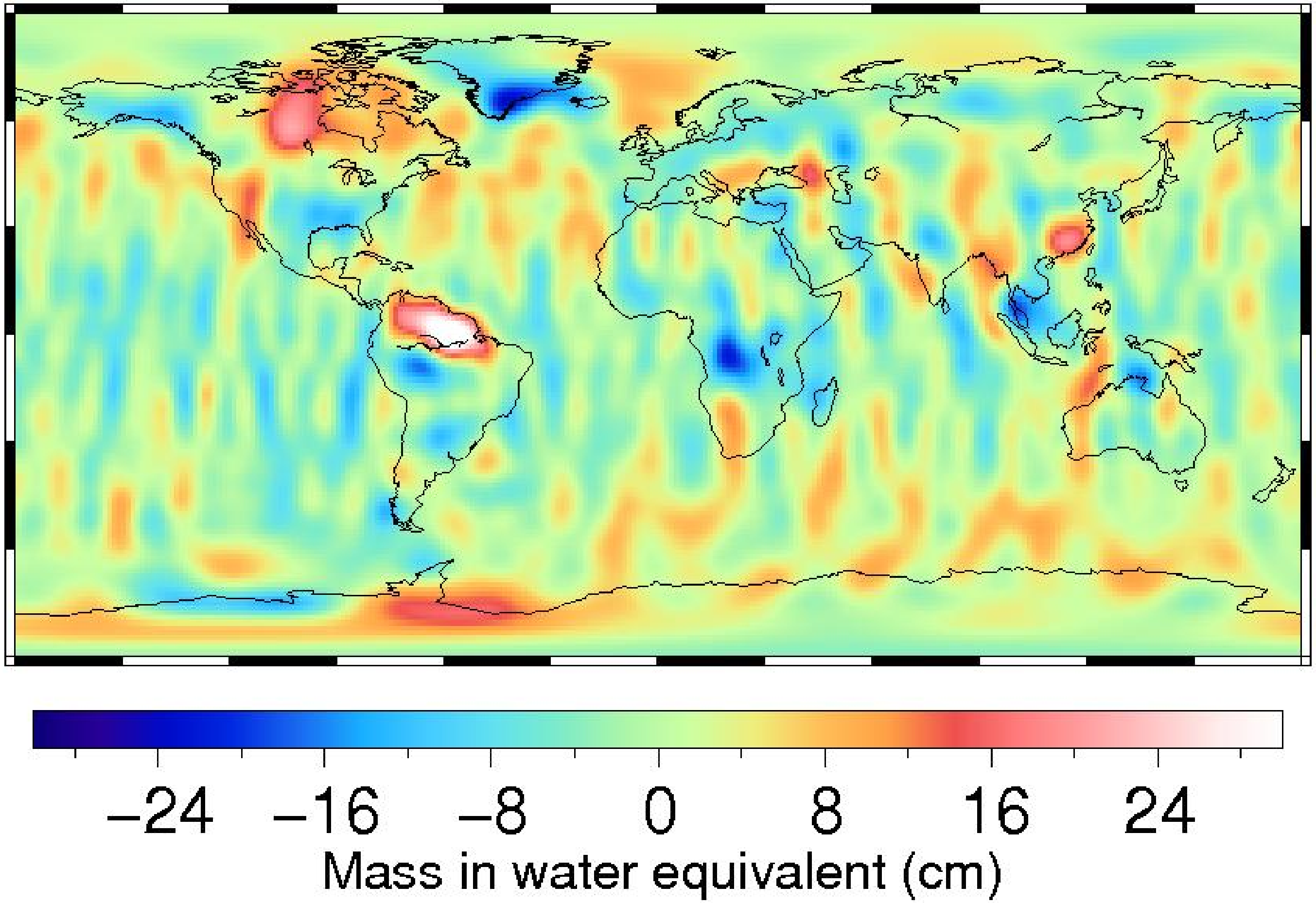

Geoid Variation - August 2006

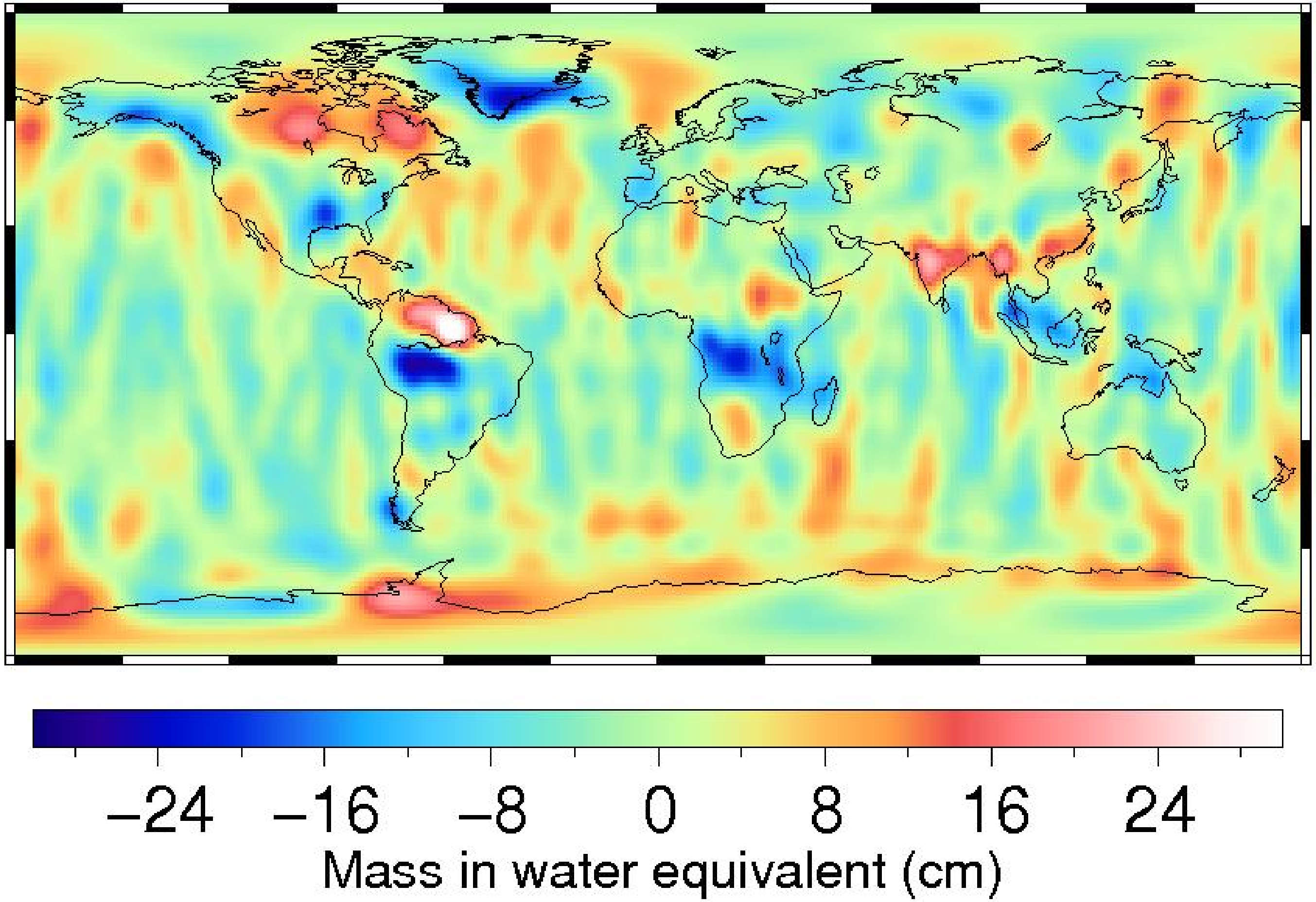

Geoid Variation - September 2006

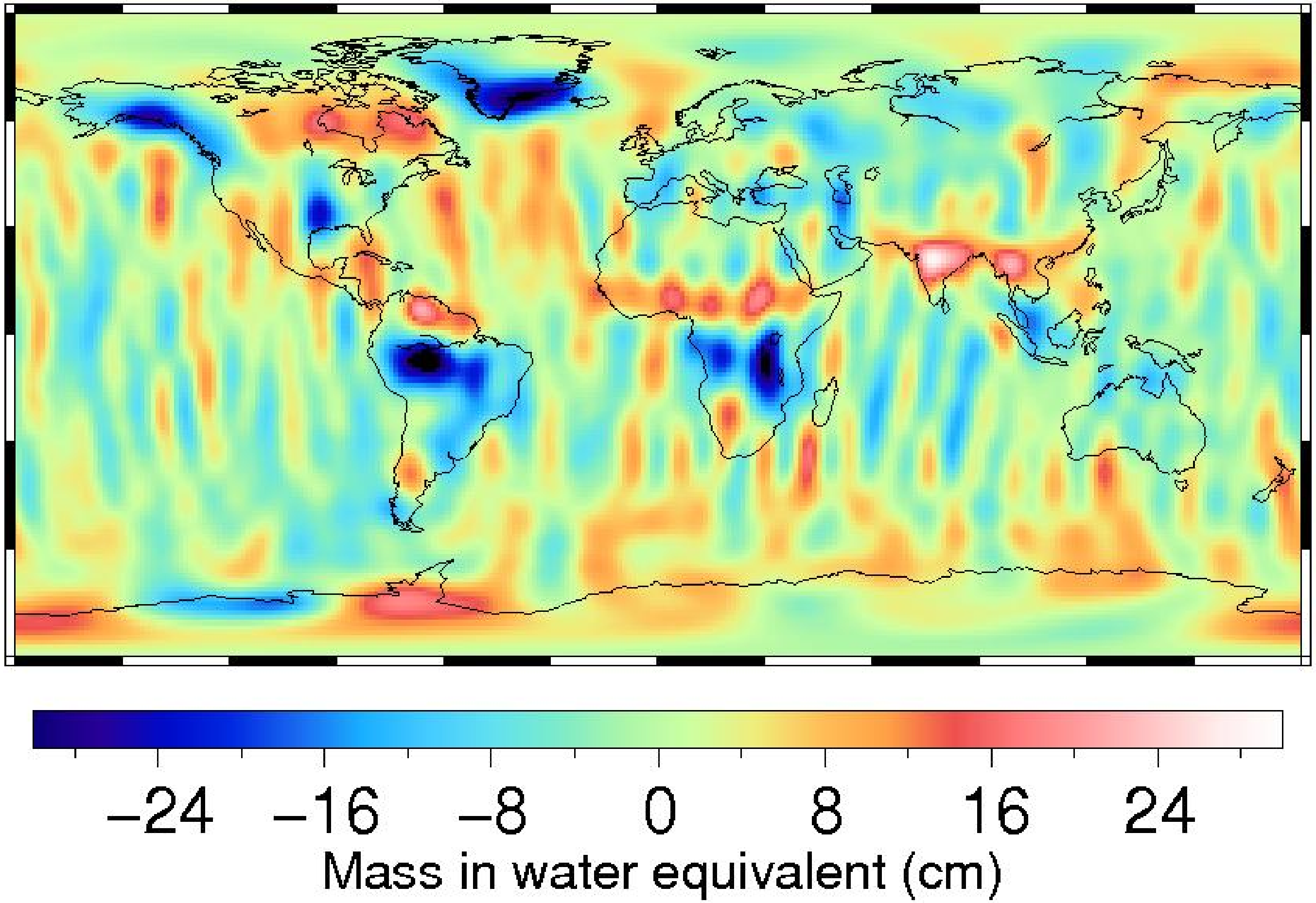

Geoid Variation - October 2006

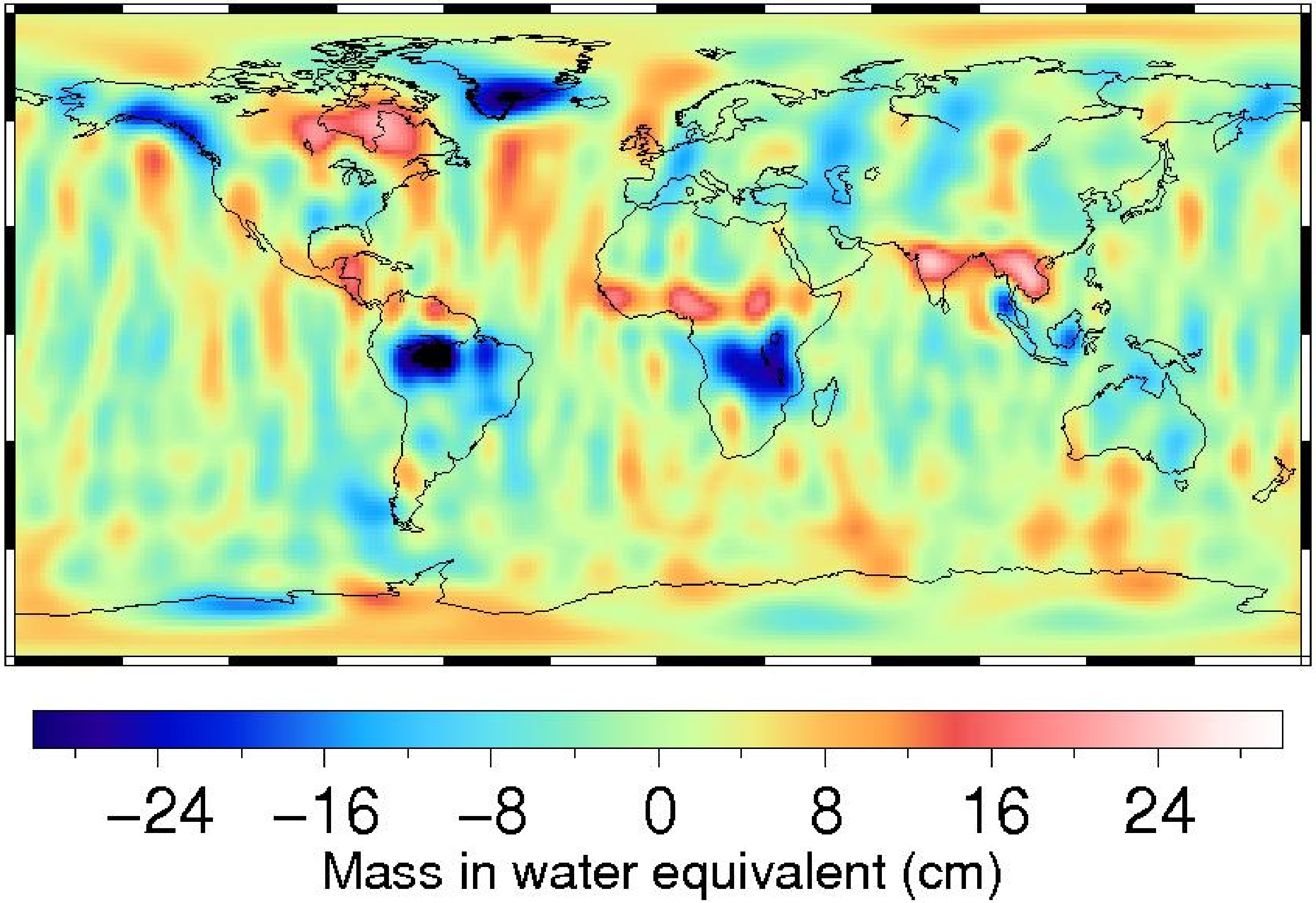

Geoid Variation - November 2006

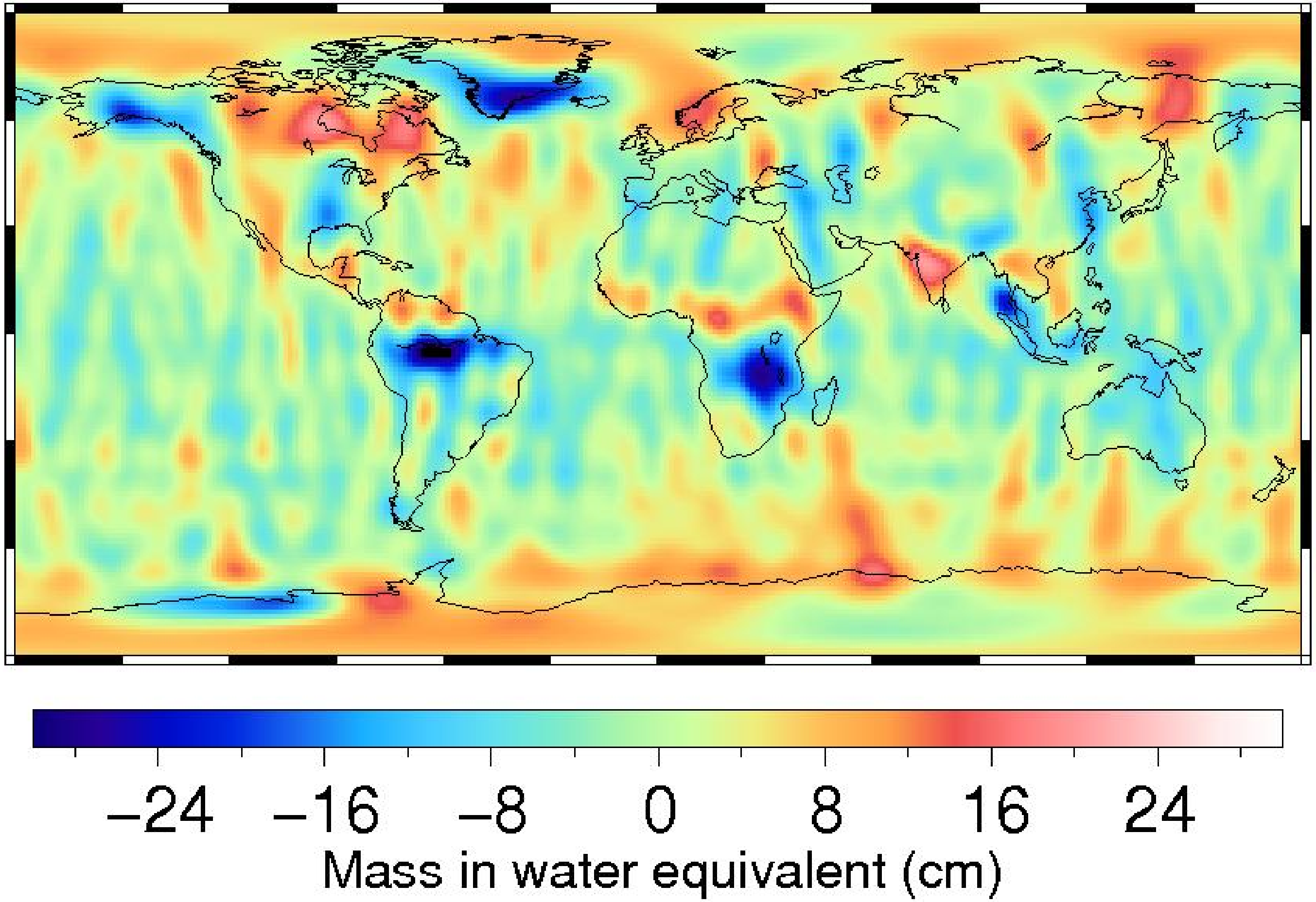

Geoid Variation - December 2006

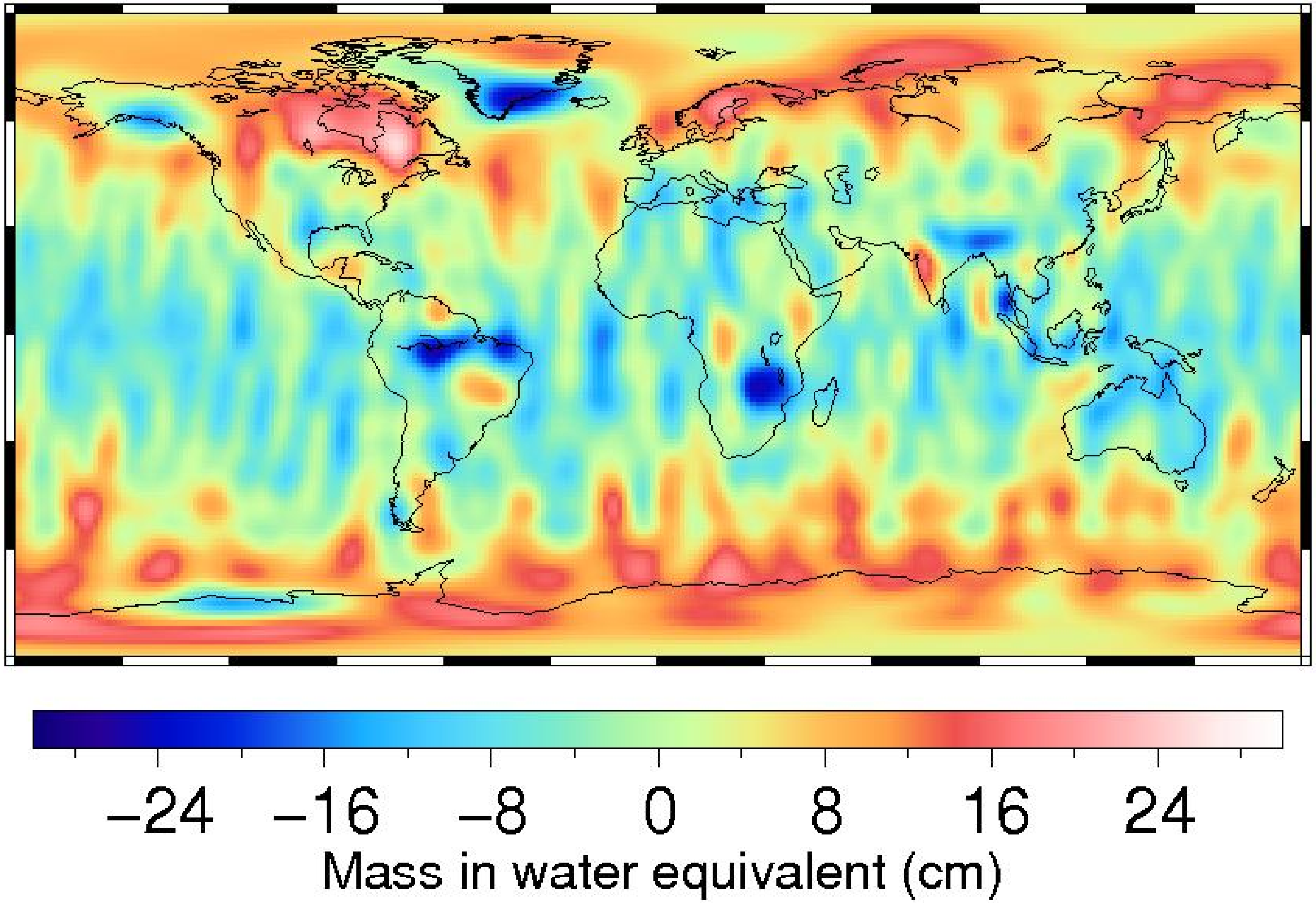

Geoid Variation - January 2007

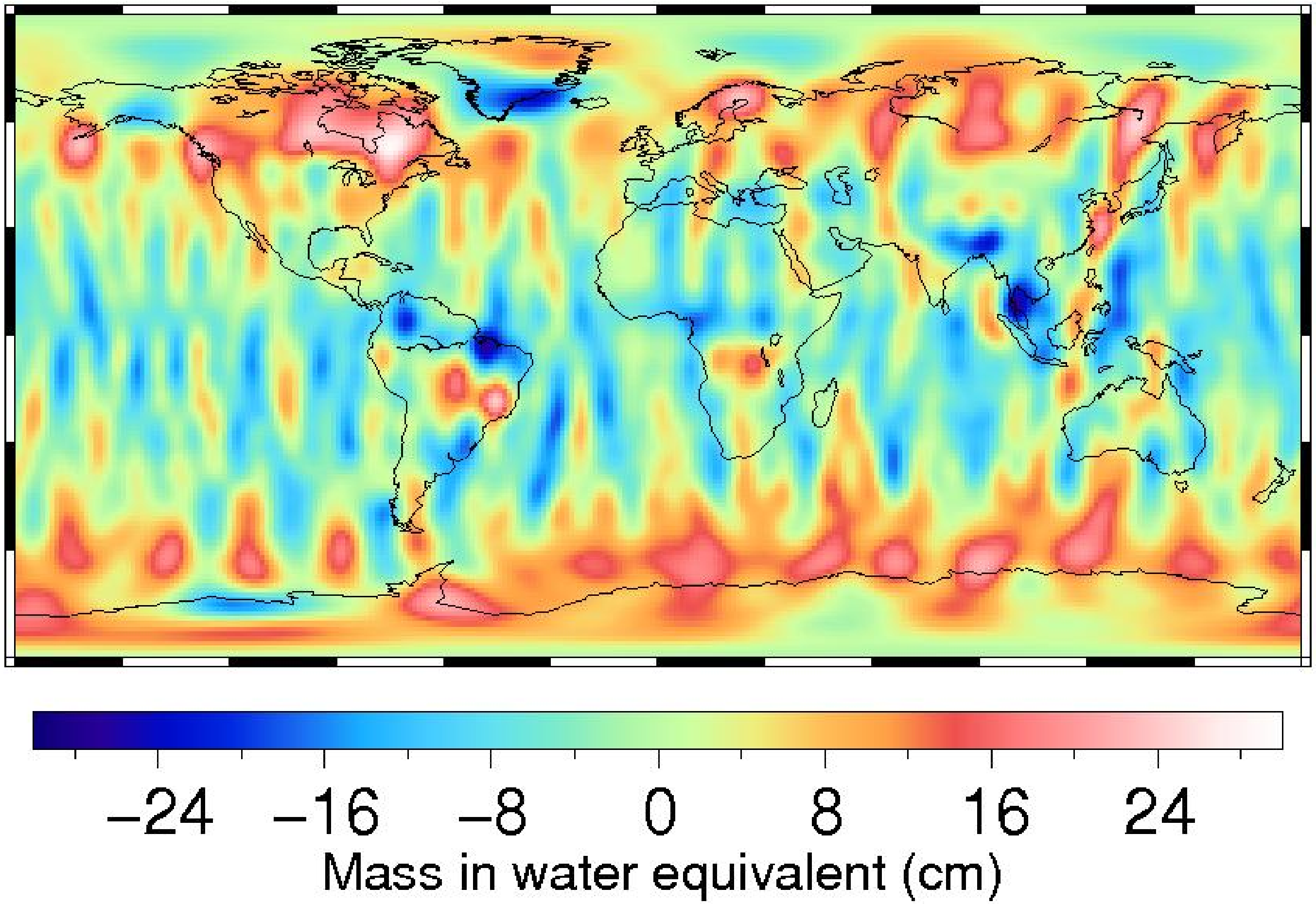

Geoid Variation - February 2007

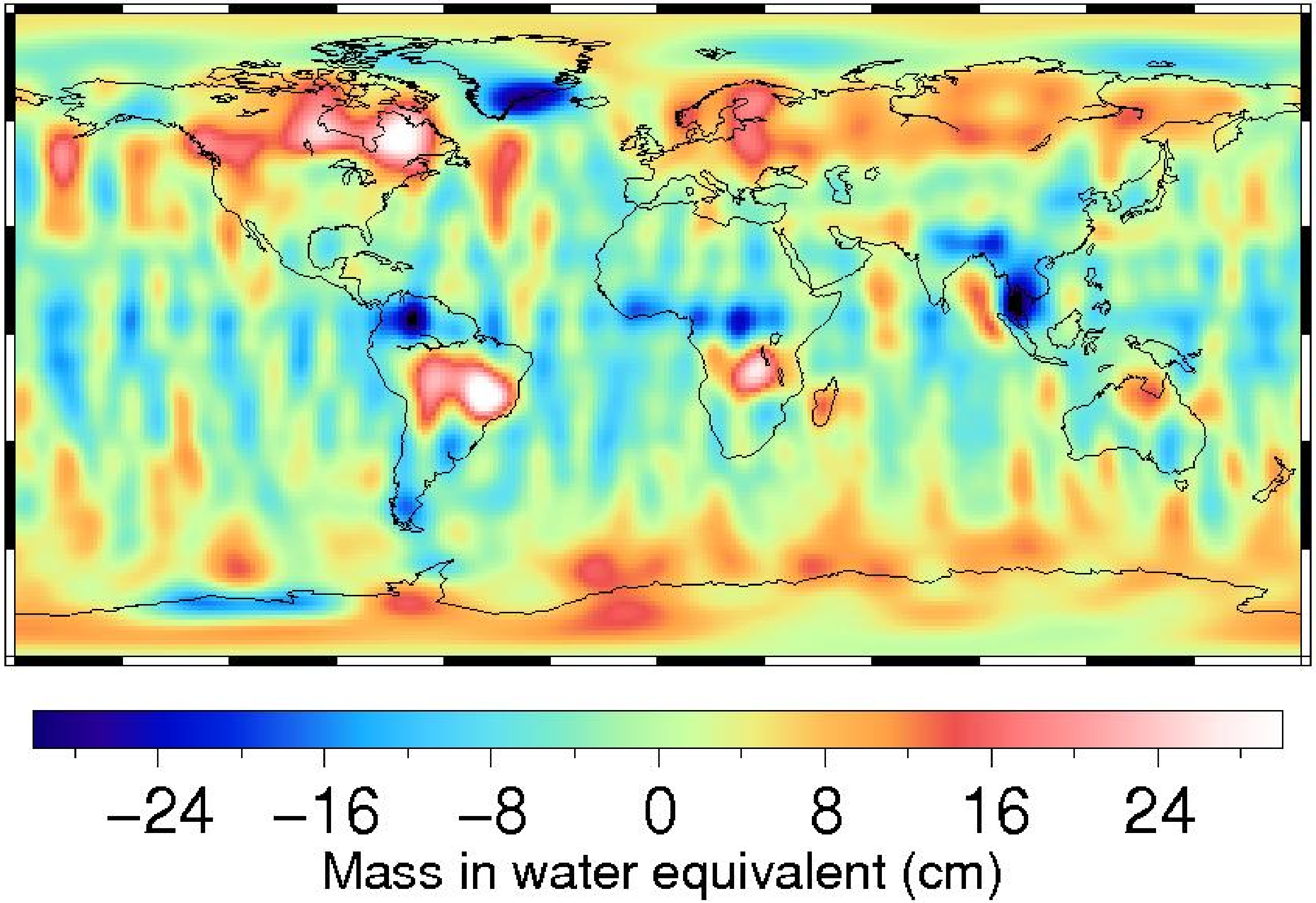

Geoid Variation - March 2007

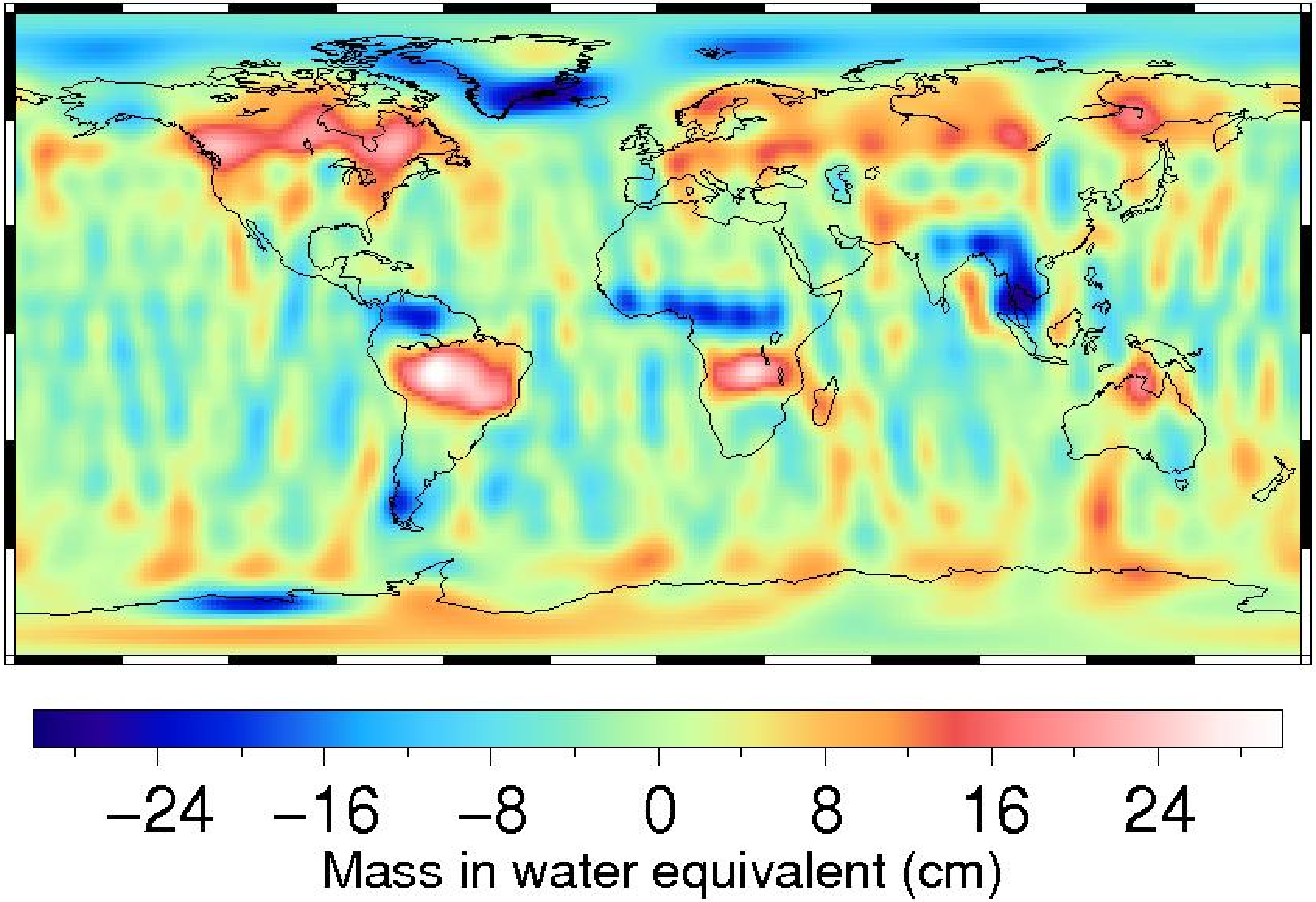

Geoid Variation - April 2007

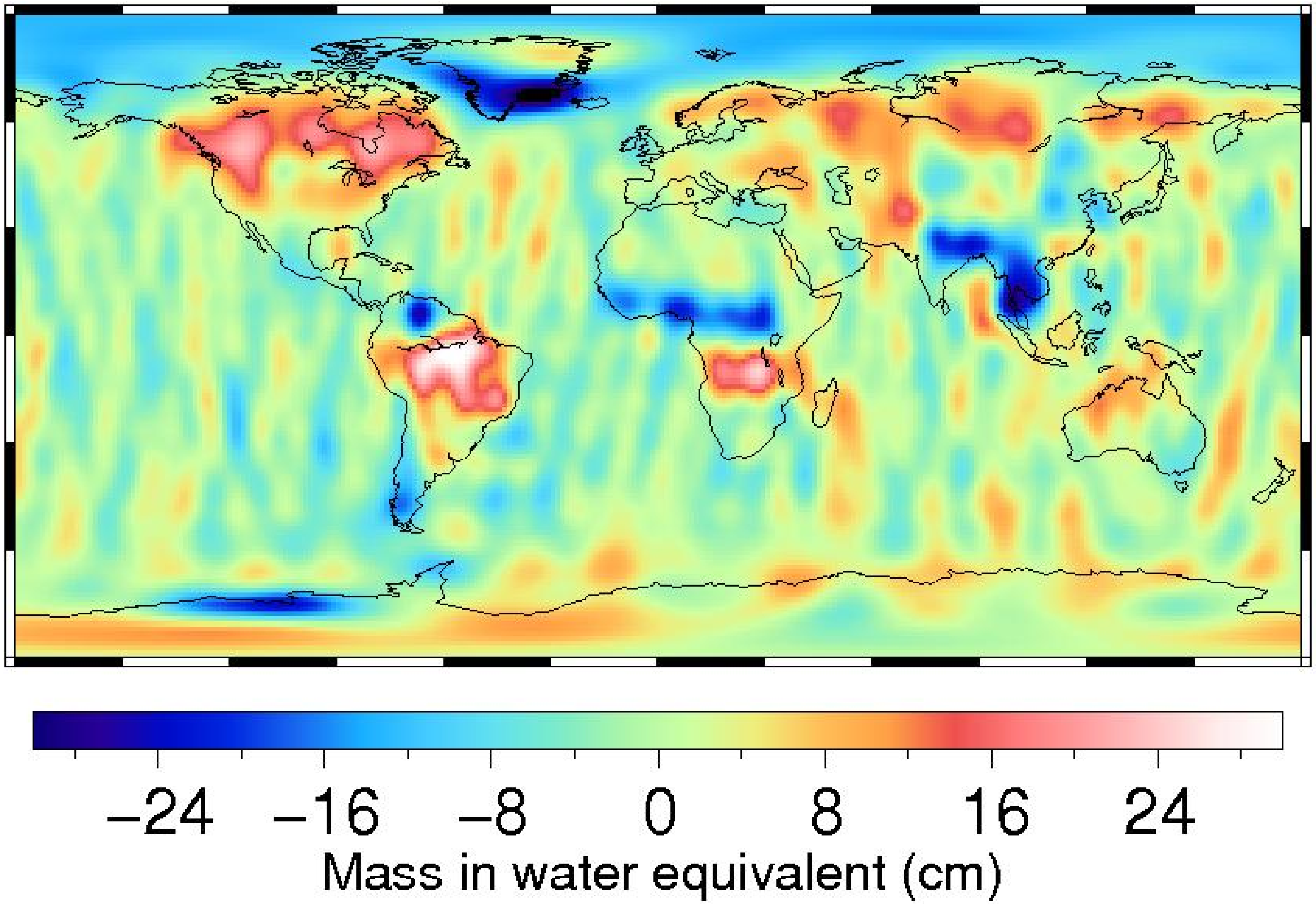

Periodic Signal

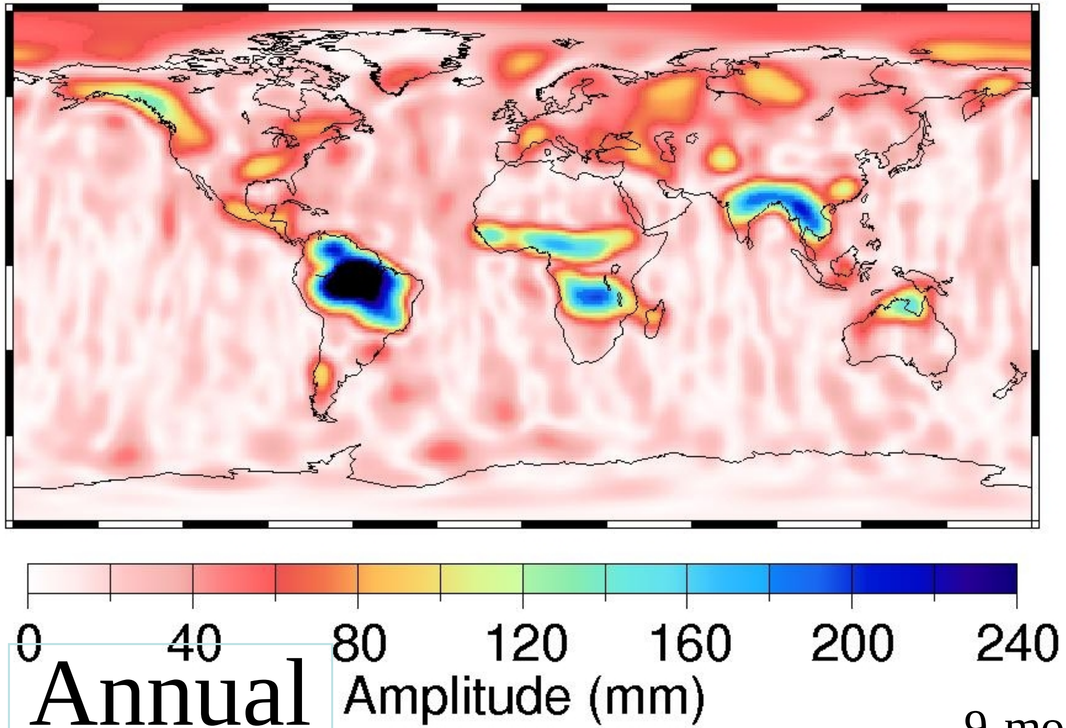

Annual

Semi-Annual

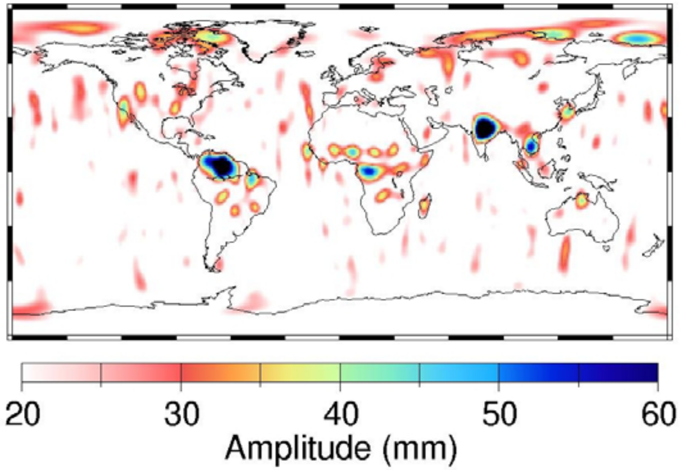

9-month

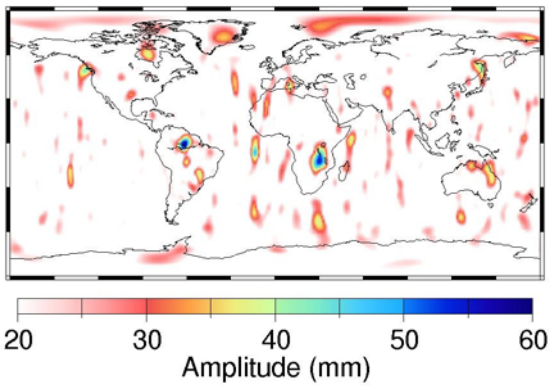

7.2-month

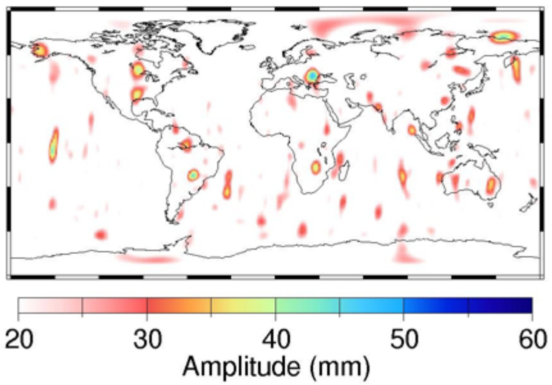

The Map of Mass Variation Trend - Filtered

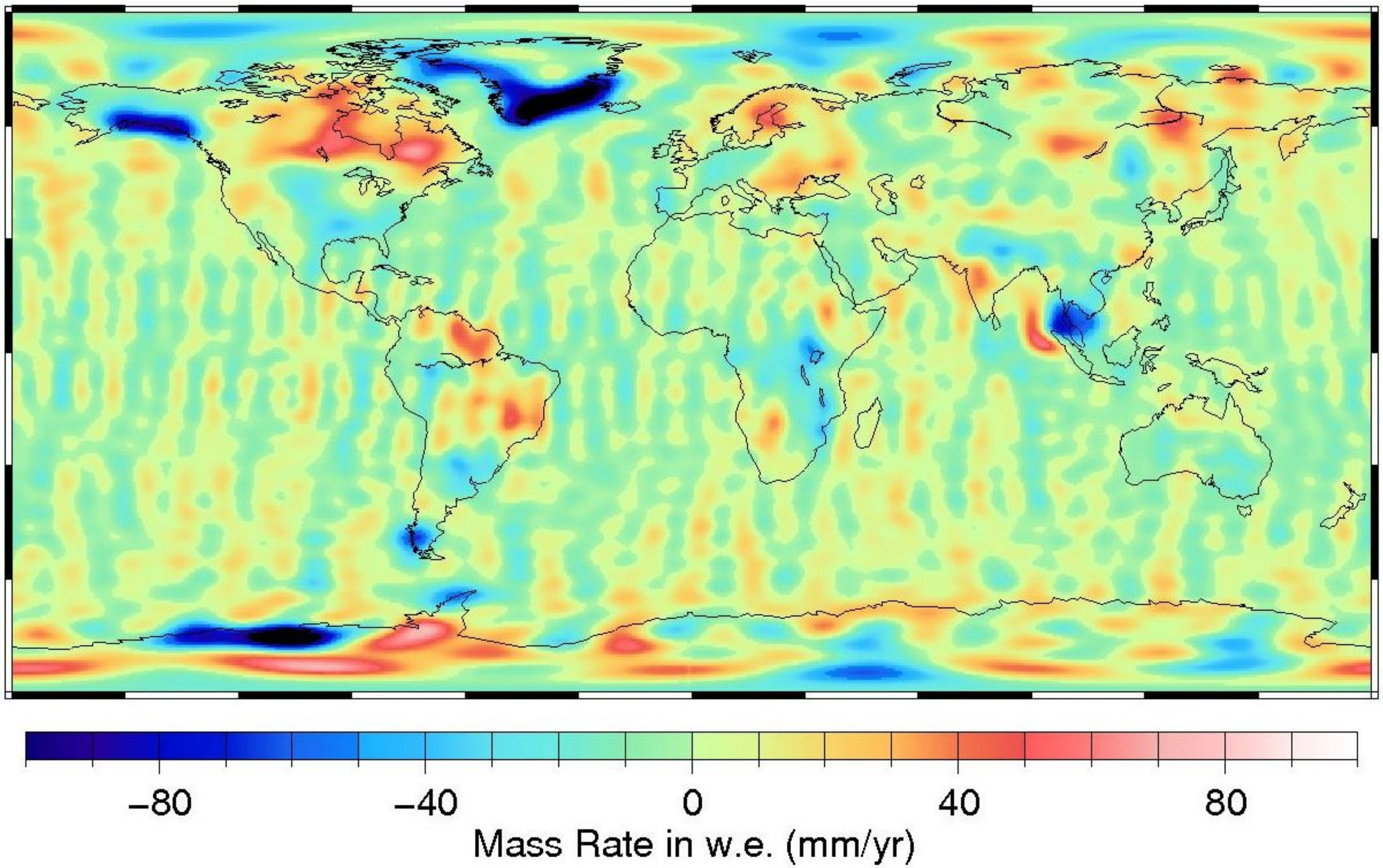

Details: Greenland and Antarctica

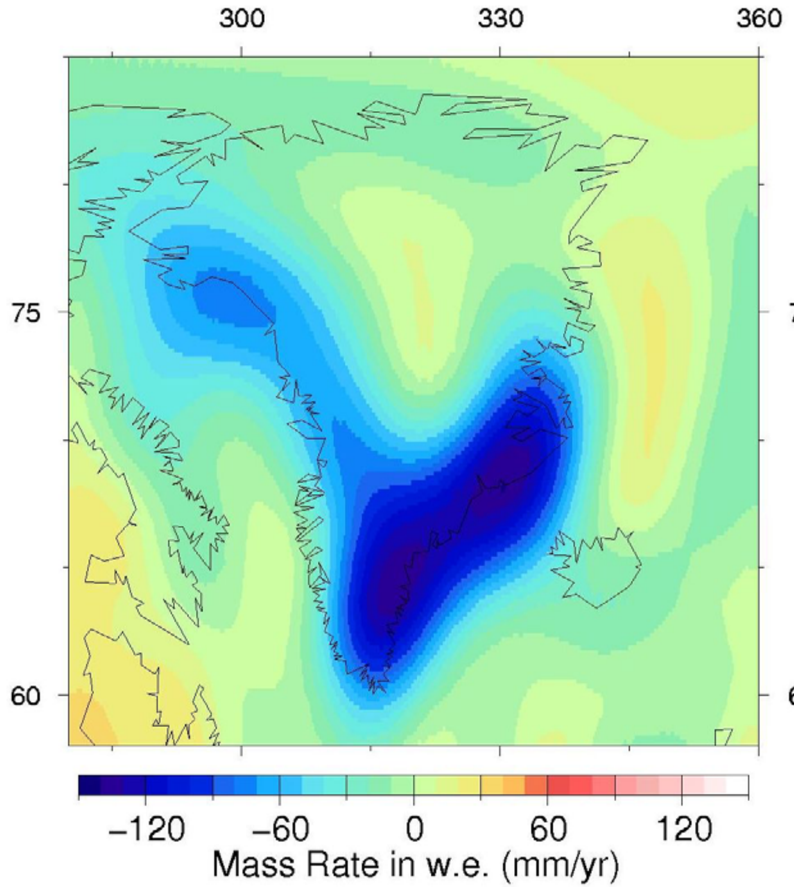

Water Equivalent in mm/yr

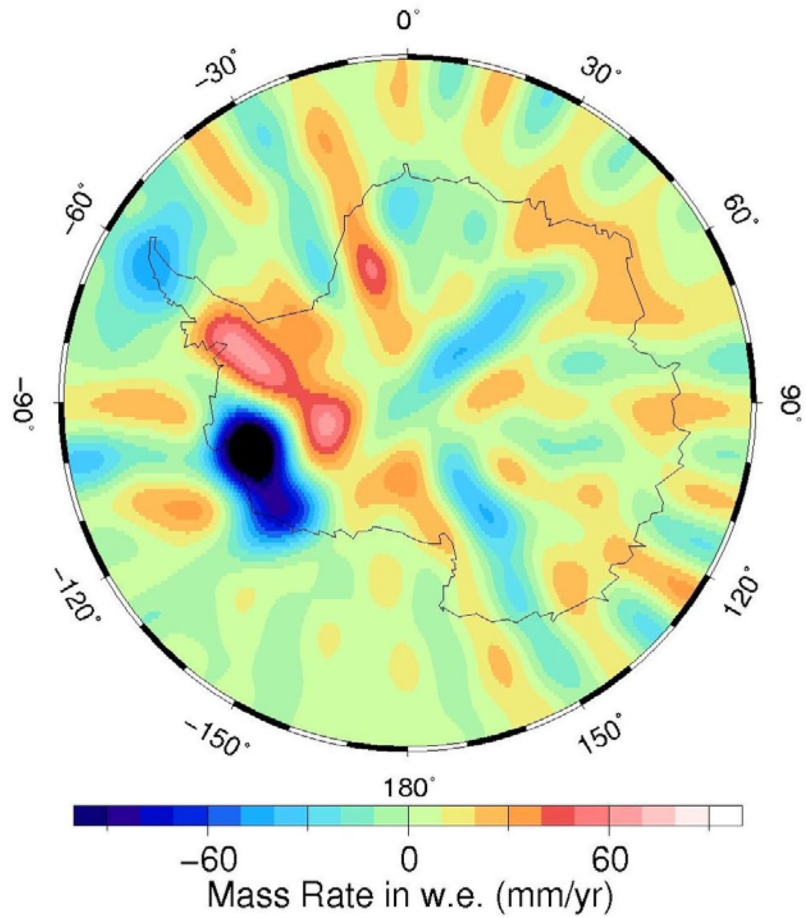

Water Equivalent in mm/yr

Details: Fennoscandia and Hudson Bay

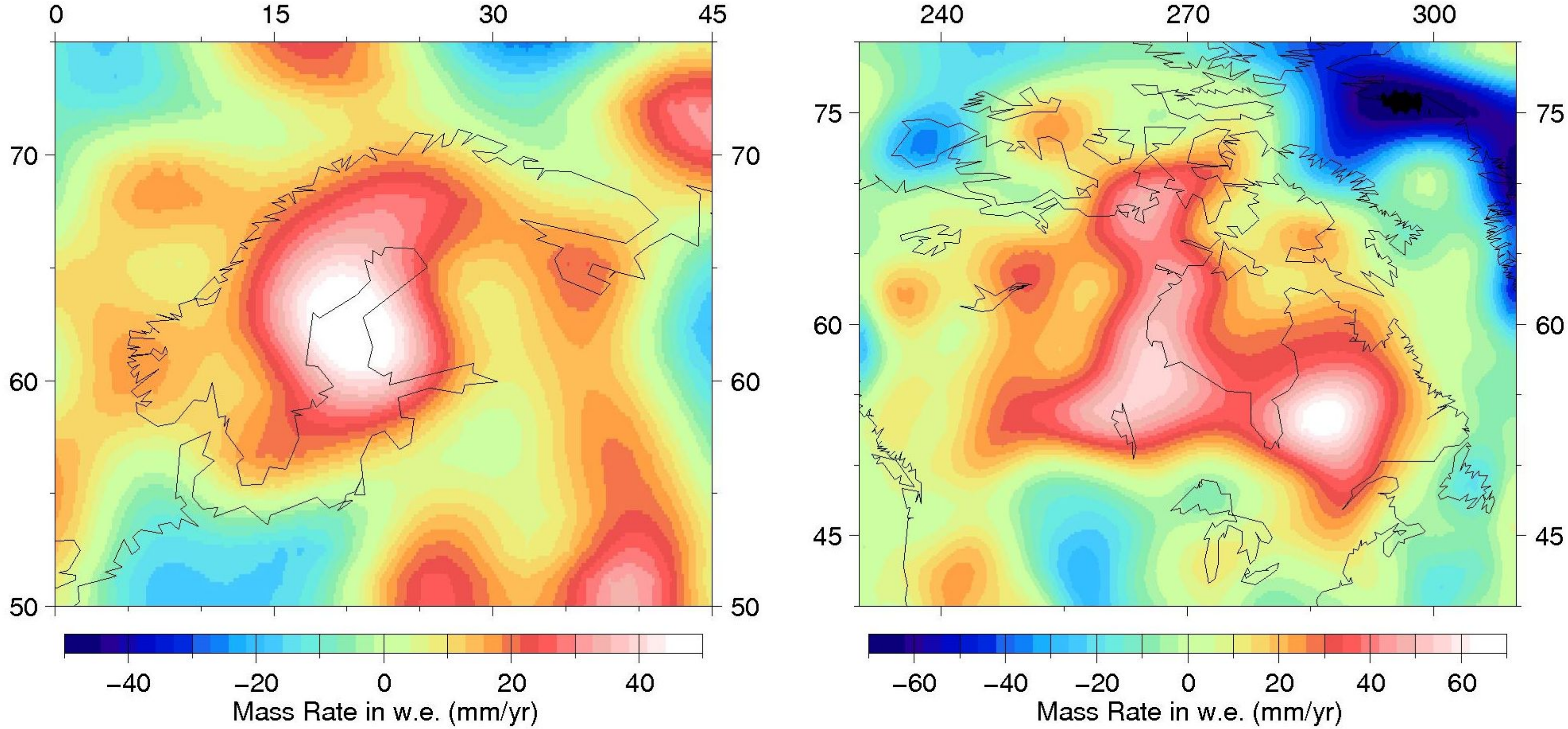

The Post Glacial Rebound

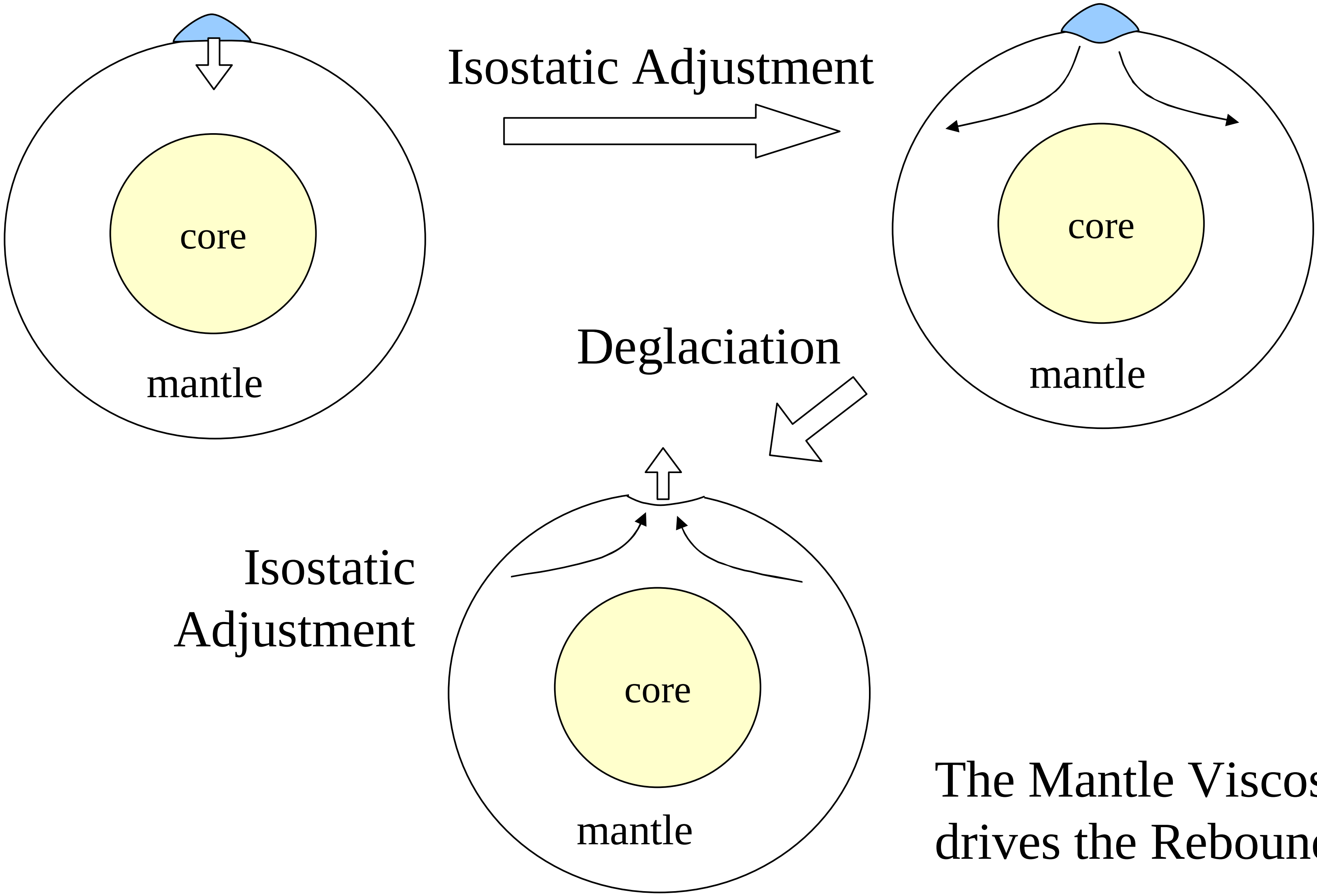

The Mantle Viscosity
drives the Rebound

Pleistocene Deglaciation Model

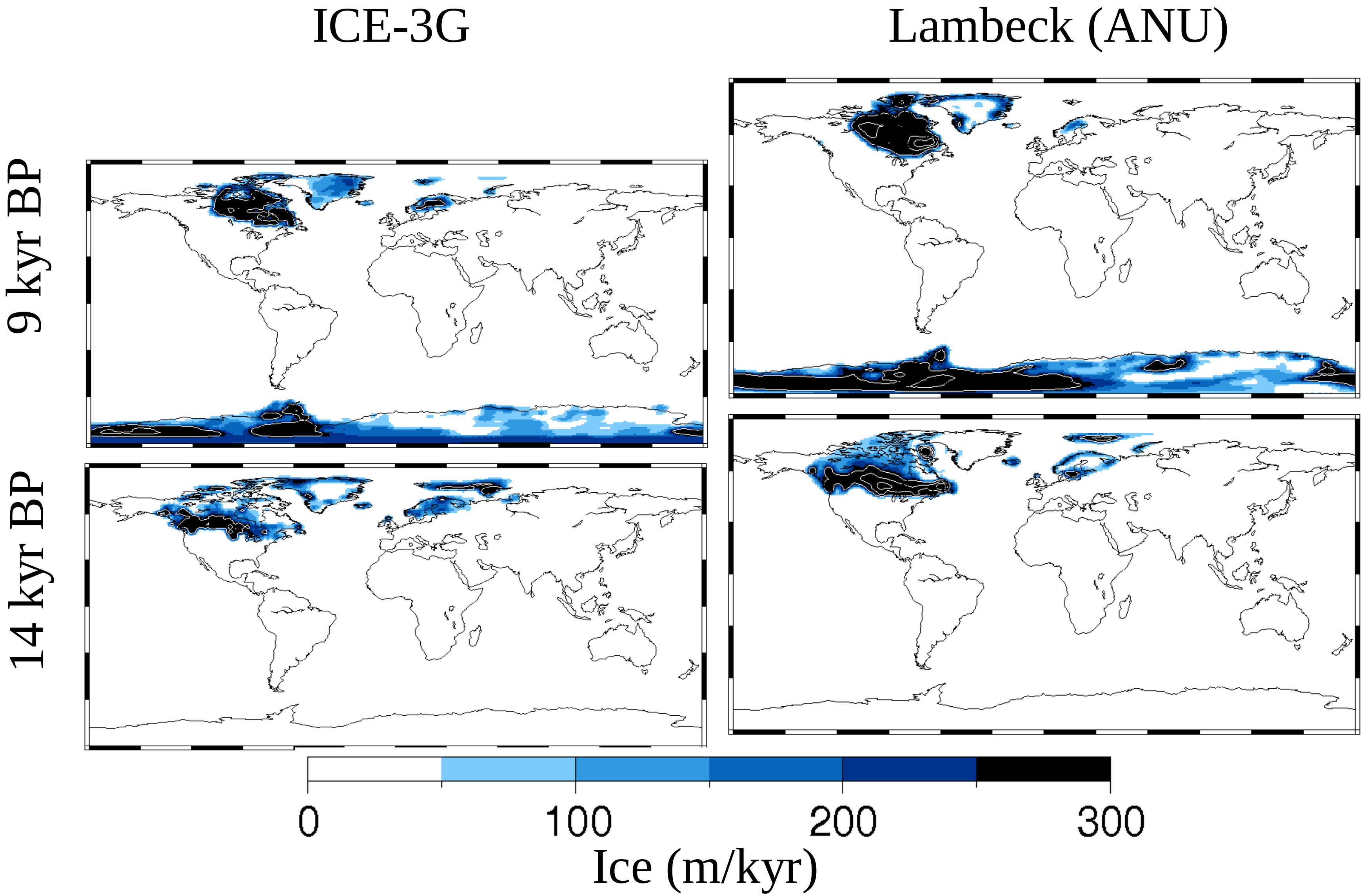

The Post Glacial Rebound: *Geoid Rate*

Lambeck (ANU) $\nu_{UP} = 5x10^{20}$ Pa s $\nu_{LW} = 2.5x10^{21}$ Pa s

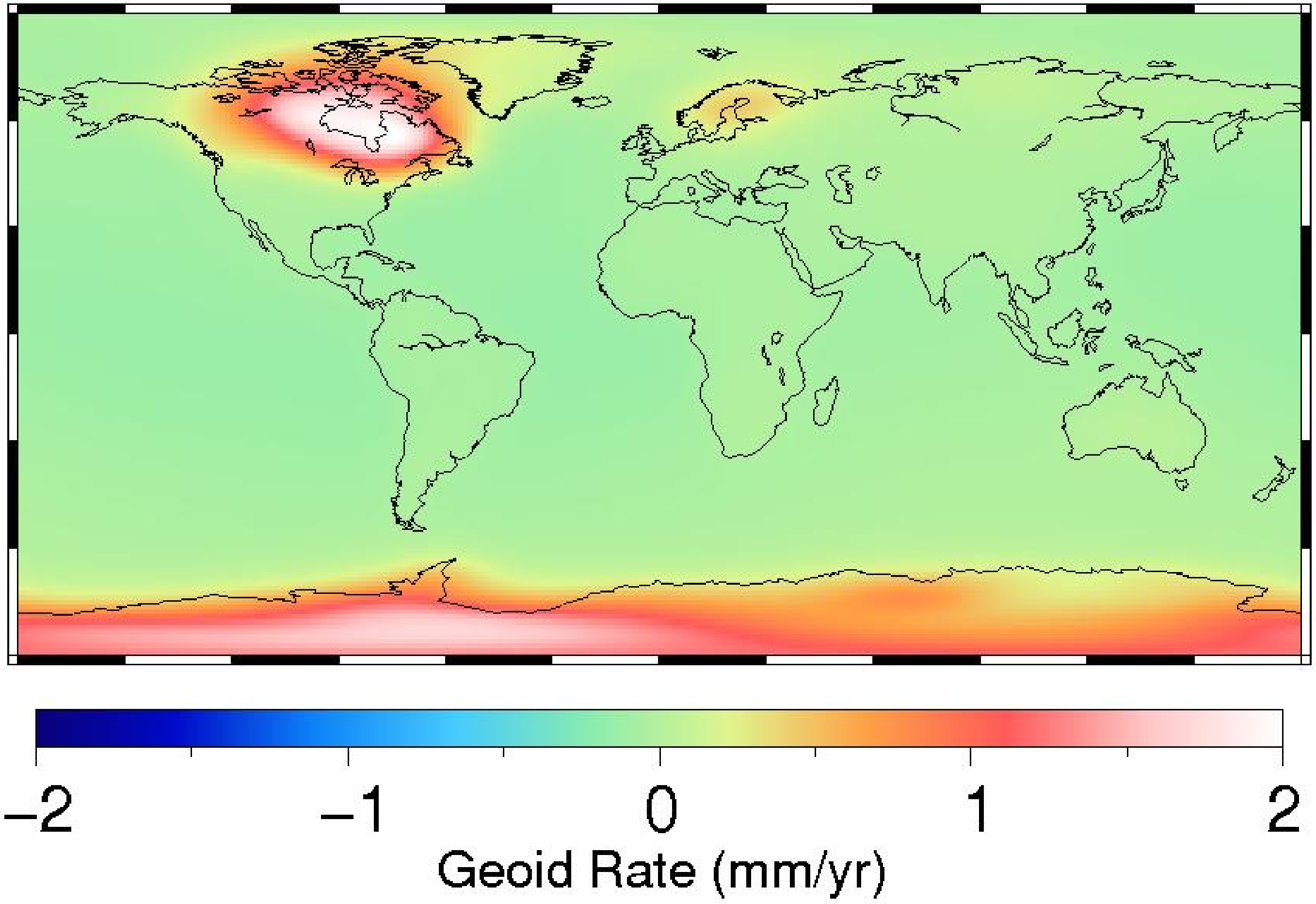

The Map of Mass Variation Trend - Filtered

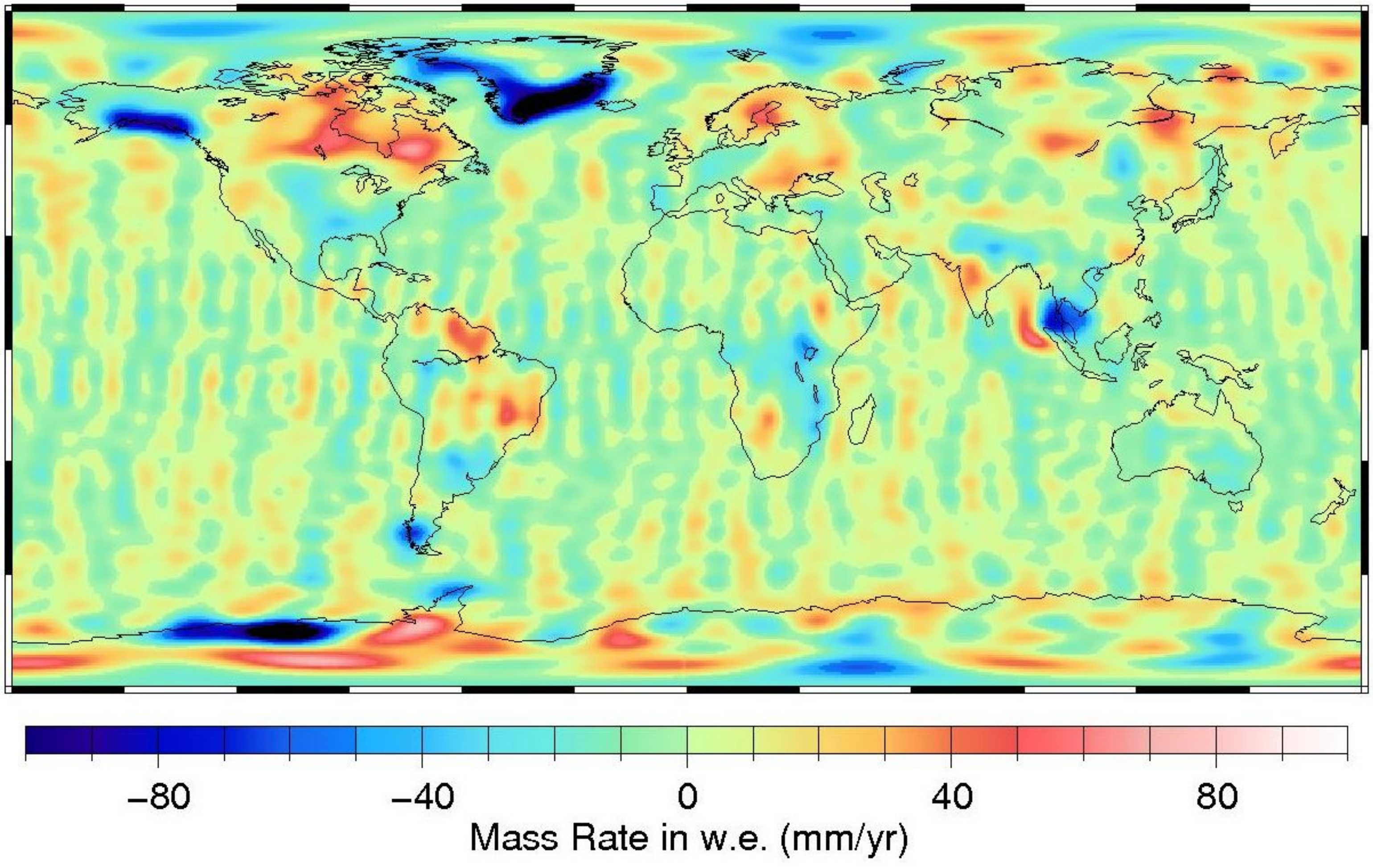

Mass Distribution

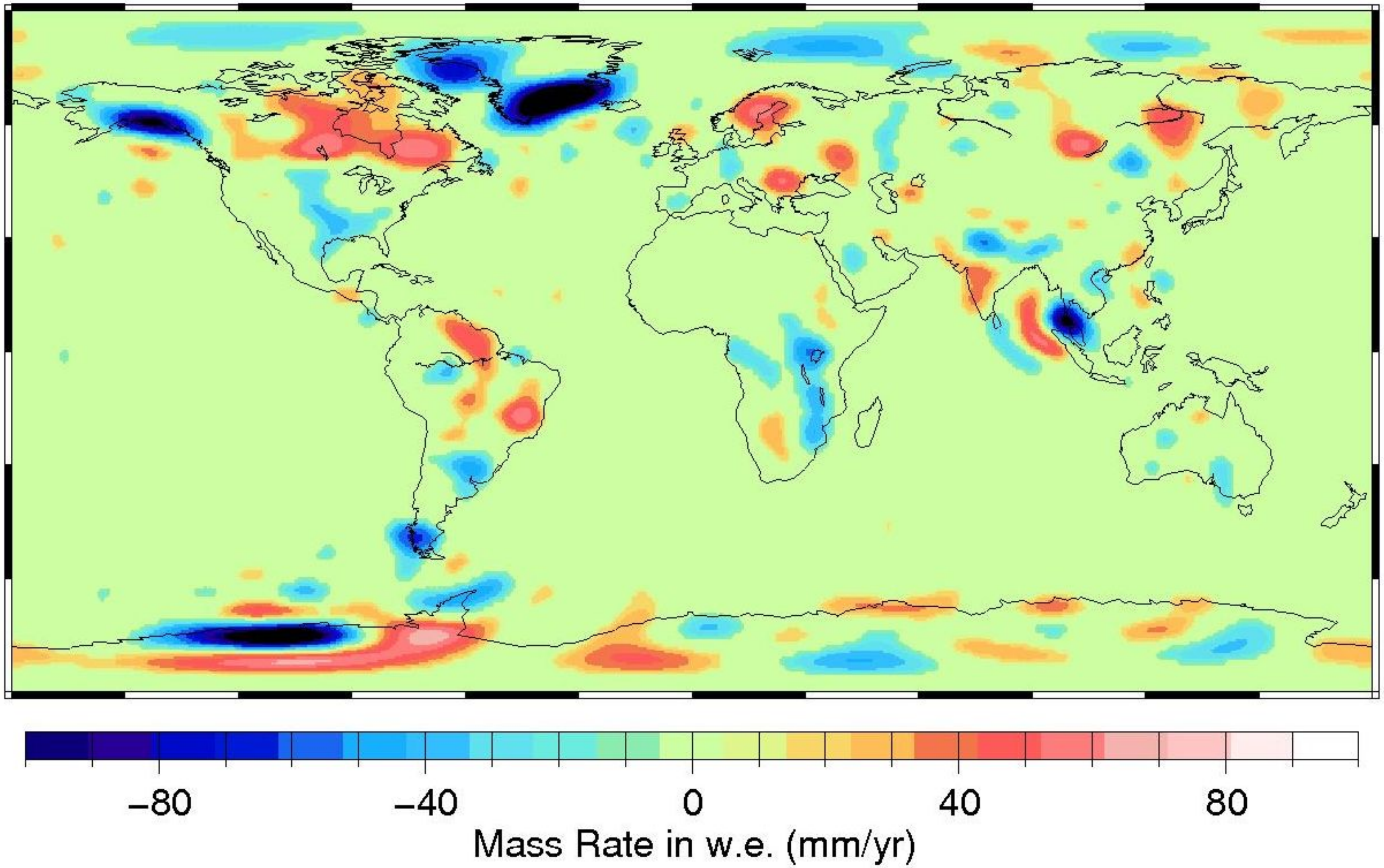

Mass Distribution over Oceans

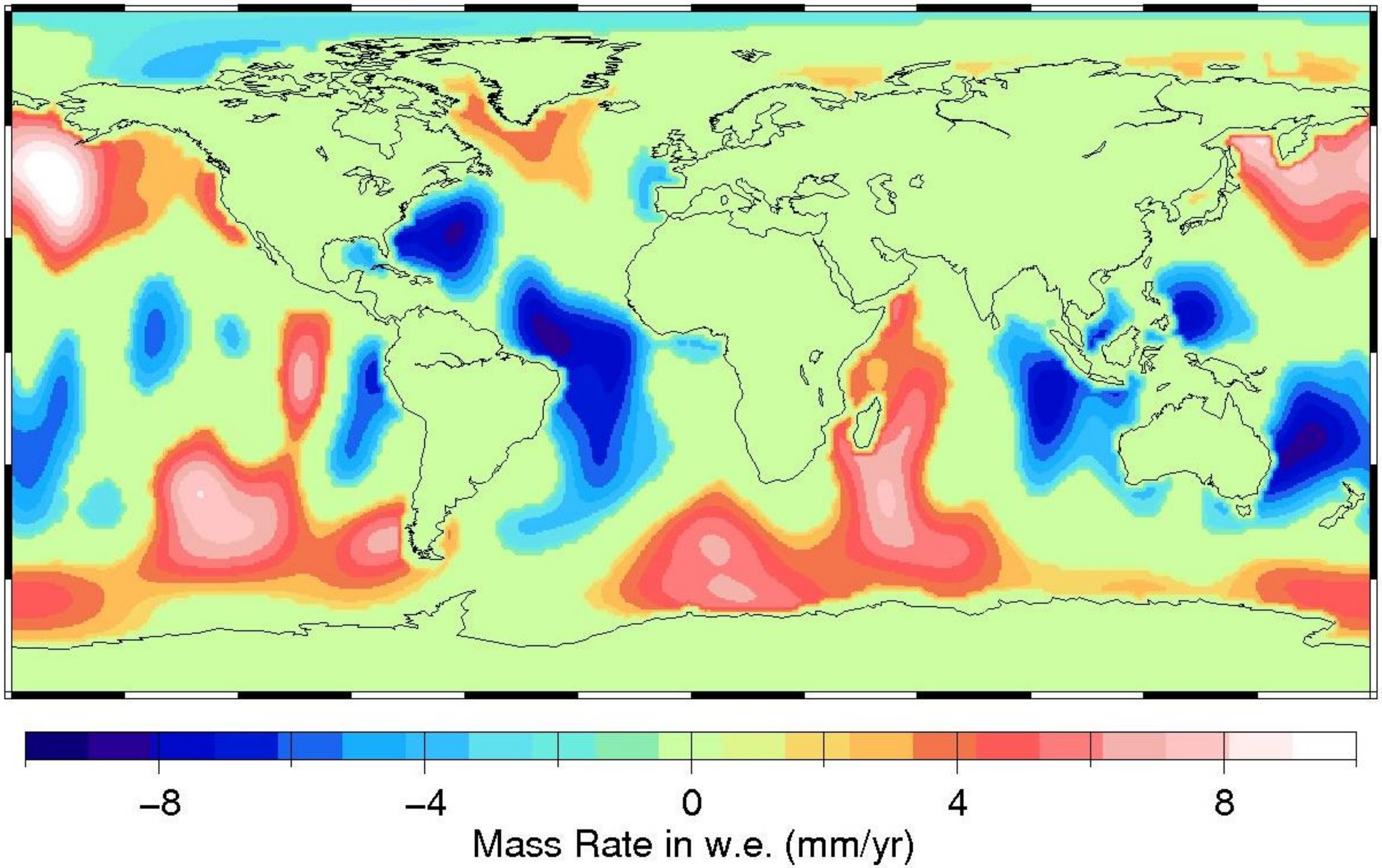

GRACE up 30 - Sea *Removed*

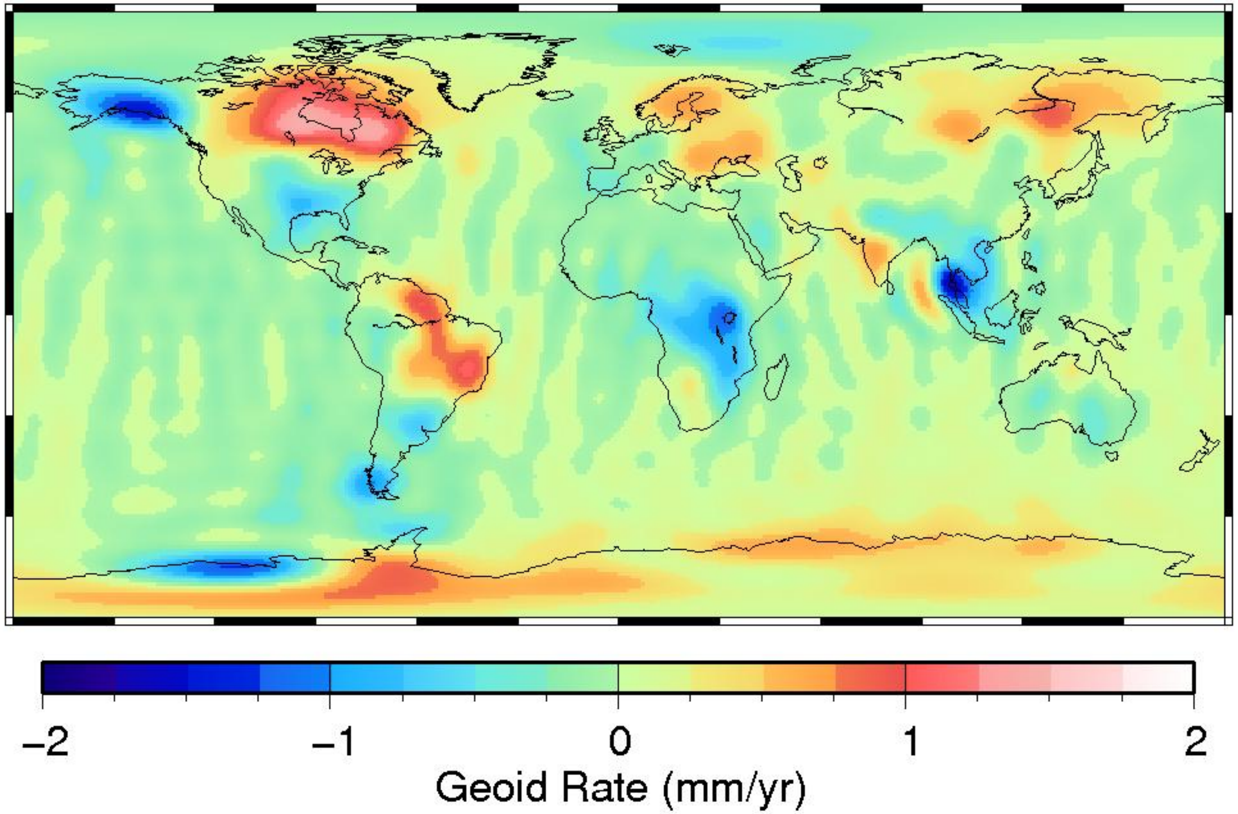

GRACE up 30 - Far from PGR *Removed*

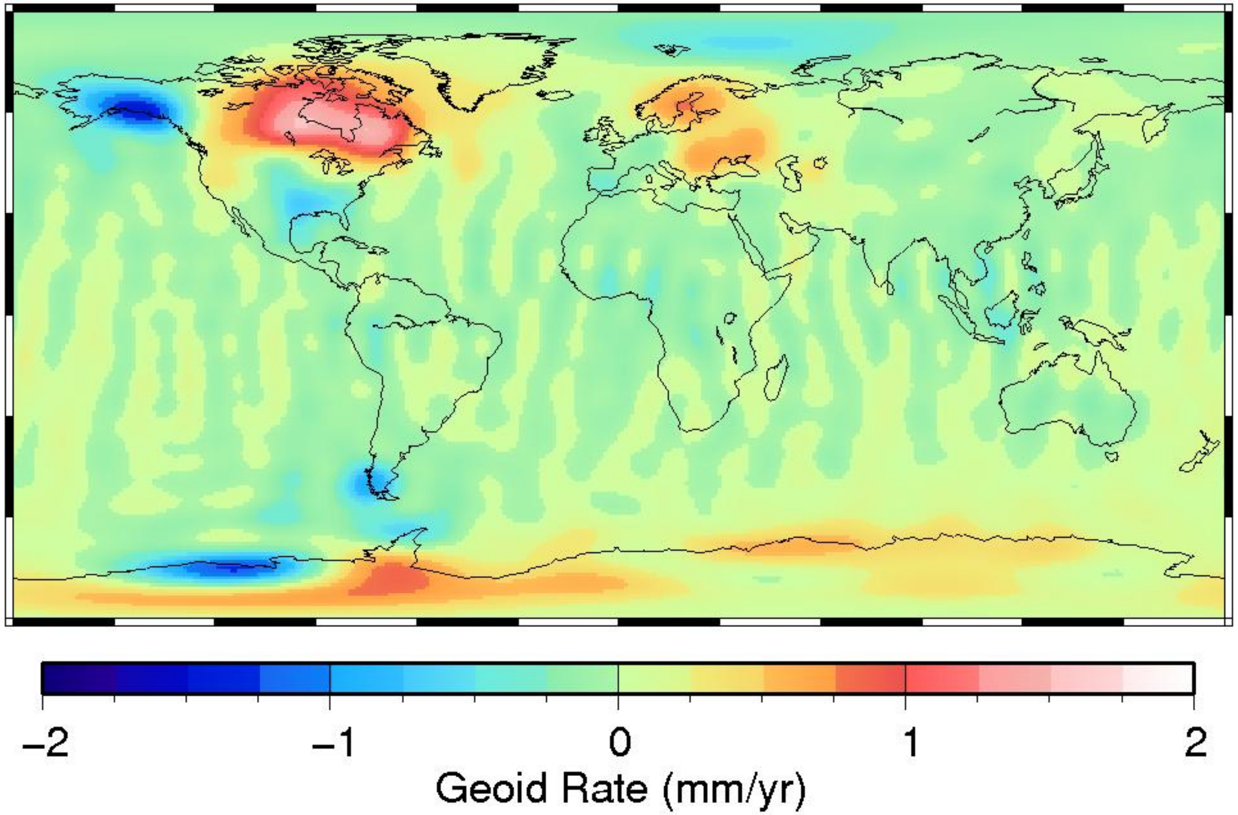

GRACE up 30 - Nearby Fennoscandia *Removed*

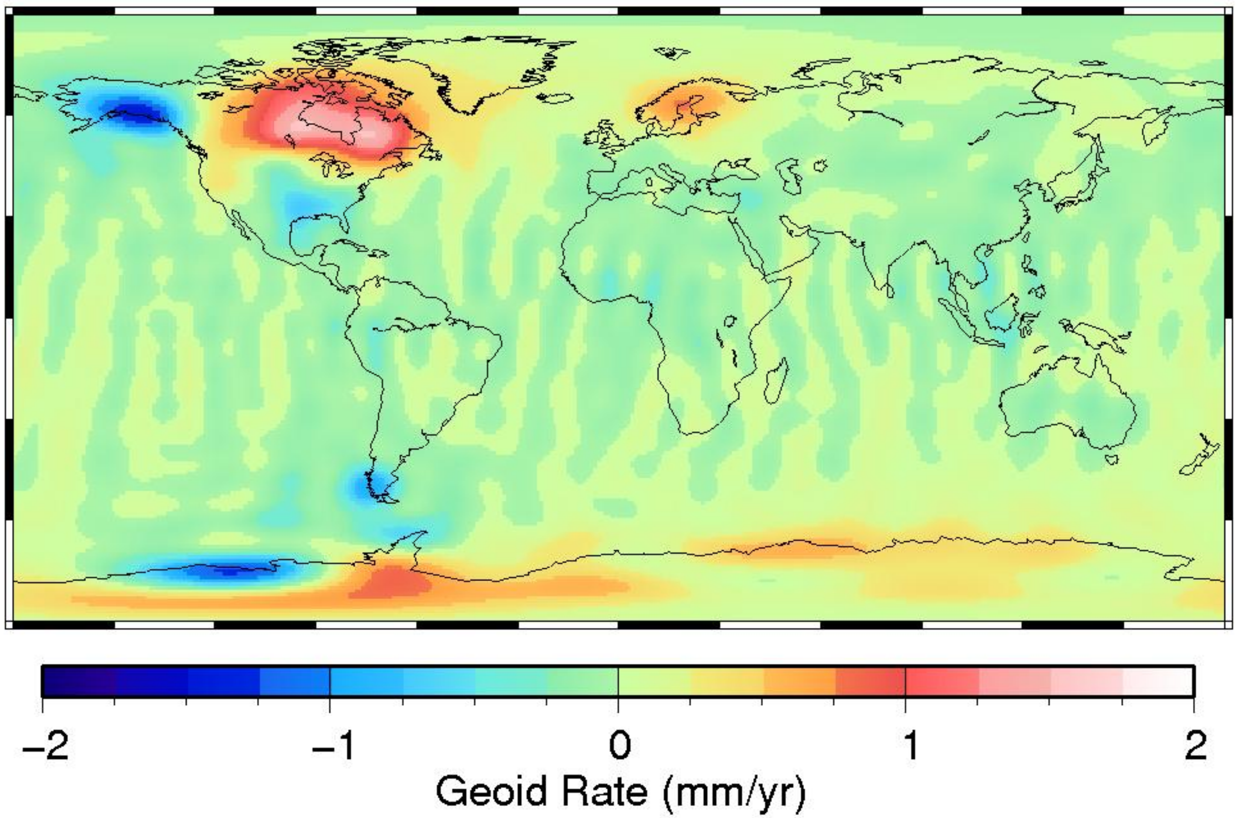

GRACE up 30 - Nearby Hudson Bay *Removed*

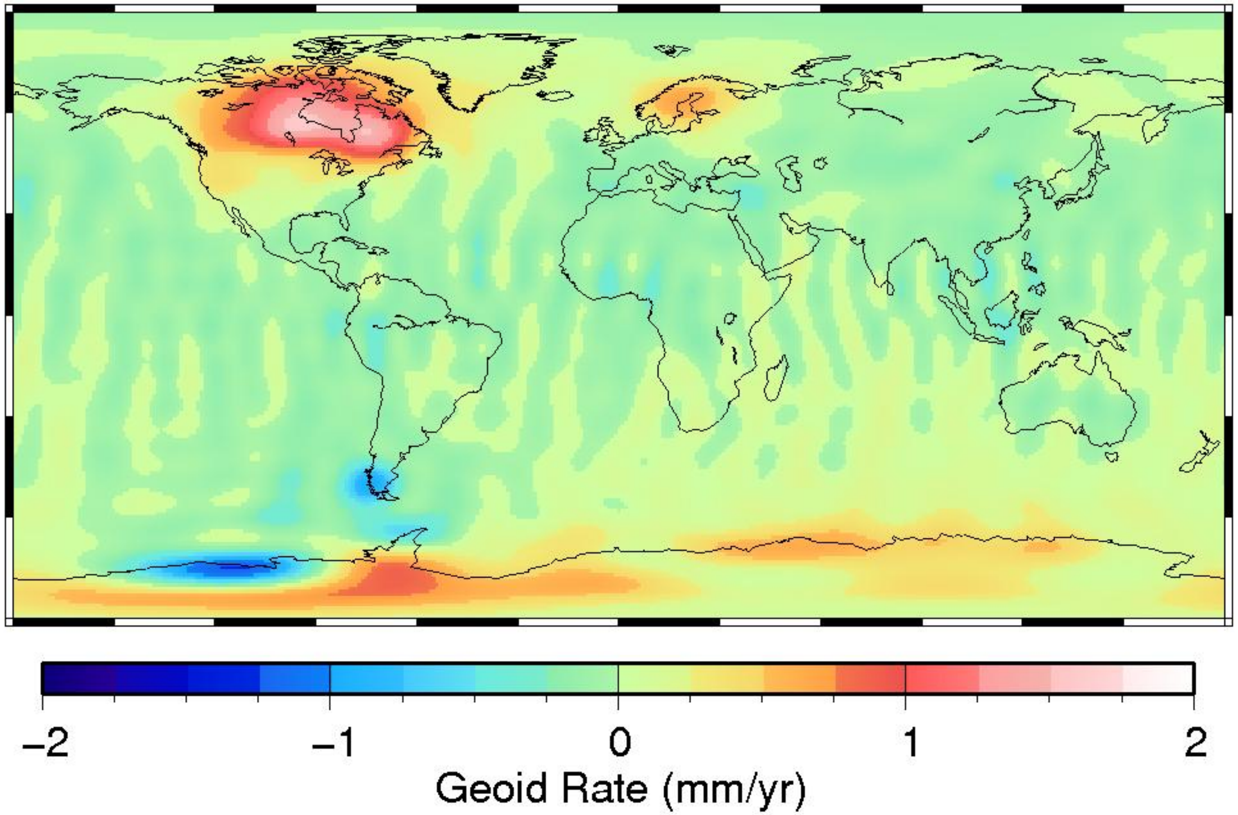

GRACE up 30 - West Antarctica *Removed*

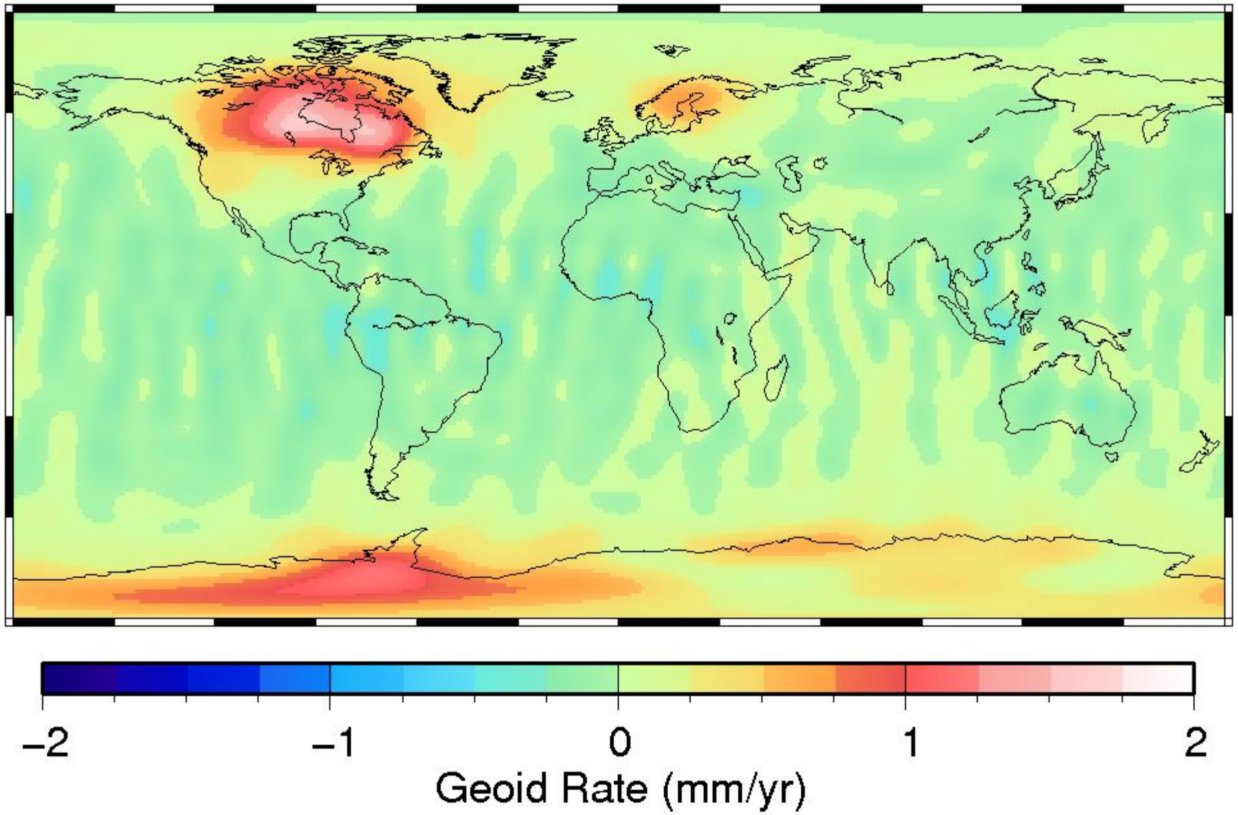

The Earth Model

Incompressible, Viscoelastic Maxwell Rheology

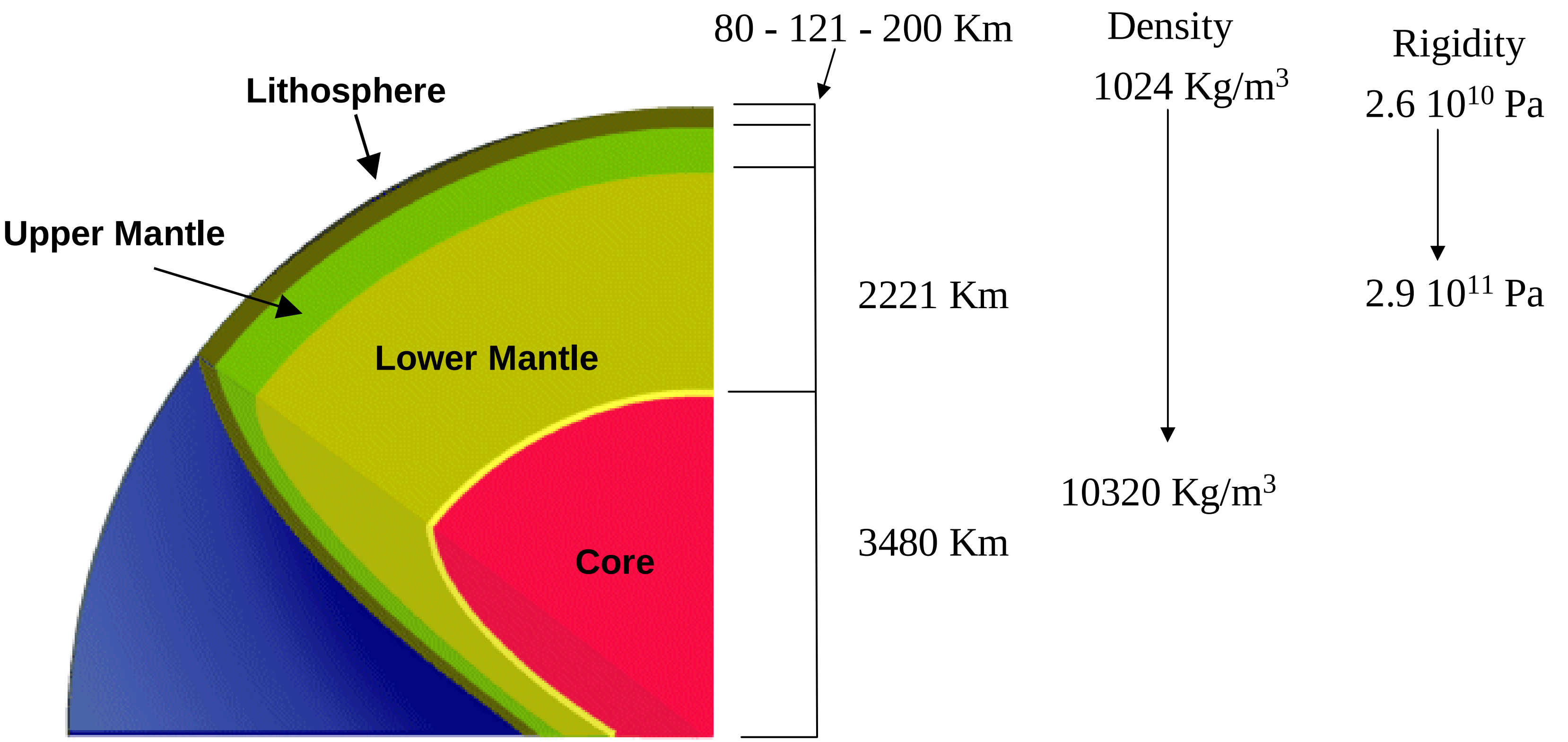

Upper Mantle Viscosity $\nu_{UP} = 10^{19}\text{-}6\text{x}10^{21}$ Pa s

Lower Mantle Viscosity $\nu_{LW} = 10^{21}\text{-}6\text{x}10^{23}$ Pa s

Global Problem - Search for best viscosity

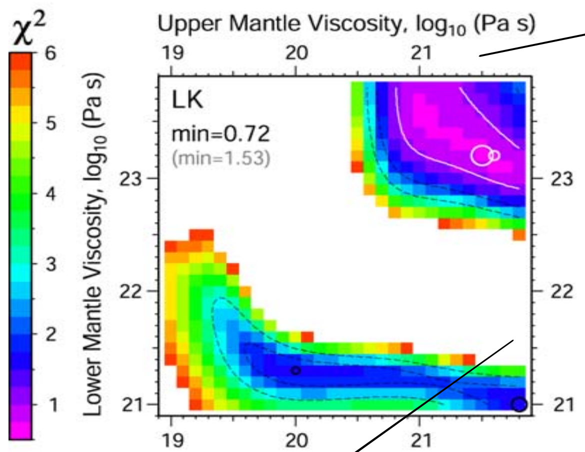

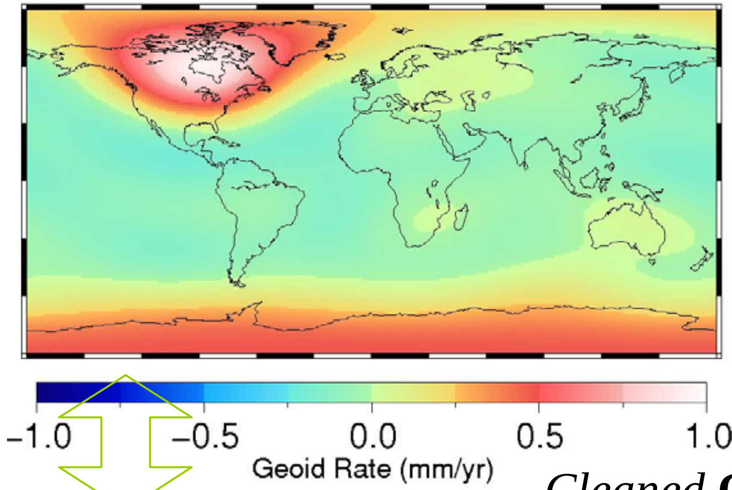

ν_{UP} = $3.1\text{x}10^{20}$ Pa s

ν_{LW} = $1.5\text{x}10^{23}$ Pa s

Cleaned **GRACE**

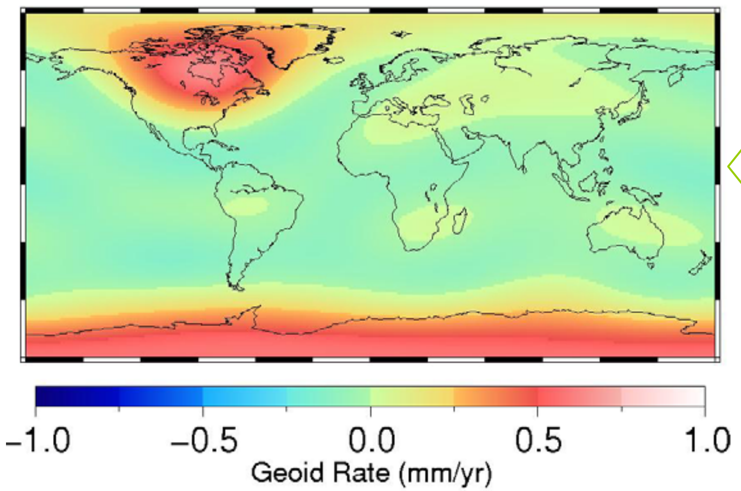

ν_{UP} = $6.3\text{x}10^{21}$ Pa s ν_{LW} = $1.0\text{x}10^{21}$ Pa s

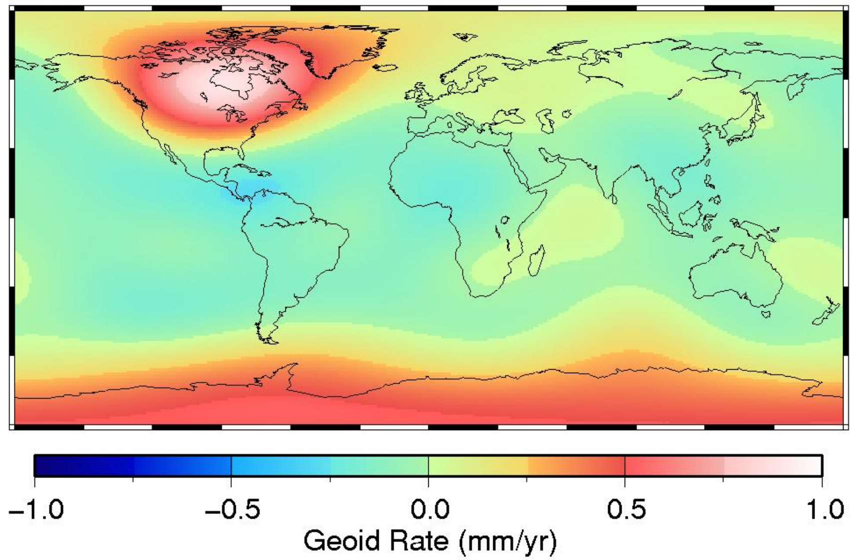

Global Problem - Search for best viscosity

Zonals $\dot{J}$

GRACE

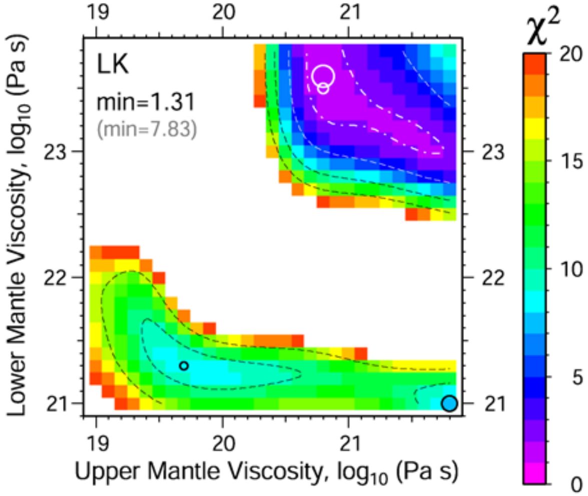

SLR

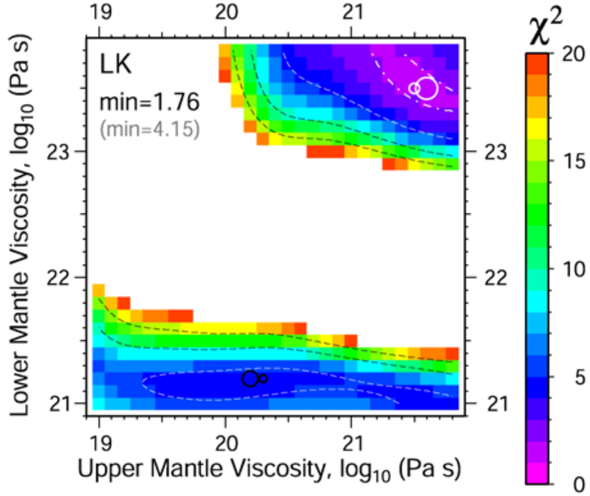

Polar Region Mass Balance from GRACE

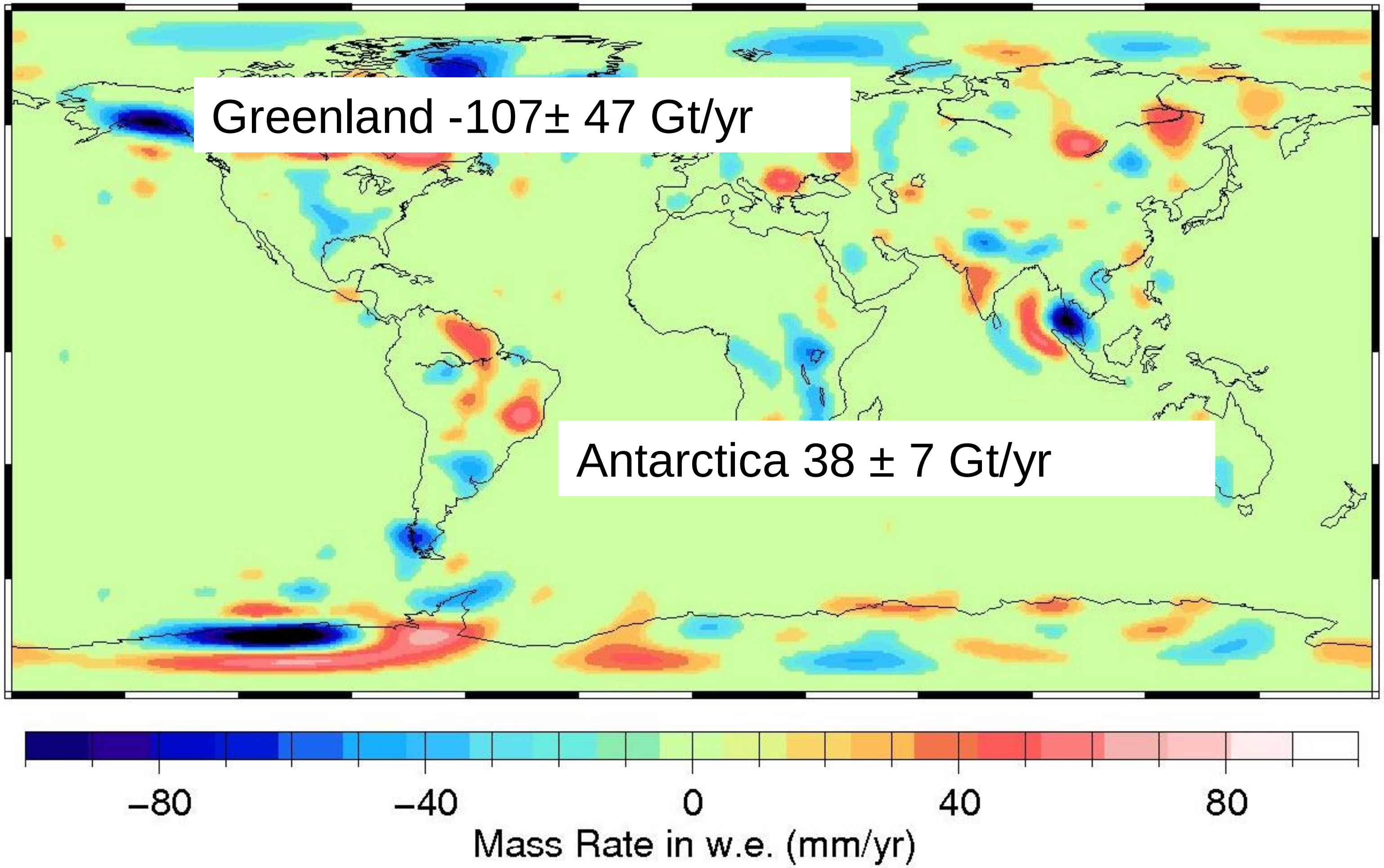

Worldwide Glacier Shrinkage

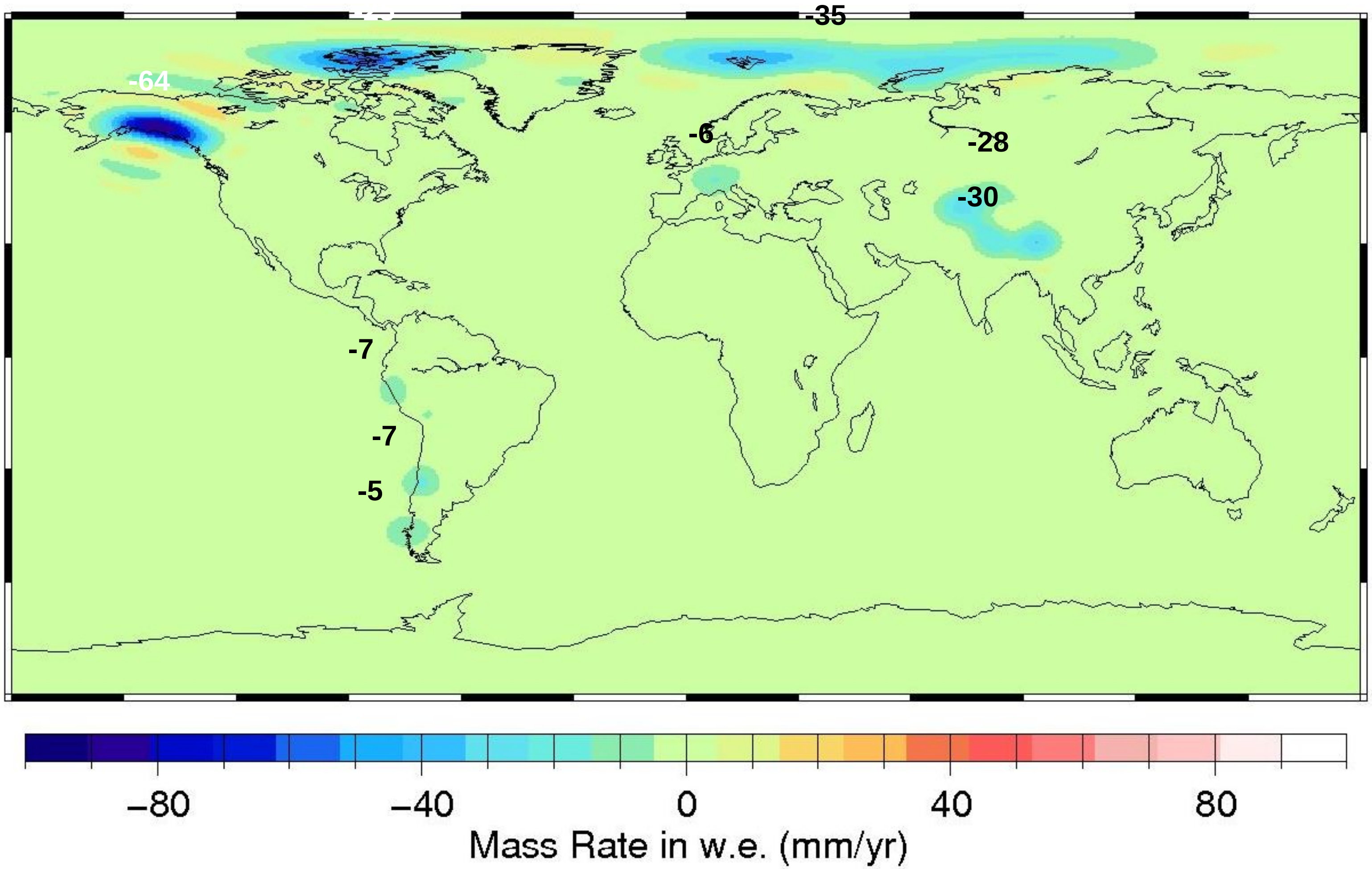

UNIVERSITA' DEGLI STUDI DI MILANO

Dep. of Earth Sciences - Sec. Geophysics

Lithosphere=80 Km

MOD 21

ν_{UM}=0.5X10^{21} Pa s ν_{LM}=1.0X10^{21} Pa s

MOD 26

ν_{UM}=0.5X10^{21} Pa s ν_{LM}=1.0X10^{22} Pa s

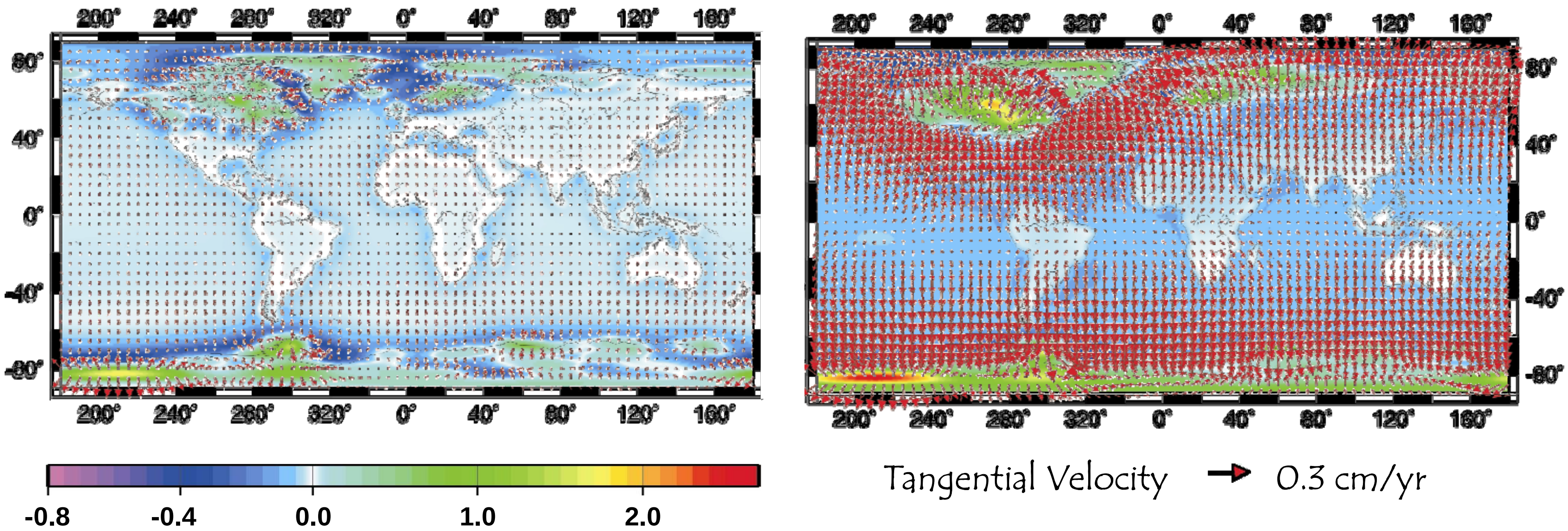

Tangential Velocity → 0.3 cm/yr

Radial velocity cm/yr

UNIVERSITA' DEGLI STUDI DI MILANO
Dep. of Earth Sciences - Sec. Geophysics

Lithosphere=80 Km

MOD 21
ν_{UM}=0.5X10^{21} Pa s ν_{LM}=1.0X10^{21} Pa s

MOD 26
ν_{UM}=0.5X10^{21} Pa s ν_{LM}=1.0X10^{22} Pa s

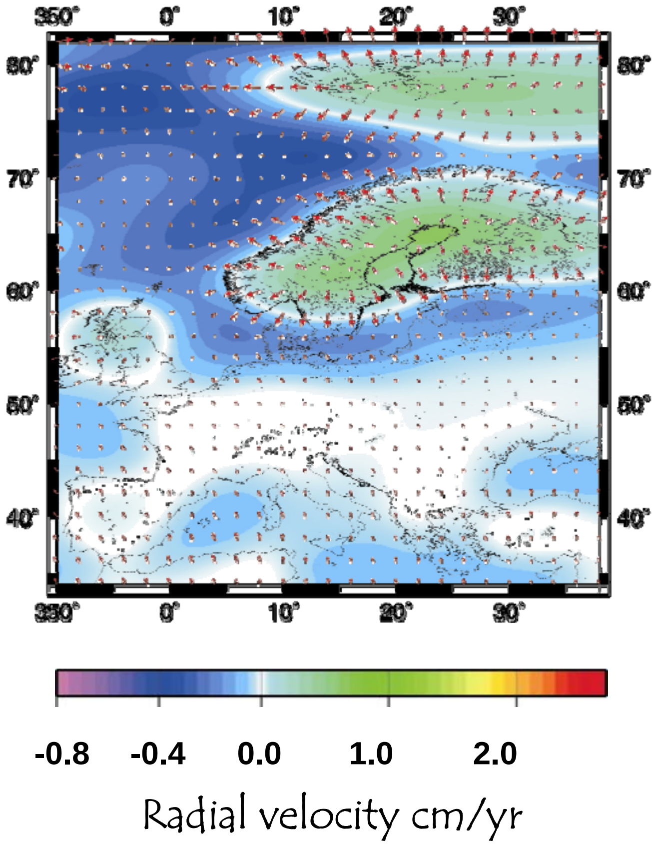

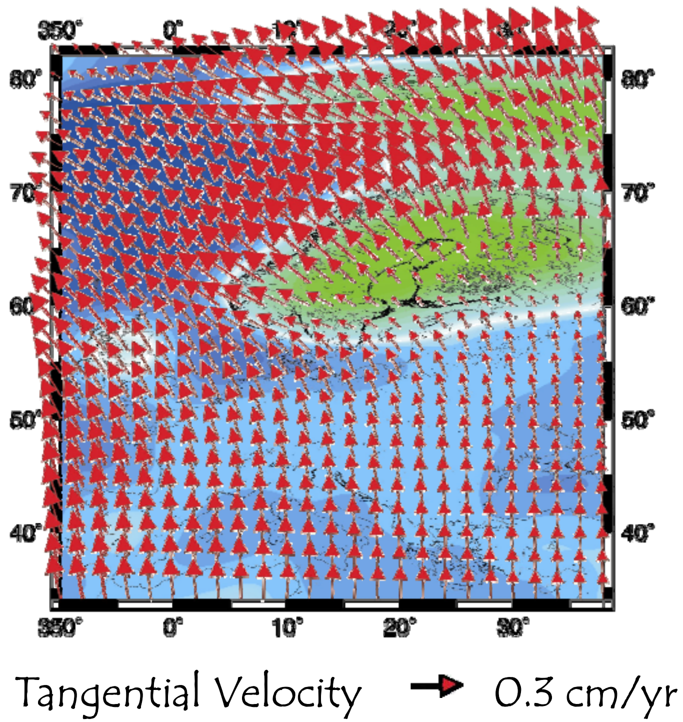

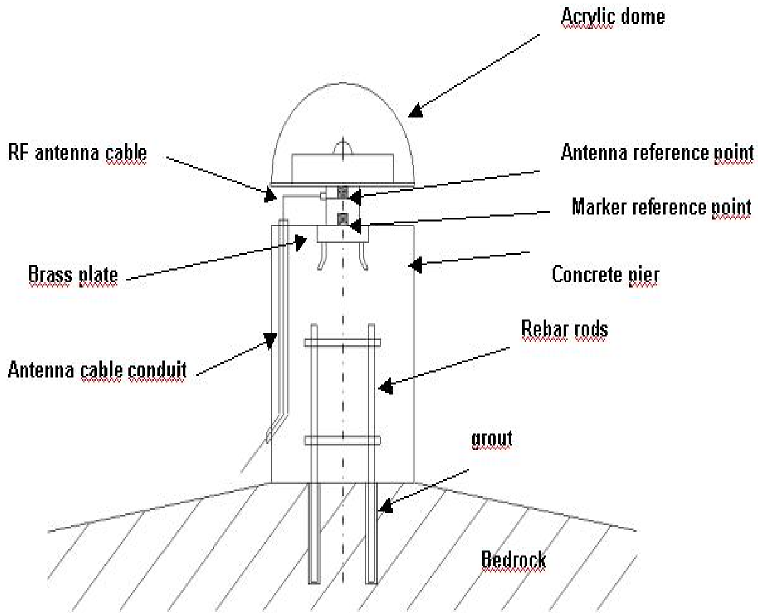
Acrylic dome
RF antenna cable
Antenna reference point
Marker reference point
Brass plate
Concrete pier
Rebar rods
Antenna cable conduit
grout
Bedrock

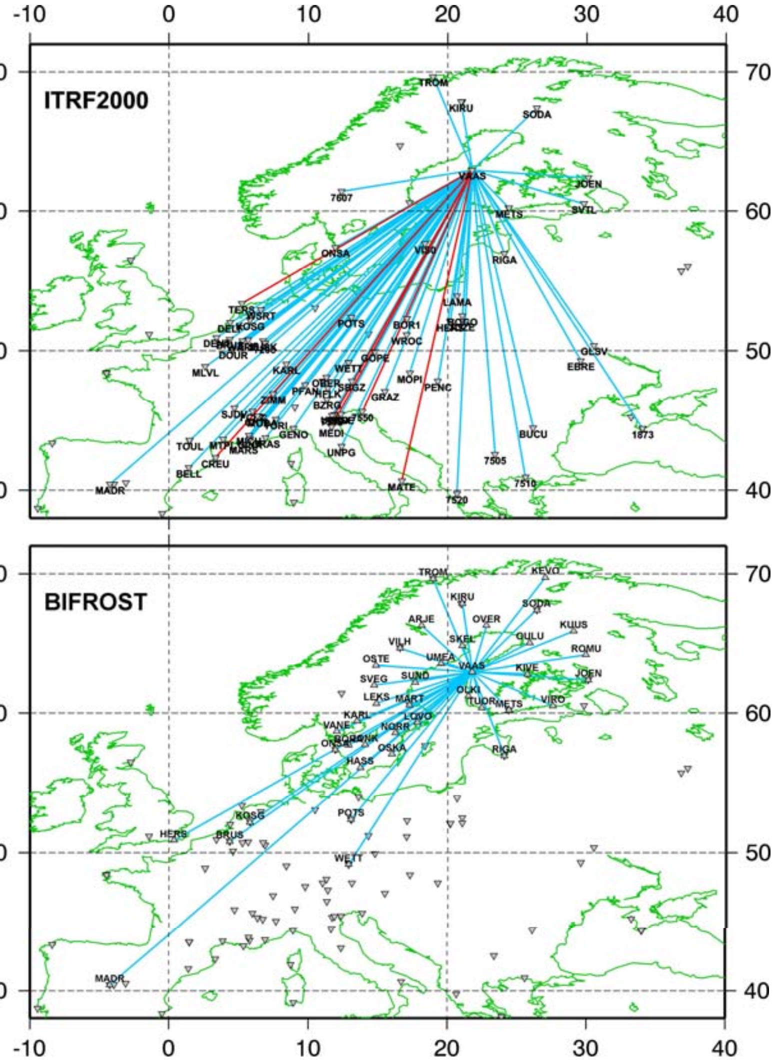
ITRF2000
BIFROST
TROM
KIRU
SODA
VAAS
JOEN
METS
ONSA
RIGA
POTS
WETT
MADR
KEVO
ARJE
OVER
OULU
KUUS
ROMU
VILH
SKEL
OSTE
UMEA
KIVE
SUND
SVEG
LEKS
MART
OLKI
TUOR
VIRO
KARL
VANE
NORR
LOVO
OSKA
HASS
KOSG
HERS
BRUS
BUCU
MATE
GRAZ
PENC
MOPI
WROC
BOR1
LAMA
GLSV
EBRE
TOUL
BELL
CREU
GENO
UNPG
MEDI
ZIMM
KOSG
TERS
DOUR
MLVL
7505
7510
7520
1873
7607

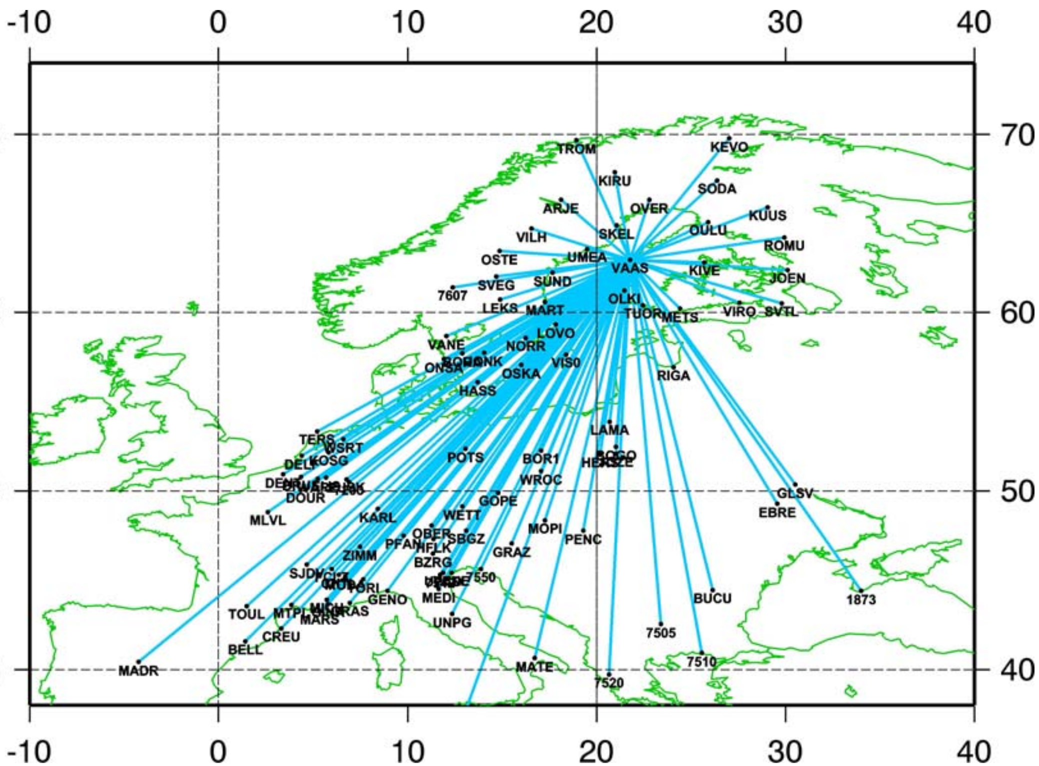
-10
0
10
20
30
40
70
60
50
40
TROM
KEVO
KIRU
SODA
ARJE
OVER
KUUS
SKEL
OULU
VILH
ROMU
OSTE
UMEA
VAAS
KIVE
JOEN
SVEG
SUND
7607
OLKI
LEKS
MART
TUOR
METS
VIRO
SVTL
LOVO
VANE
NORR
VIS0
ONSA
OSKA
RIGA
HASS
LAMA
TERS
WSRT
KOSG
DELF
POTS
BOR1
WROC
DOUR
GOPE
GLSV
EBRE
MLVL
KARL
WETT
MOPI
PENC
OBER
PFAN
HFLK
SBGZ
GRAZ
ZIMM
BZRG
7550
SJDV
GENO
MEDI
BUCU
TOUL
MARS
UNPG
7505
CREU
BELL
MADR
MATE
7510
7520
1873

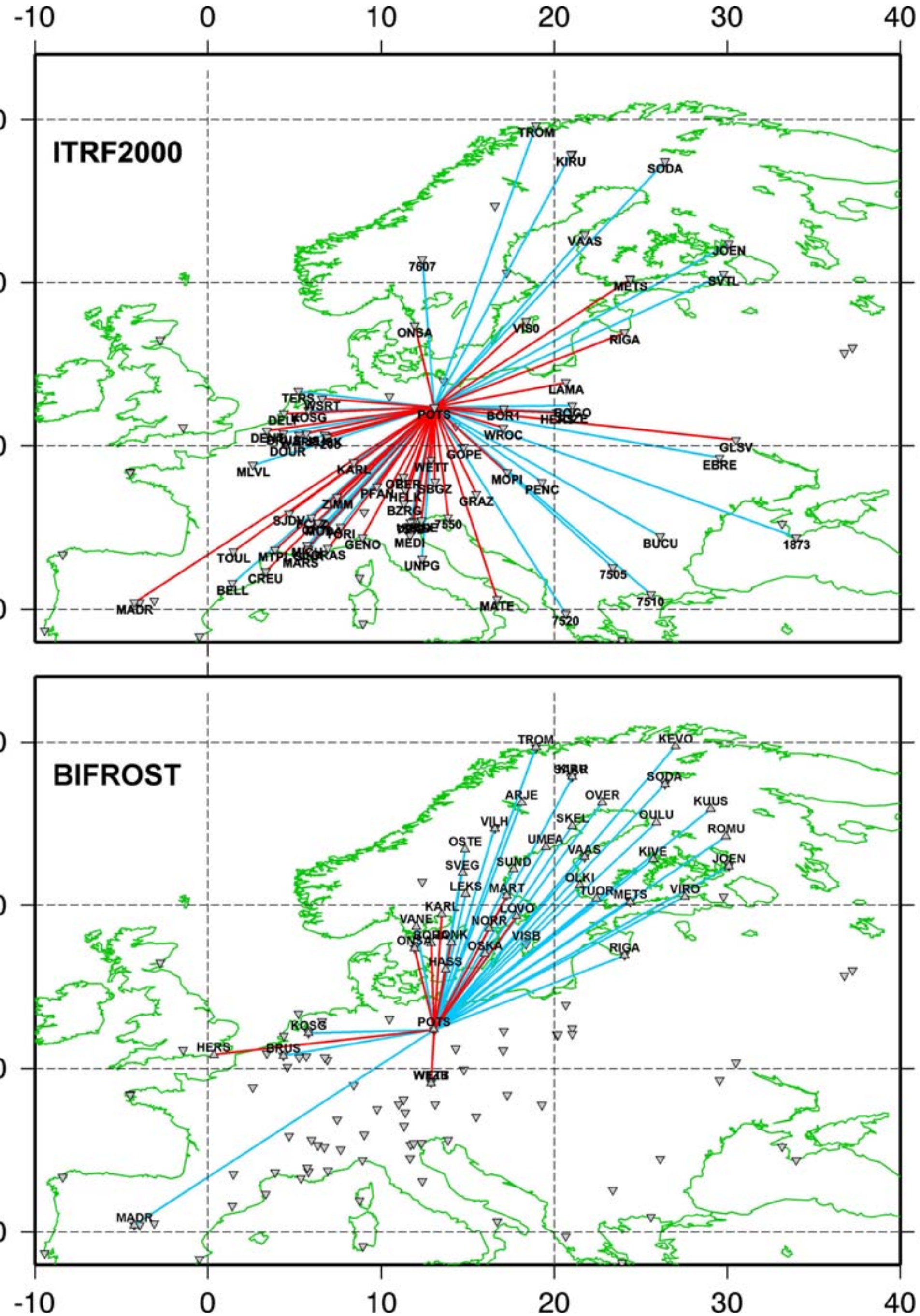

ITRF2000
BIFROST
-10
0
10
20
30
40
70
60
50
40
TROM
KIRU
SODA
VAAS
JOEN
7607
METS
SVTL
ONSA
VIS0
RIGA
LAMA
TERS
WSRT
KOSG
DELF
POTS
BOR1
WROC
GLSV
EBRE
DOUR
MLVL
KARL
WETT
GOPE
MOPI
PENC
OBER
HFLK
SBGZ
GRAZ
PFAN
ZIMM
BZRG
SJDV
GENO
MEDI
BUCU
1873
TOUL
MTPL
MARS
CREU
BELL
UNPG
7505
7510
MADR
MATE
7520
KEVO
ARJE
OVER
KUUS
VILH
SKEL
OULU
ROMU
OSTE
UMEA
SVEG
SUND
KIVE
LEKS
MART
OLKI
TUOR
VIRO
VANE
LOVO
NORR
VISB
OSKA
HASS
HERS
BRUS

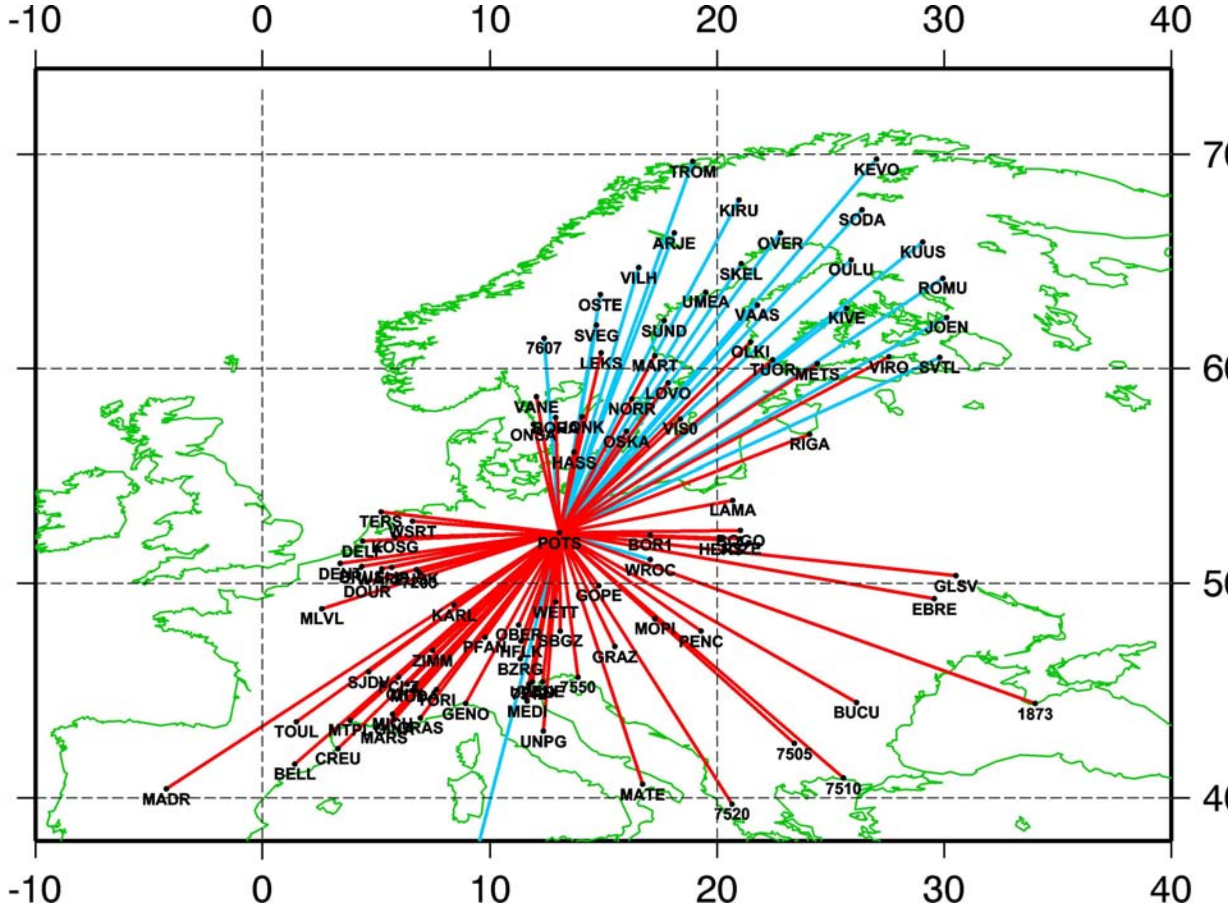

-10
0
10
20
30
40
70
60
50
40
TROM
KEVO
KIRU
SODA
ARJE
OVER
KUUS
OULU
SKEL
VILH
ROMU
UMEA
OSTE
VAAS
KIVE
SUND
SVEG
JOEN
7607
OLKI
LEKS
MART
TUOR
METS
VIRO
SVTL
LOVO
NORR
VANE
VIS0
ONSA
OSKA
RIGA
HASS
LAMA
TERS
WSRT
POTS
BOR1
KOSG
DELF
WROC
GLSV
DOUR
GOPE
EBRE
MLVL
KARL
WETT
MOPI
OBER
PENC
SBGZ
PFAN
HFLK
GRAZ
ZIMM
BZRG
SJDV
7550
GENO
MEDI
BUCU
1873
TOUL
MARS
UNPG
7505
CREU
BELL
7510
MADR
MATE
7520

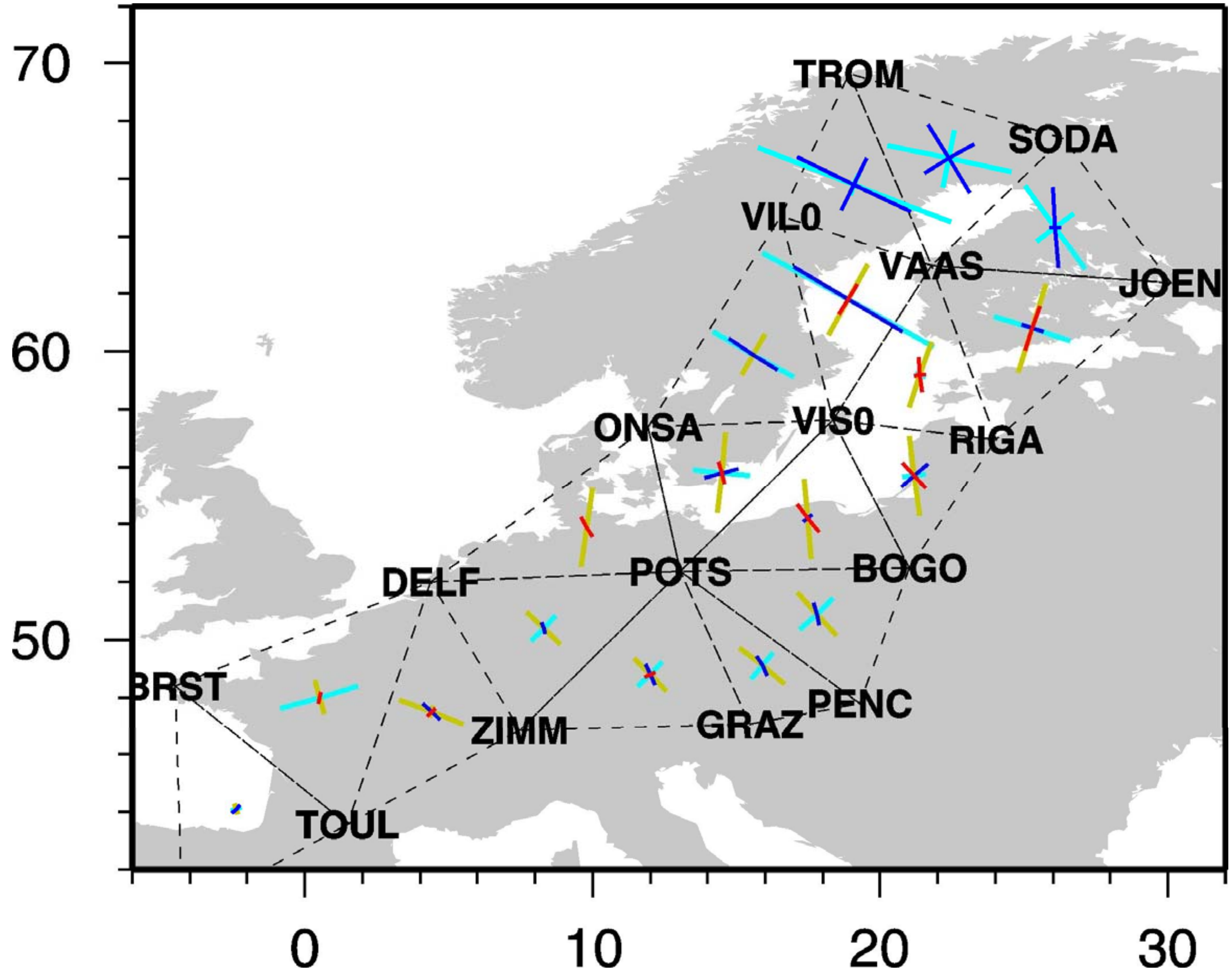

TROM
SODA
VIL0
VAAS
JOEN
ONSA
VIS0
RIGA
DELF
POTS
BOGO
BRST
ZIMM
GRAZ
PENC
TOUL
70
60
50
0
10
20
30

Geophysical modelling and GPS, SAR, GRACE and GOCE data for the understanding of lithospheric and mantle processes - 2

Roberto Sabadini

Dipartimento di Scienze della Terra “A. Desio”
Università di Milano

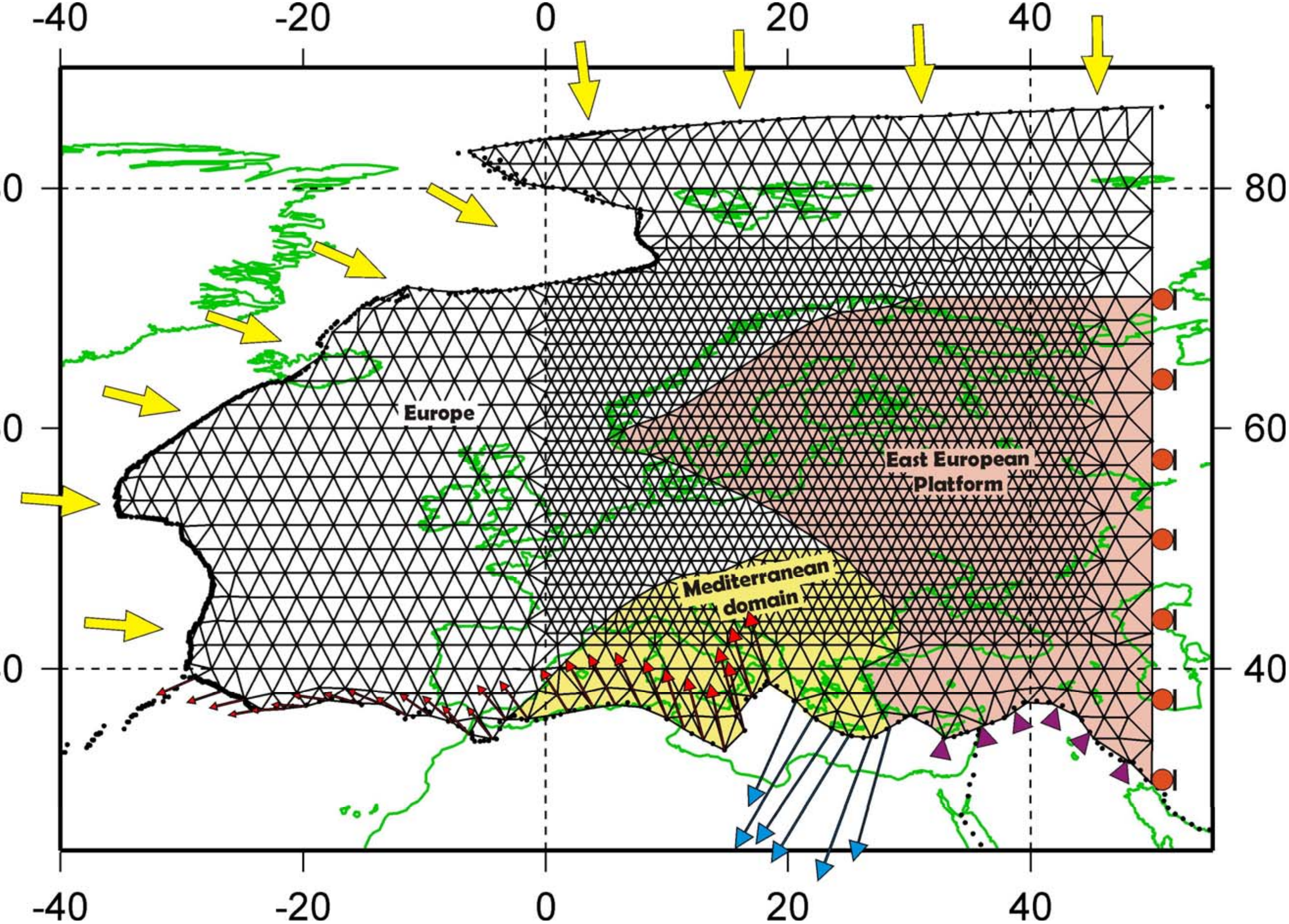
-40
-20
0
20
40
80
60
40
Europe
East European Platform
Mediterranean domain

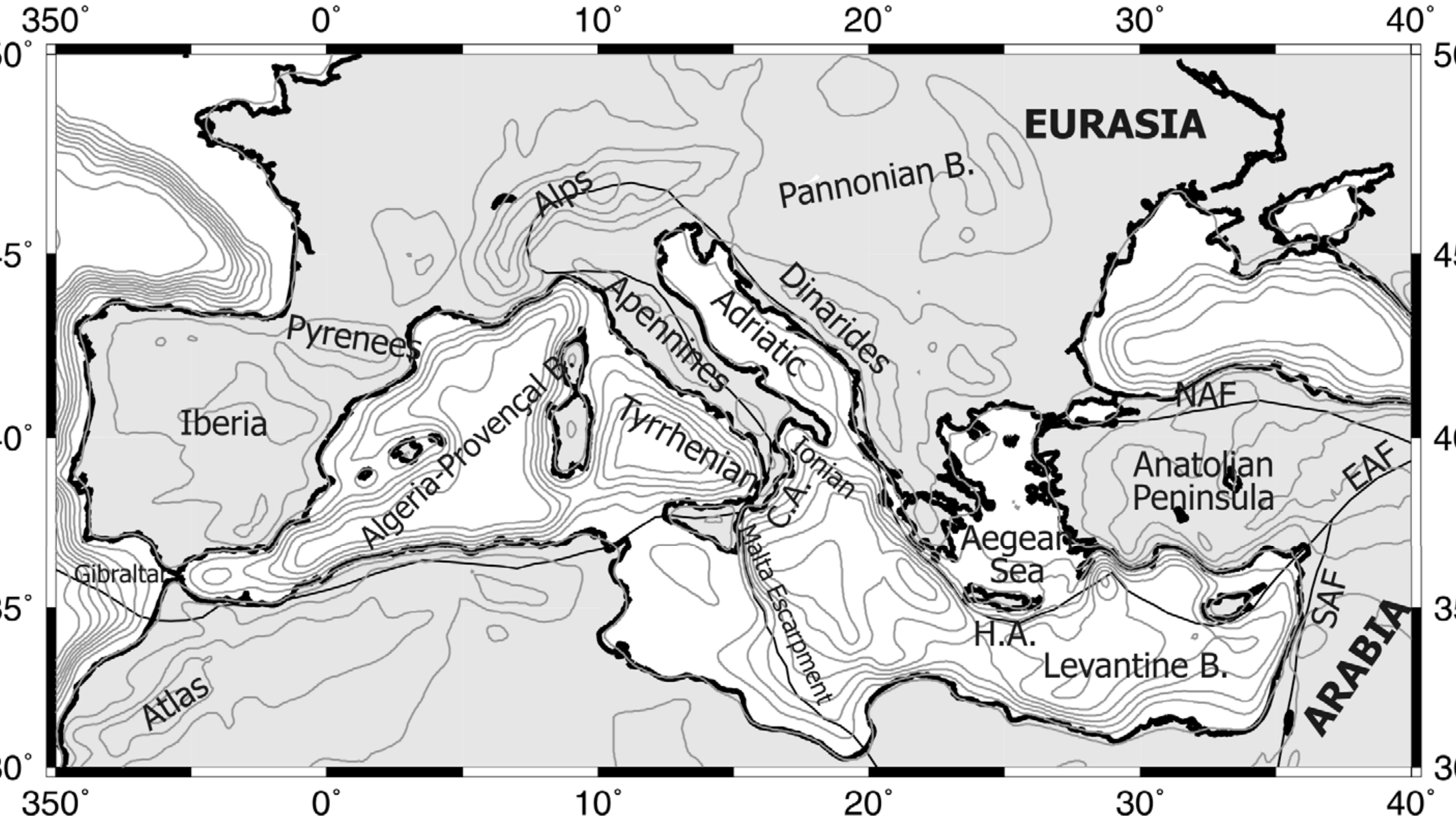

350°
0°
10°
20°
30°
40°
50°
45°
40°
35°
30°
EURASIA
Pannonian B.
Alps
Dinarides
Adriatic
Apennines
Pyrenees
Iberia
Algeria-Provençal B.
Tyrrhenian
Ionian
C.A.
Malta Escarpment
NAF
Anatolian
Peninsula
EAF
Aegean
Sea
SAF
ARABIA
H.A.
Levantine B.
Gibraltar
Atlas

Implementation of numerical and analytical forward and inverse modeling of crust and lithosphere deformation

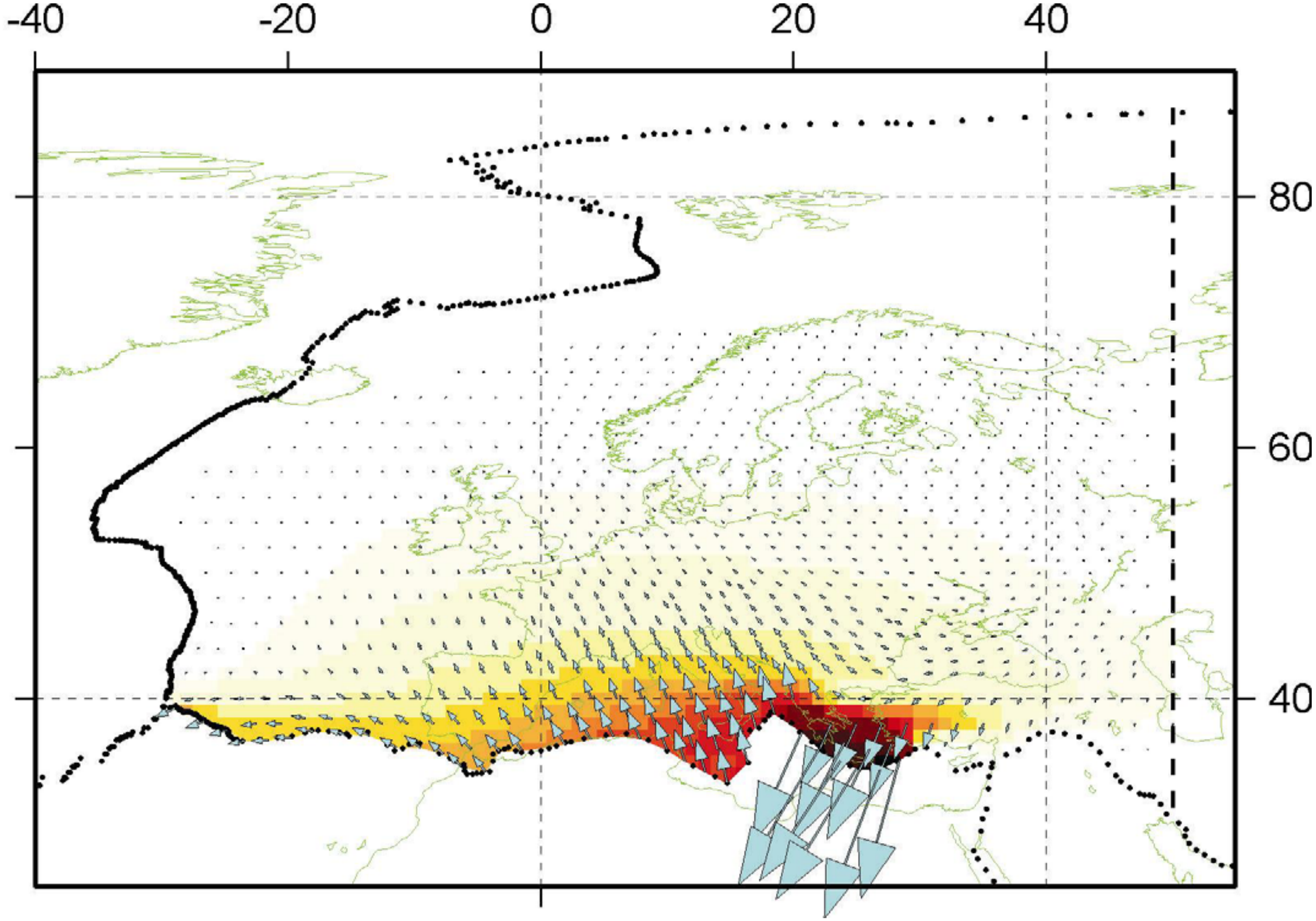

Marotta, A. M. et al., JGR 2004 – Combined effects of tectonics and glacial isostatic adjustment on intraplate deformation in central and northern Europe: Application to Geodetic baseline analysis.

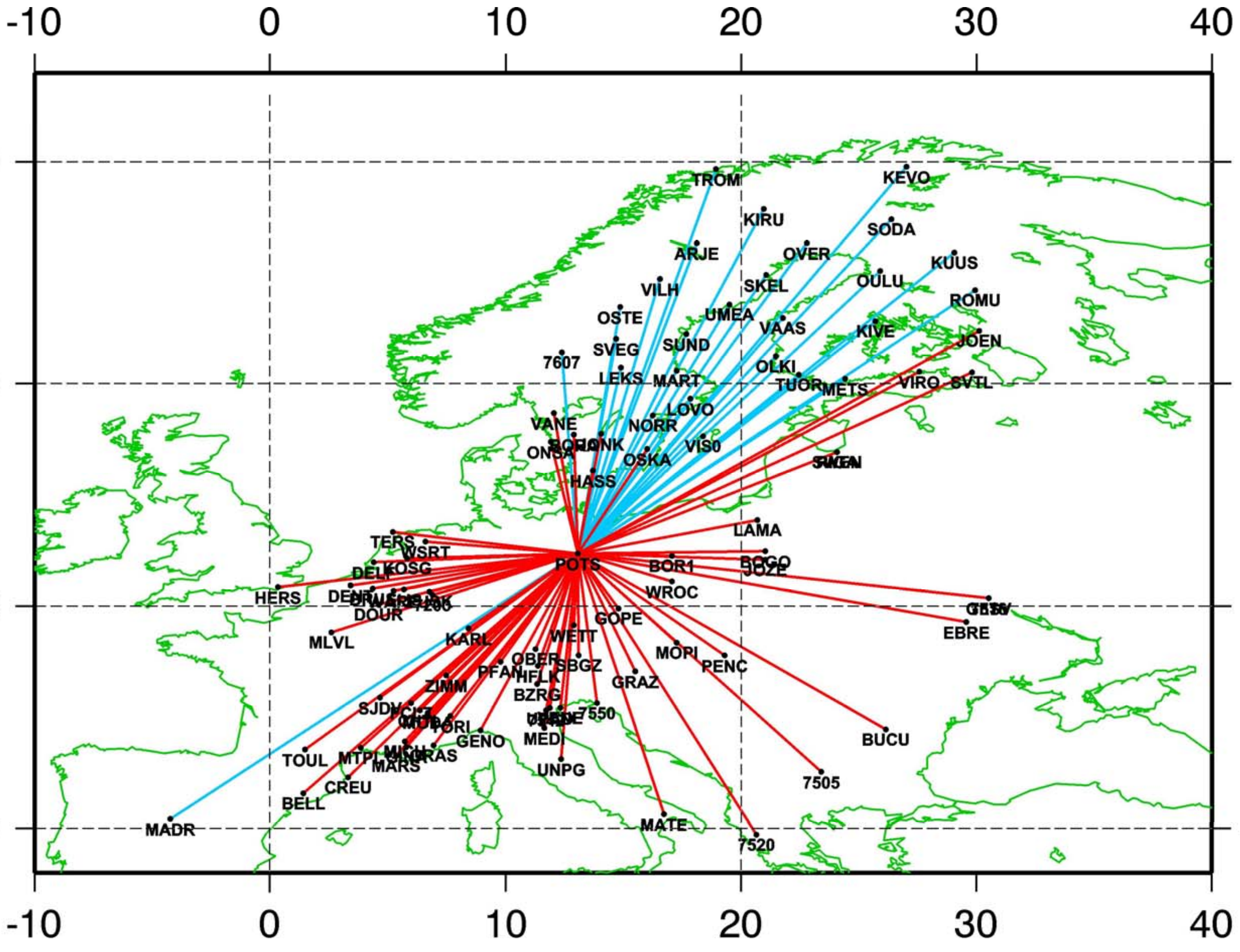

-10
0
10
20
30
40
70
60
50
40
TROM
KEVO
KIRU
SODA
ARJE
OVER
KUUS
OULU
VILH
SKEL
ROMU
OSTE
UMEA
VAAS
KIVE
SUND
SVEG
JOEN
7607
OLKI
LEKS
MART
TUOR
METS
VIRO
SVTL
LOVO
VANE
NORR
ONSA
VIS0
OSKA
HASS
LAMA
TERS
WSRT
POTS
BOR1
JOZE
KOSG
DELF
WROC
HERS
DENT
7200
DOUR
GOPE
EBRE
MLVL
KARL
WETT
MOPI
OBER
SBGZ
PENC
PFAN
HFLK
GRAZ
ZIMM
BZRG
SJDV
7550
PORI
GENO
MEDI
BUCU
TOUL
MTPL
MARS
GRAS
CREU
UNPG
7505
BELL
MADR
MATE
7520

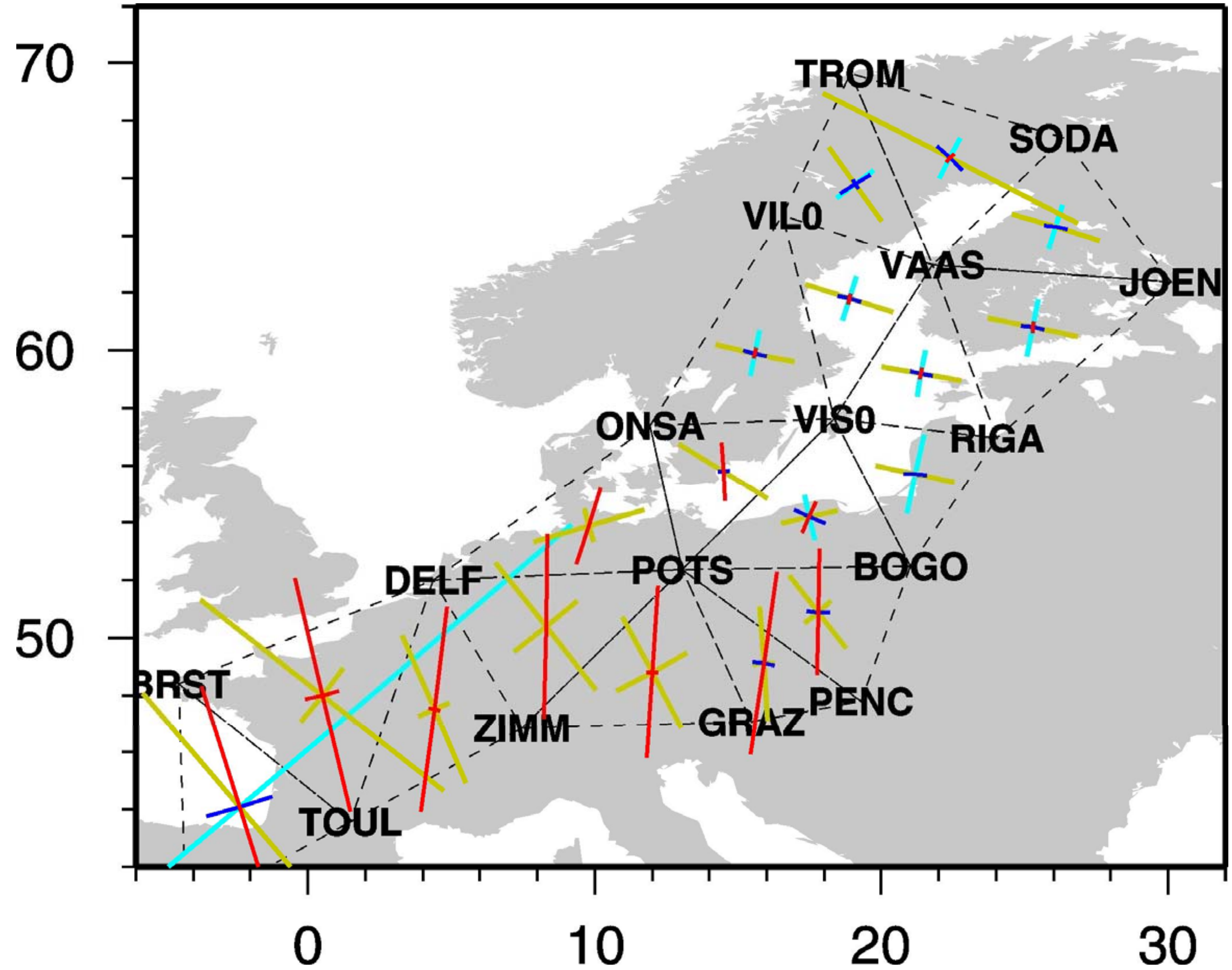

70
60
50
0
10
20
30
TROM
SODA
VIL0
VAAS
JOEN
ONSA
VIS0
RIGA
DELF
POTS
BOGO
BRST
ZIMM
GRAZ
PENC
TOUL

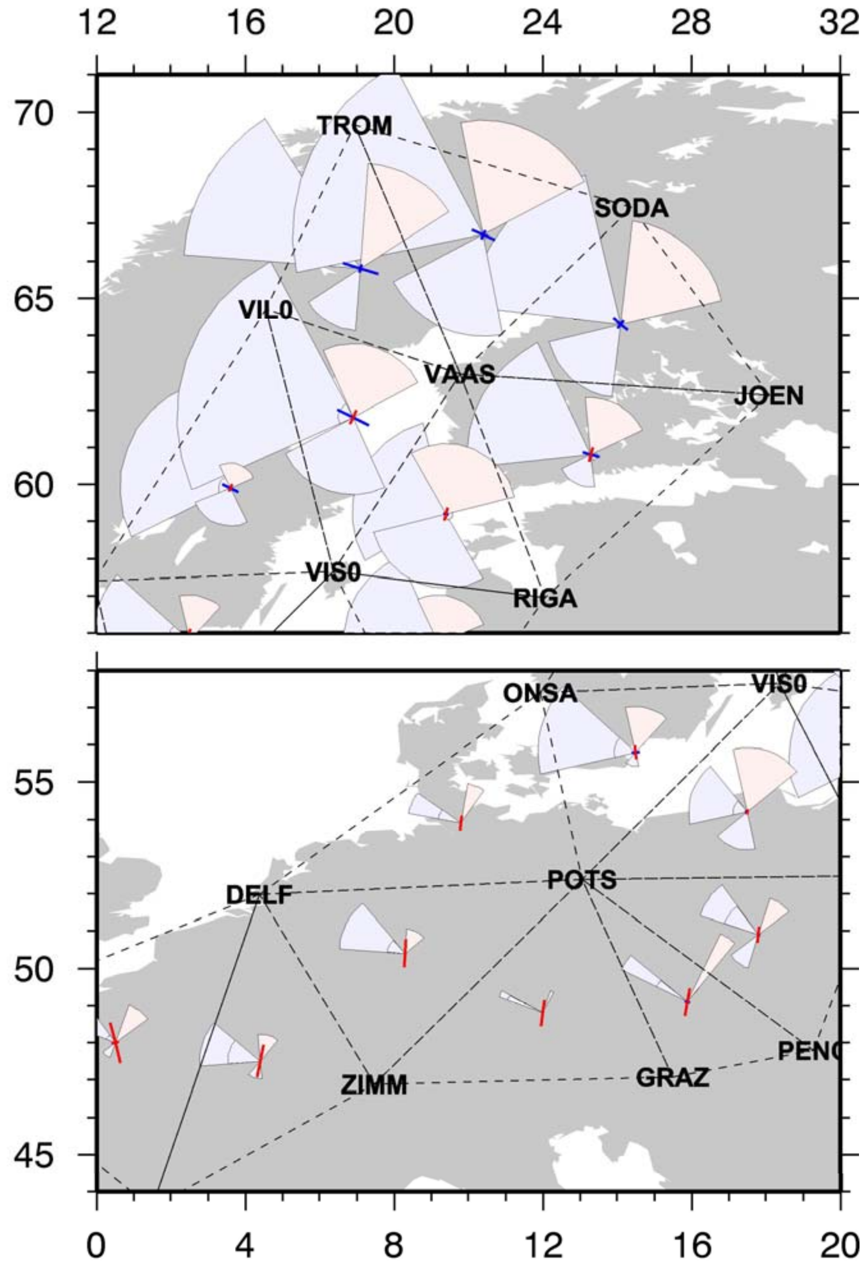

12
16
20
24
28
32
70
65
60
TROM
SODA
VIL0
VAAS
JOEN
VIS0
RIGA
55
50
45
ONSA
VIS0
DELF
POTS
ZIMM
GRAZ
PENC
0
4
8
12
16
20

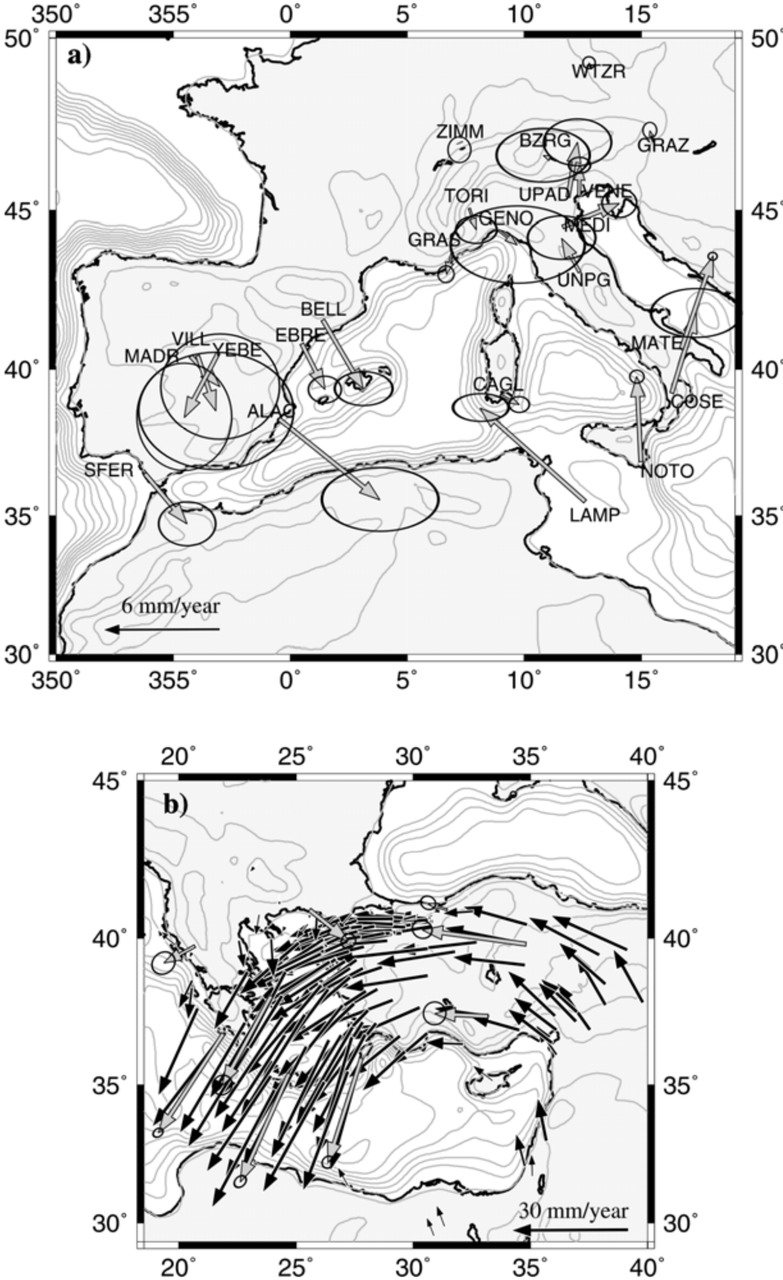
a)
WTZR
ZIMM
BZRG
GRAZ
TORI
UPAD
VENE
GENO
MEDI
GRAS
UNPG
BELL
EBRE
VILL
MADR
YEBE
ALAC
MATE
CAGL
COSE
SFER
NOTO
LAMP
6 mm/year
350° 355° 0° 5° 10° 15°
30° 35° 40° 45° 50°
b)
30 mm/year
20° 25° 30° 35° 40°
30° 35° 40° 45°

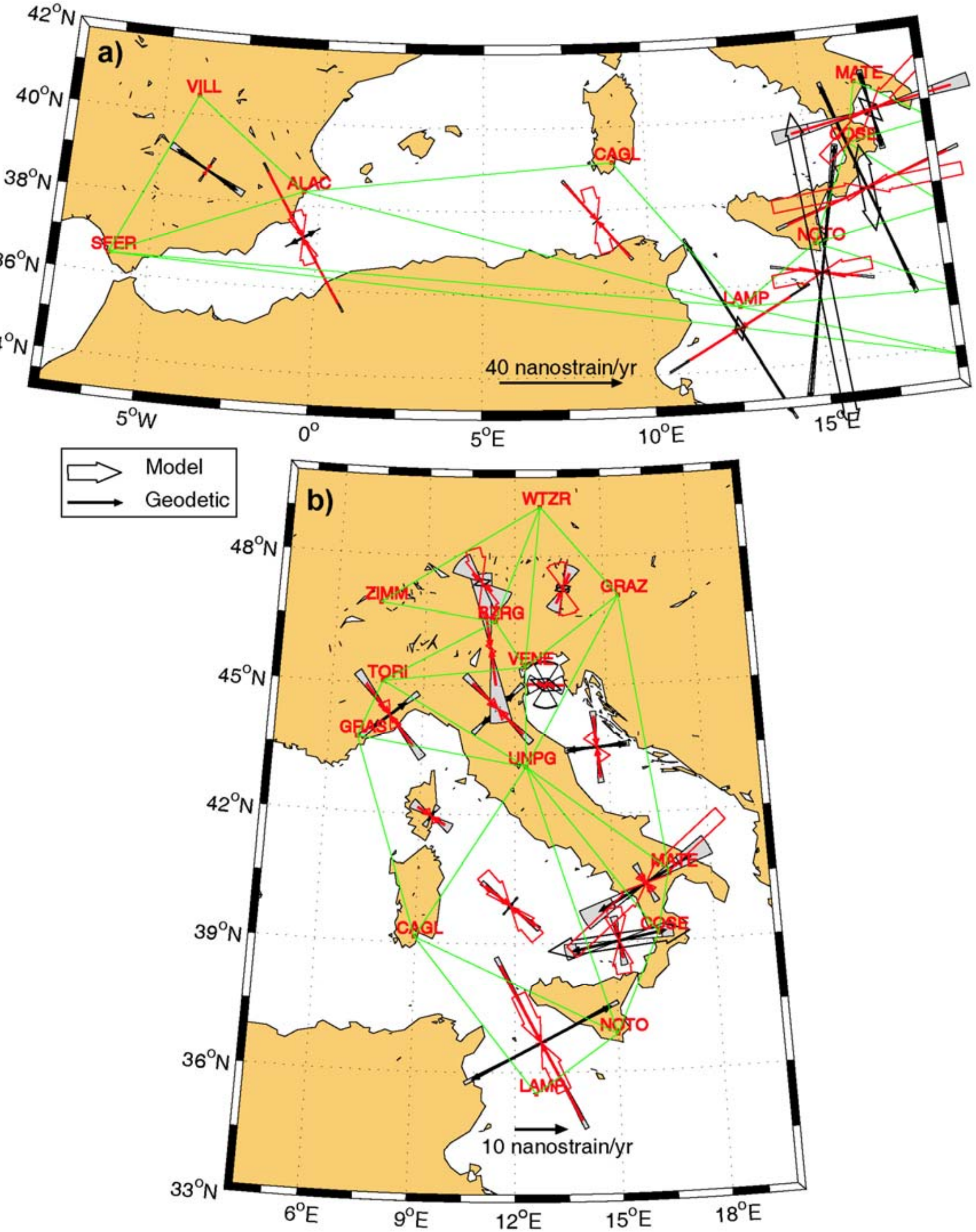

a)
VILL
ALAC
SFER
CAGL
MATE
COSE
NOTO
LAMP
40 nanostrain/yr
42°N
40°N
38°N
36°N
34°N
5°W
0°
5°E
10°E
15°E
Model
Geodetic
b)
WTZR
ZIMM
BZRG
GRAZ
VENE
TORI
GRAS
UNPG
MATE
CAGL
COSE
NOTO
LAMP
10 nanostrain/yr
48°N
45°N
42°N
39°N
36°N
33°N
6°E
9°E
12°E
15°E
18°E

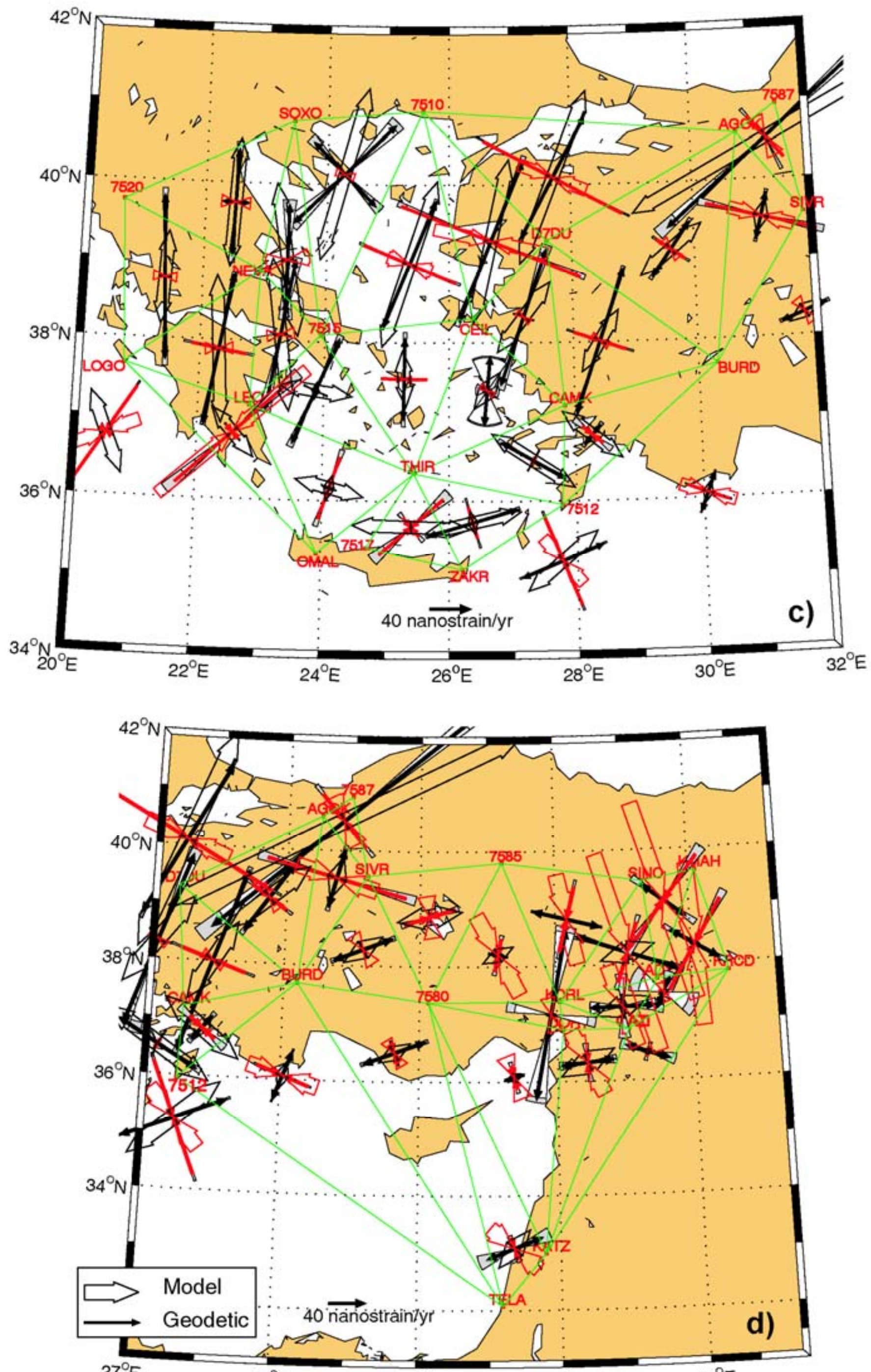

42°N
40°N
38°N
36°N
34°N
20°E
22°E
24°E
26°E
28°E
30°E
32°E
SOXO
7510
7587
AGOK
7520
SIVR
NEST
7515
CEIL
BURD
LOGO
LEON
CAMK
THIR
7512
7517
OMAL
ZAKR
40 nanostrain/yr
c)
42°N
40°N
38°N
36°N
34°N
27°E
30°E
33°E
36°E
39°E
7587
AGOK
SIVR
7585
SINO
MAAH
BURD
7580
CAMK
7512
KATZ
TELA
Model
Geodetic
40 nanostrain/yr
d)

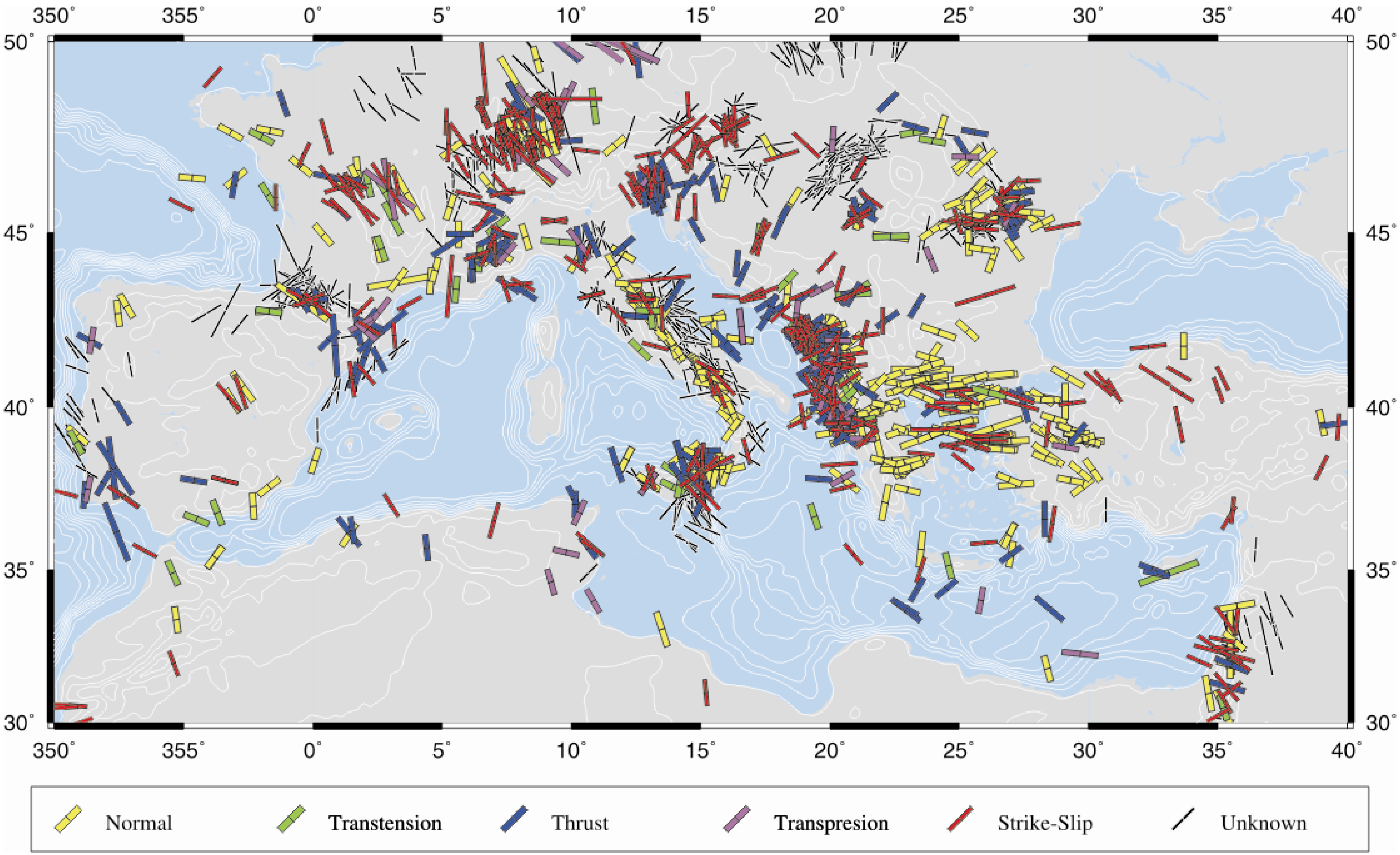
350° 355° 0° 5° 10° 15° 20° 25° 30° 35° 40°
50° 45° 40° 35° 30°
Normal
Transtension
Thrust
Transpresion
Strike-Slip
Unknown

Seismicity (M_s, NEIC 1903-1999) and calculated seismic strain rate

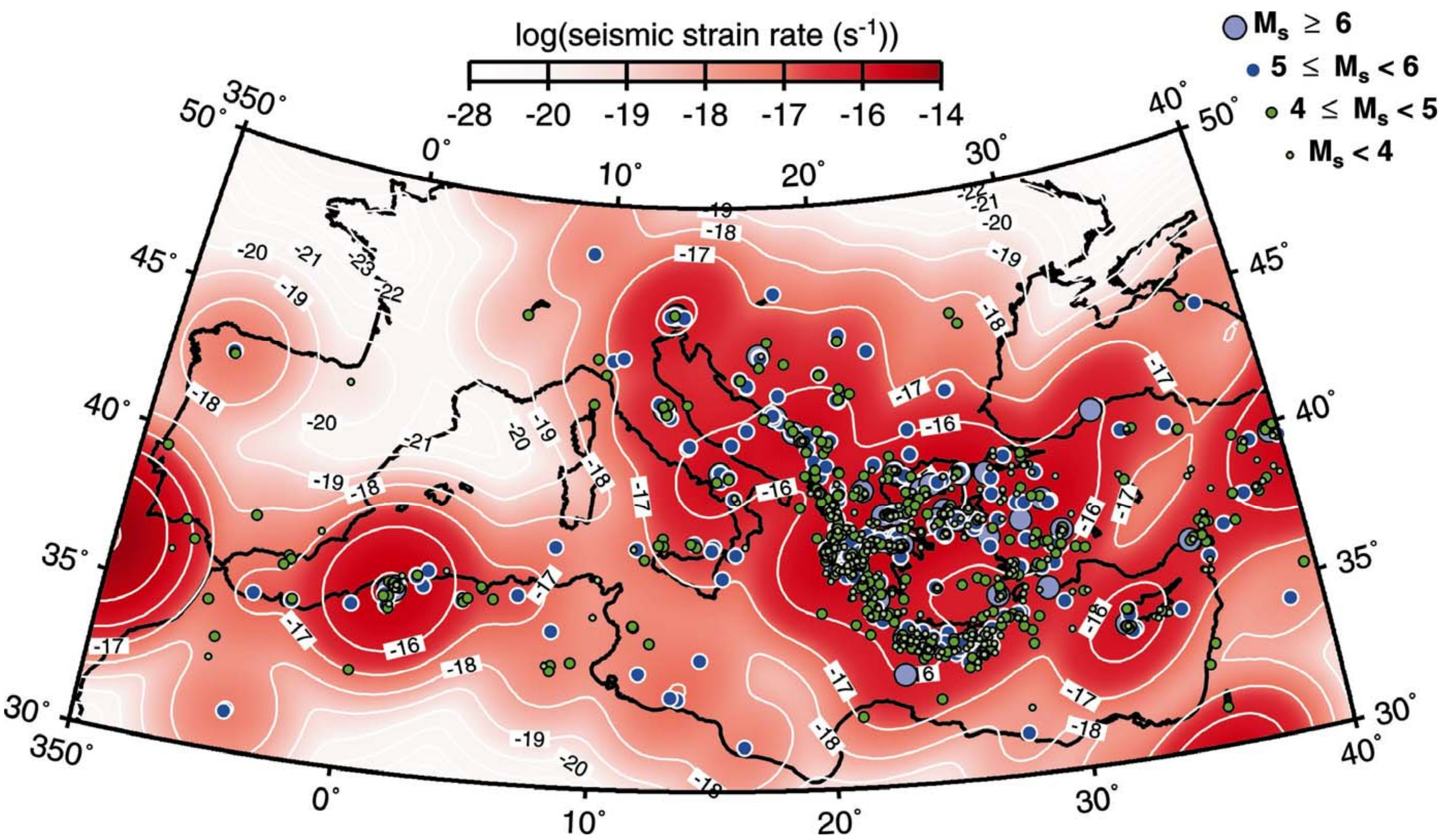

SAR: data acquisition

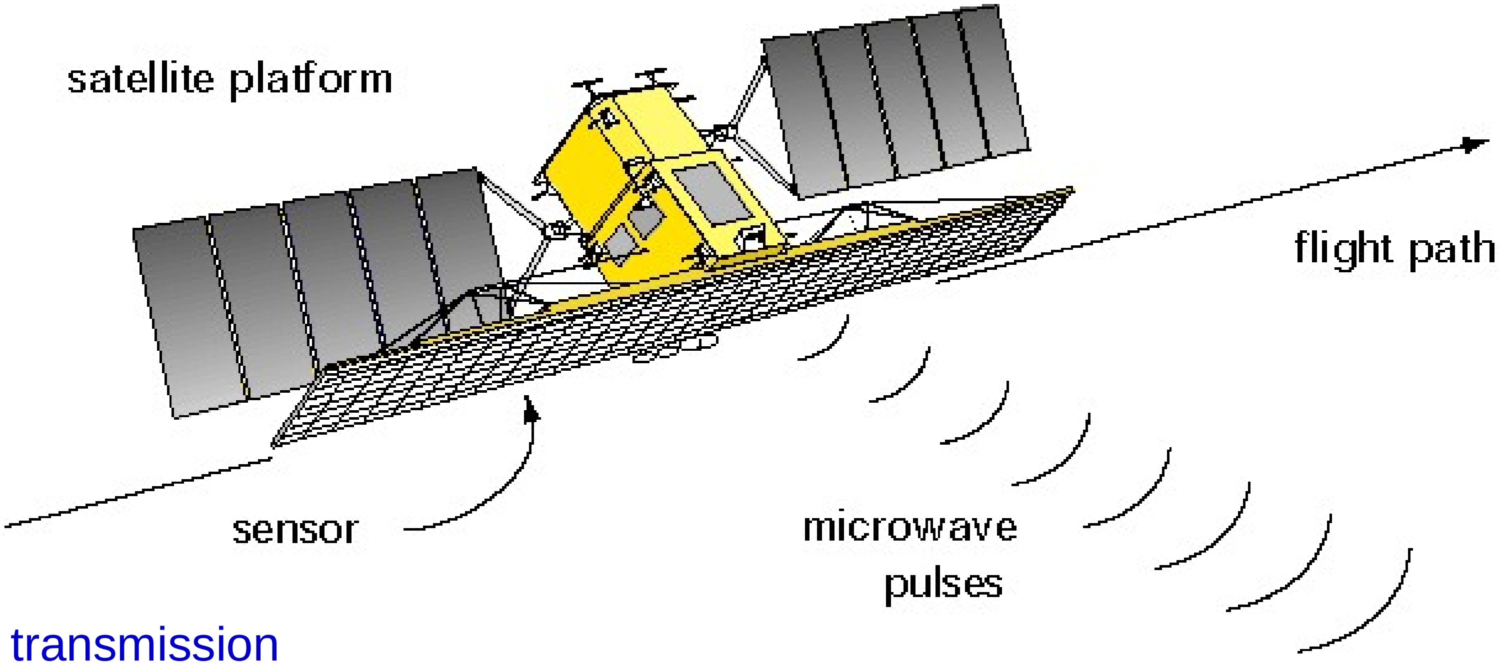

- Pulse transmission
- Propagation, interaction with surface ➔ echoes
- Acquisition of echoes, with a delay: $t = 2\, R\, /\, c$
  ➔ the system measures distances
- Transmission of pulses along the orbit ➔ 2D sampling of terrain

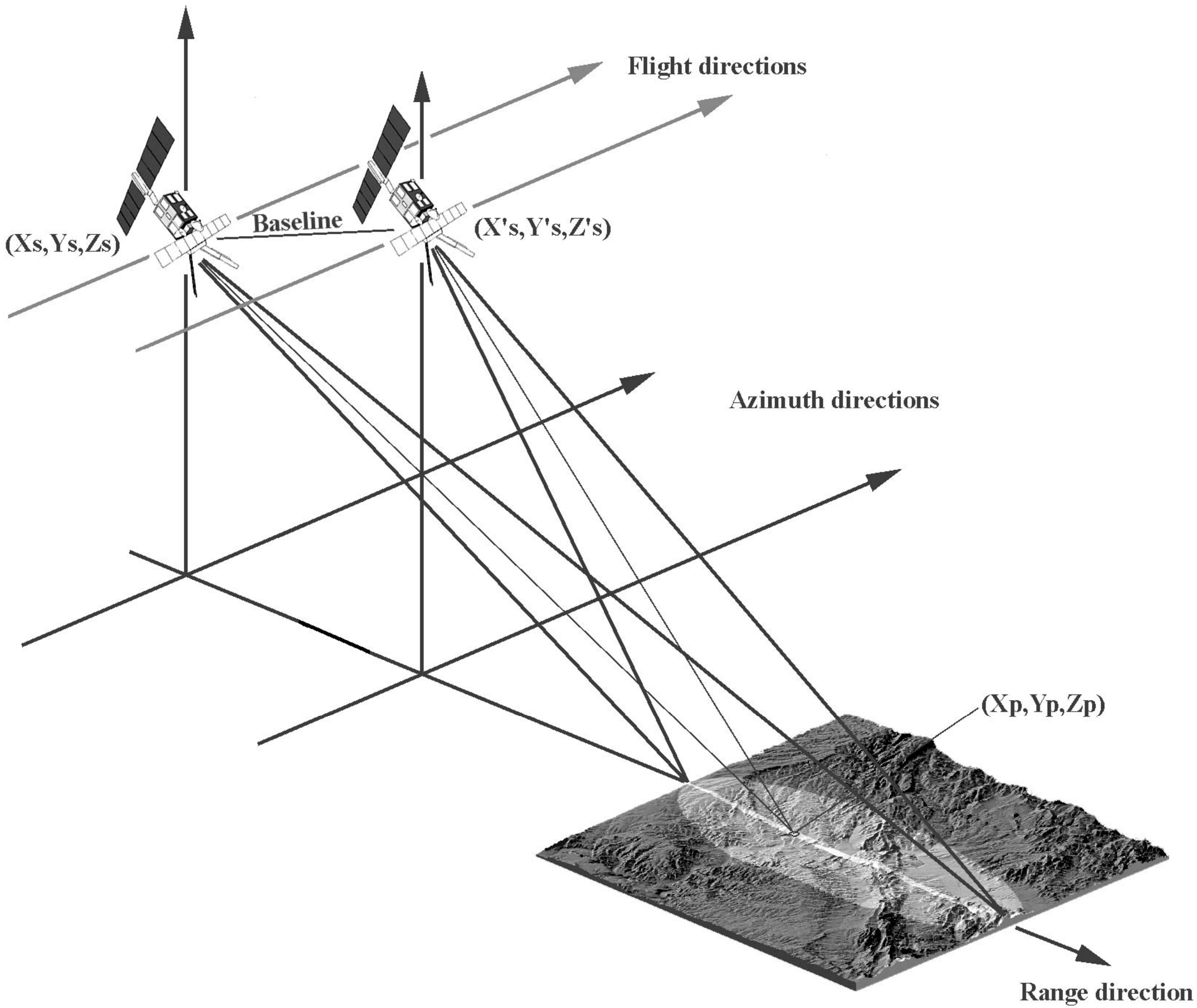
Flight directions
Baseline
(Xs,Ys,Zs)
(X's,Y's,Z's)
Azimuth directions
(Xp,Yp,Zp)
Range direction

Methodology for detecting the vertical movements during the

pre-seismic, co-seismic and post-seismic phases in earthquake prone areas

(**Crippa B. et al., An advanced slip model for the Umbria-Marche earthquake sequence: coseismic displacements observed by SAR interferometry and model inversion, GJI, 2005, in press**).

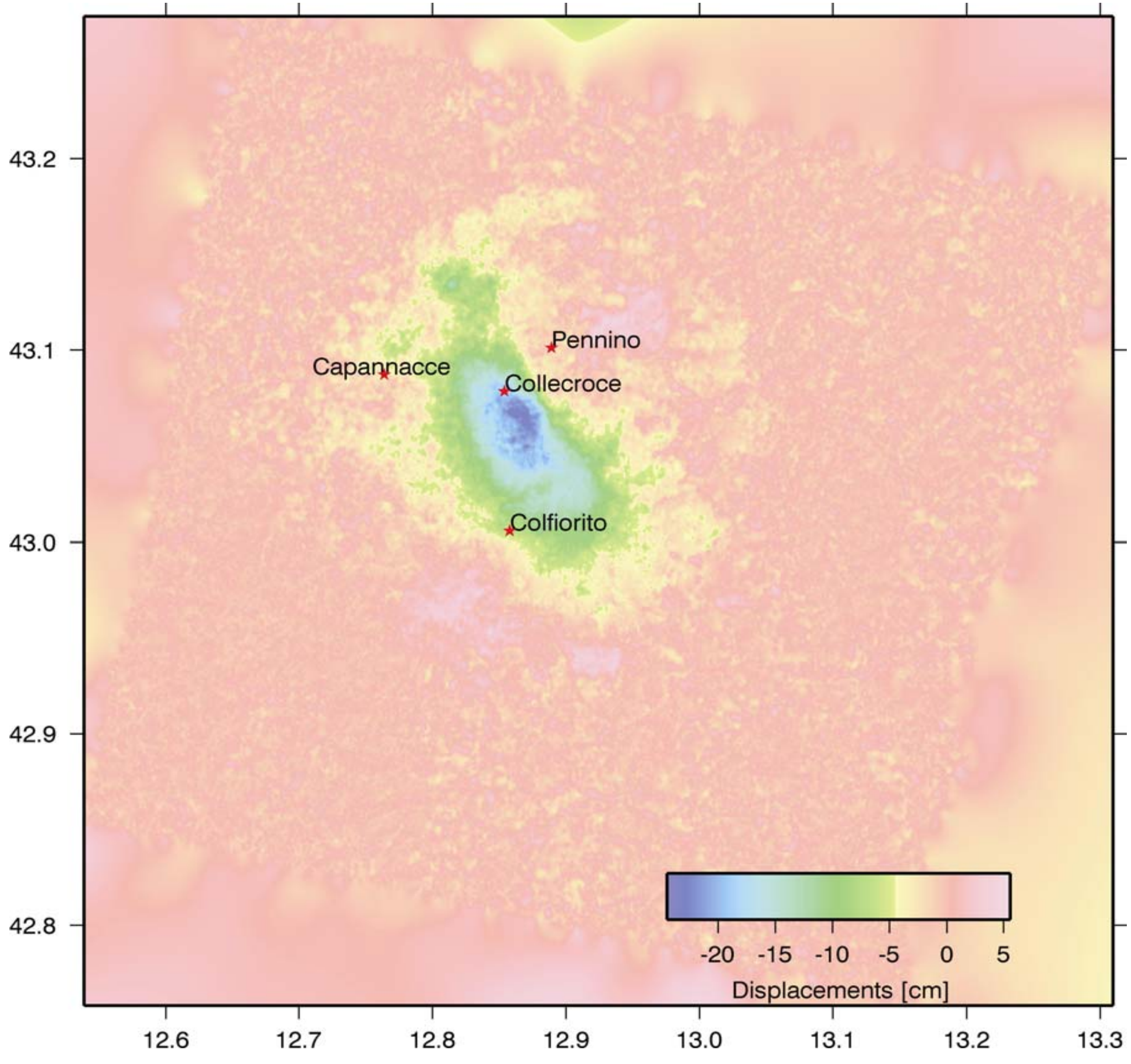

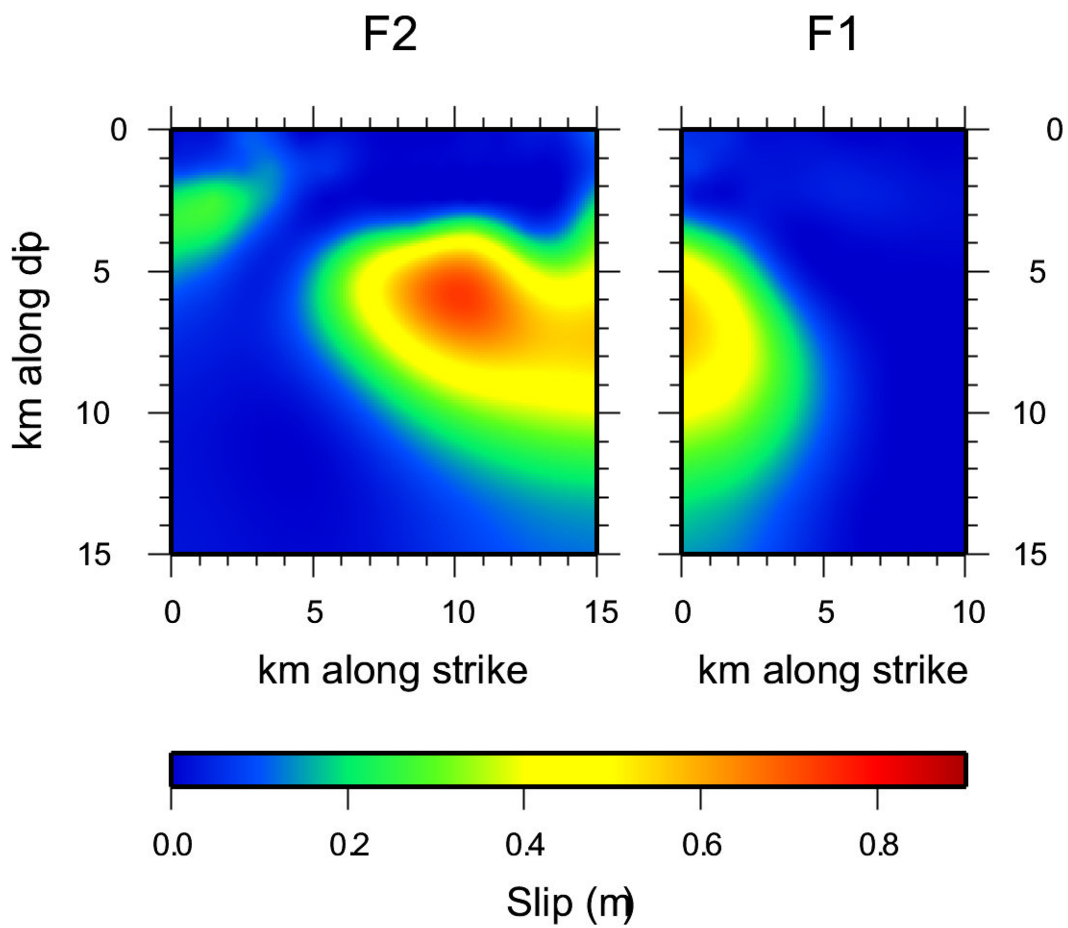

F2
F1
0
5
10
15
km along dp
0
5
10
15
0
5
10
15
km along strike
0
5
10
km along strike
0.0
0.2
0.4
0.6
0.8
Slip (m)

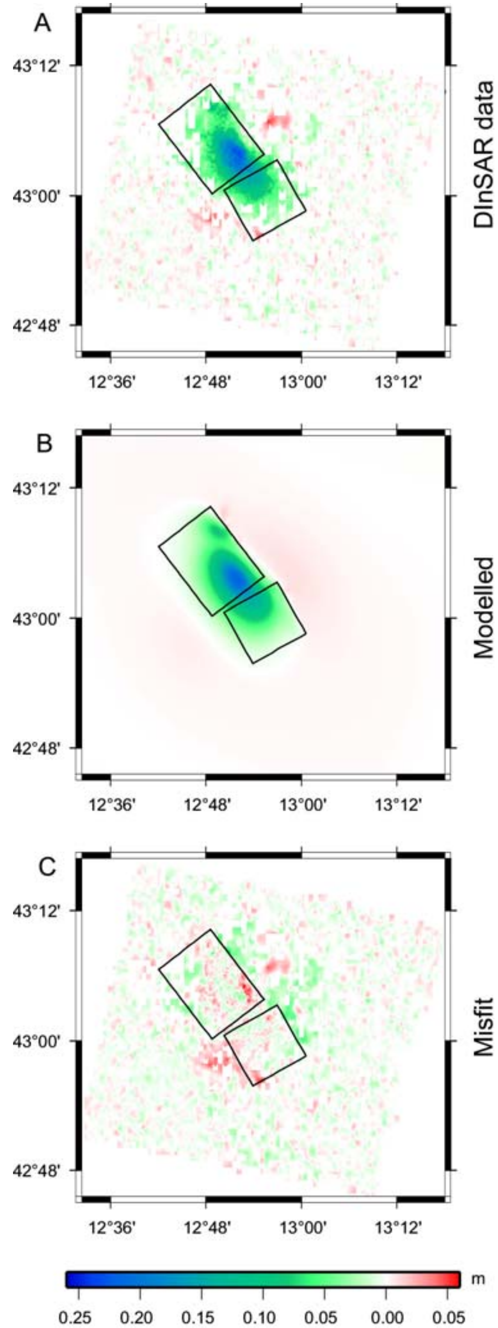
A
B
C
DInSAR data
Modelled
Misfit
43°12'
43°00'
42°48'
12°36'
12°48'
13°00'
13°12'
m
0.25
0.20
0.15
0.10
0.05
0.00
0.05

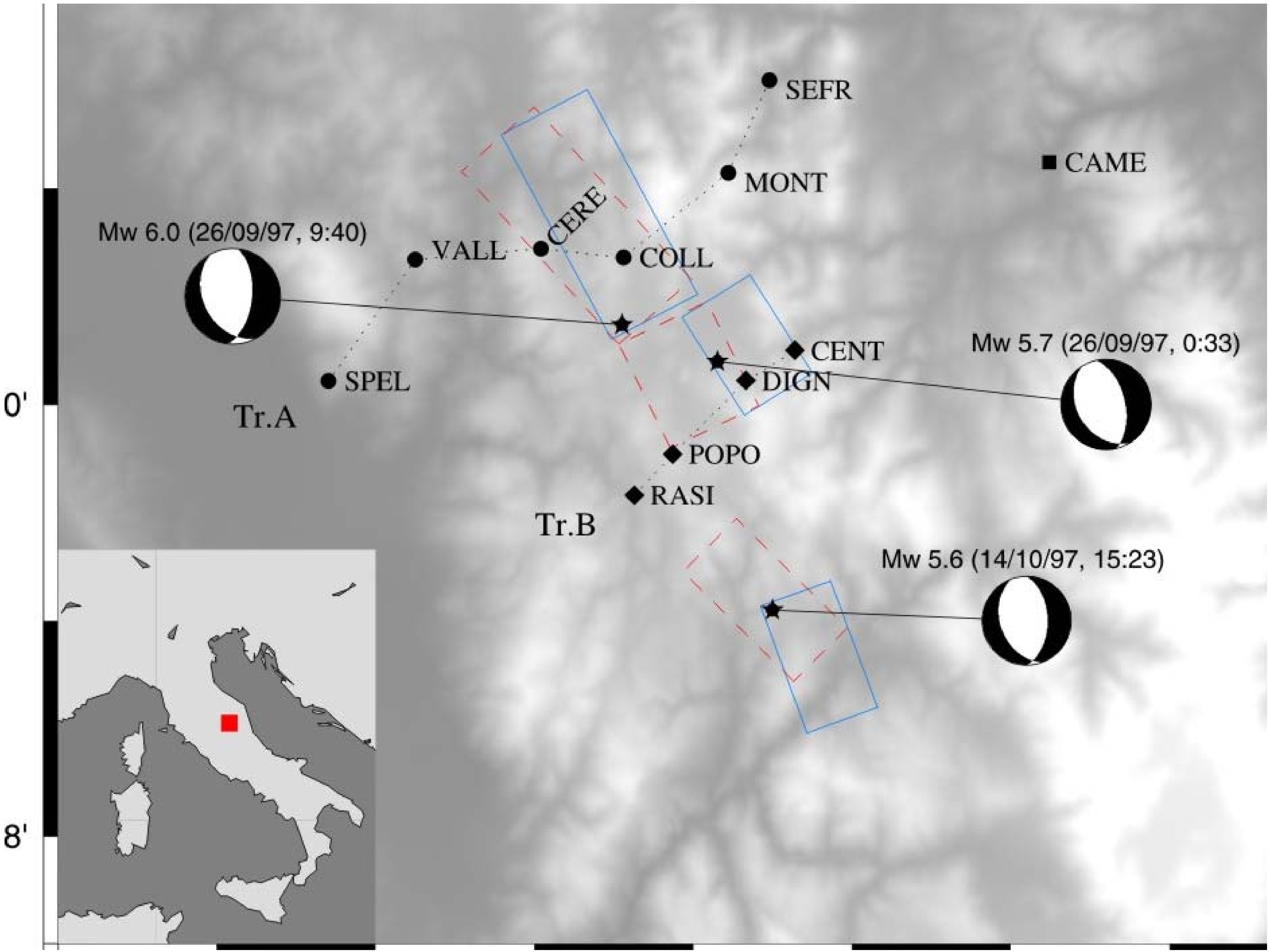
SEFR
CAME
MONT
CERE
Mw 6.0 (26/09/97, 9:40)
VALL
COLL
CENT
Mw 5.7 (26/09/97, 0:33)
SPEL
DIGN
0'
Tr.A
POPO
RASI
Tr.B
Mw 5.6 (14/10/97, 15:23)
8'

Non-permanent GPS networks

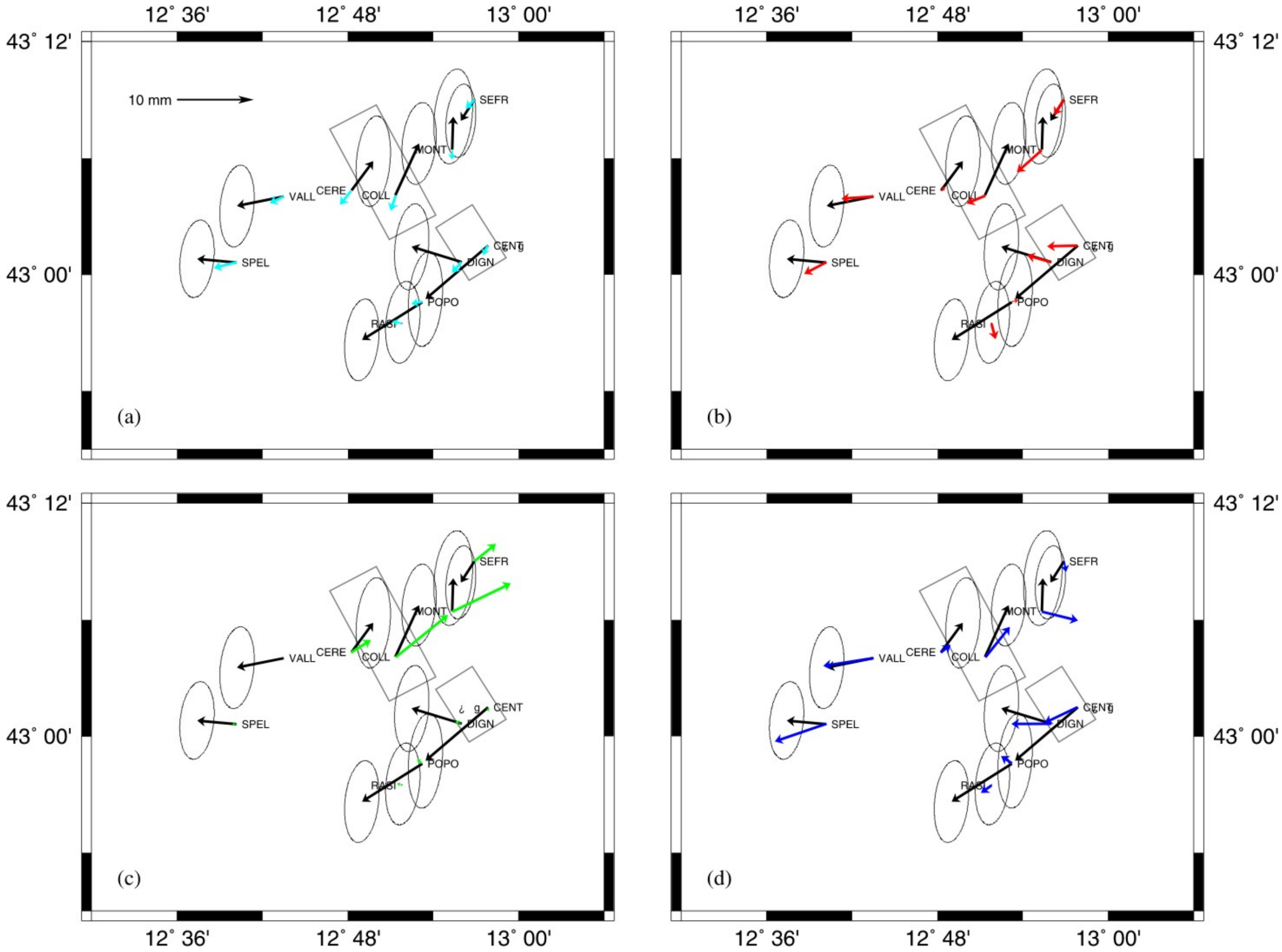

3B: Dignano 4B: Centare

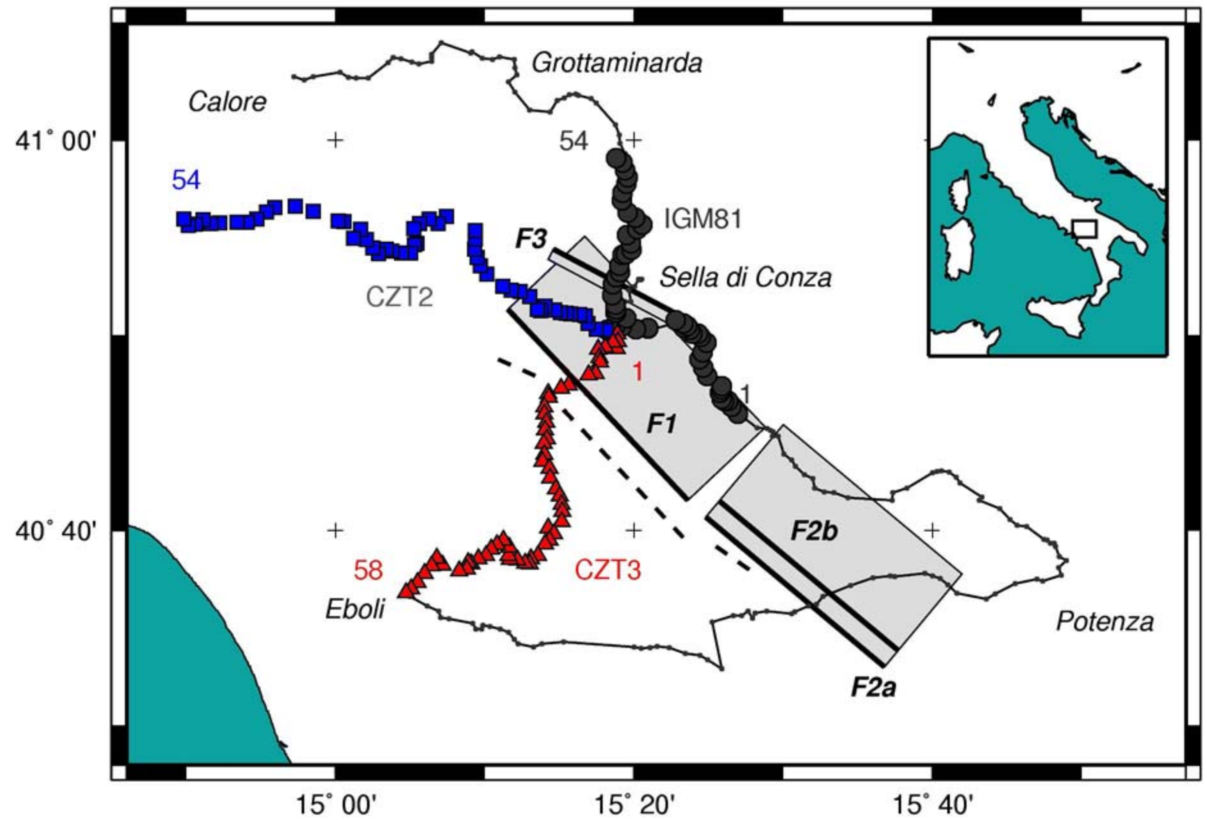

Dalla Via, G. et al., Lithospheric rheology in southern Italy inferred from postseismic viscoelastic relaxation following the 1980 Irpinia earthquake, JGR, 2005

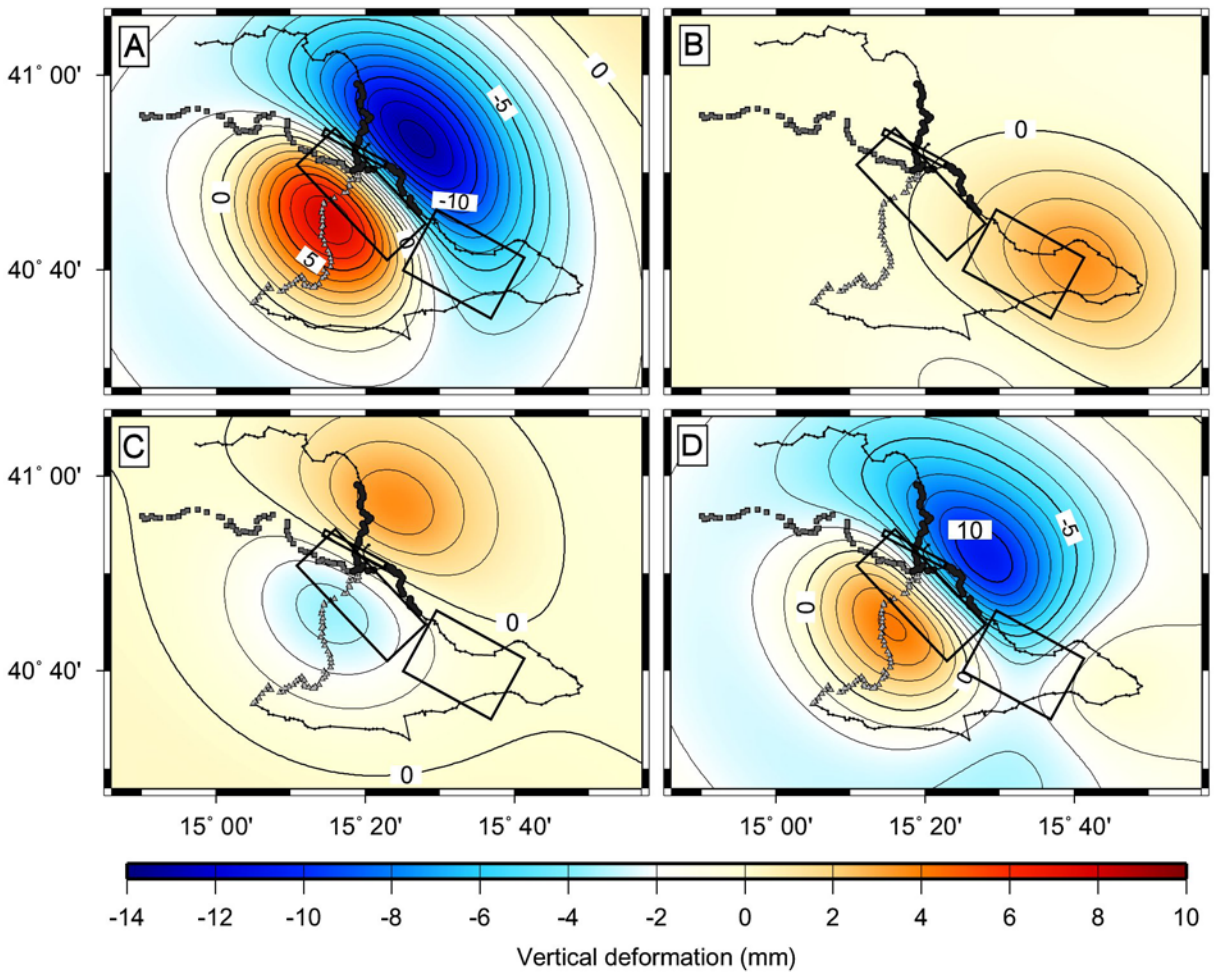
A
B
C
D
41° 00'
40° 40'
15° 00'
15° 20'
15° 40'
0
-5
-10
5
10
-14
-12
-10
-8
-6
-4
-2
0
2
4
6
8
10
Vertical deformation (mm)

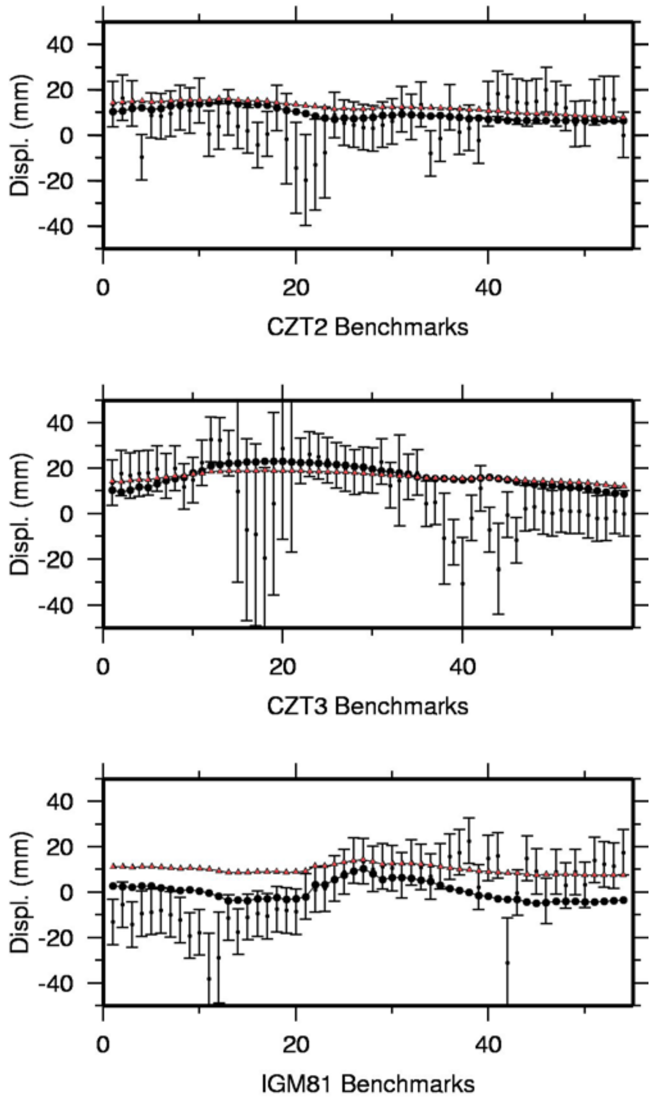

Dalla Via, G. et al., Lithospheric rheology in southern Italy inferred from postseismic Viscoelastic relaxation following the 1980 Irpinia earthquake, JGR, 2005

CONCLUSIONS (1)

- **Although the seismic classification of the Italian territory has been recently revised, the evaluation of seismic hazard continue to be based on the traditional probabilistic approach, i.e. on the probabilistic analysis of earthquake catalogue and of ground motion information, retrieved by macroseismic observations and instrumental recordings, that may lead to severe underestimations of seismic hazard.**

- **Recently this approach showed its limitation in providing a reliable seismic hazard assessment, possibly due to the insufficient information about historical seismicity, which can introduce relevant errors in the purely statistical approach mainly based on the seismic history. Indeed, some areas where low seismic hazard was foreseen, and consequently were not included in the seismic classification, have been subsequently struck by relatively strong and damaging earthquakes (e.g. the Sicily, September 2002, and the Molise, October 2002, earthquakes).**

CONCLUSIONS (2)

- To overcome the mentioned limitations and, above all, to improve the pre-seismic information which may lead to an effective mitigation of seismic risk, we are proposing an innovative approach, that combines EO data and new advanced approaches in seismological and geophysical data analysis.

- The proposed system, in fact, is proposing a deterministic approach to the estimation of seismic ground motion, integrated with the space and time dependent information provided by EO data analysis through geophysical forward modeling. The reason of the proposed integration of different geophysical observables appears almost obvious analyzing the earthquake “life cycle”, i.e. its process of preparation and occurrence: the lithosphere accumulates stress, according to strain and strain rates fields due to tectonic movements, which is partly released during the earthquake occurrence.